Supporting Information

Large Stimuli-Responsive Azobenzene Macrocycles as Functional Cavitands: Synthesis and Detection by NMR and MS Methods

Helena Roithmeyer[a]*, Merle Uudsemaa[a], Aleksander Trummal[a], Mari-Liis Brük[a], Sebastian Krämer, Indrek Reile[a], Vitalijs Rjabovs[a], Kirsti Palmi[a], Matt Rammo[a], Riina Aav[b], Elina Kalenius[c] and Jasper Adamson[a]*

[a] National Institute of Chemical Physics and Biophysics, Akadeemia tee 23, 12618 Tallinn

[b] Department of Chemistry and Biotechnology, Tallinn University of Technology

[c] University of Jyväskylä, Department of Chemistry, Finland

Current addresses:

Dr. Helena Roithmeyer
University of Zurich
Department of Chemistry
Winterthurerstrasse 190, CH-8057 Zurich
Switzerland
e-mail: helena.roithmeyer@kbfi.ee

Dr. Jasper Adamson
Laboratory of Chemical Physics, National Institute of Chemical Physics and Biophysics,
Akadeemia tee 23, 12618 Tallinn
e-mail: jasper.adamson@kbfi.ee

Contents

General Information

All solvents and reactants (azobenzene-4,4'-docarbonyl dichloride **2** and Cs_2CO_3) were purchased from Sigma-Aldrich and were used without further purification. For all reactions THF (99.8%, extra dry) was used. Compound **1** (3,3'-(1,3-phenylenebis(oxy)) diphenol) was synthesized according to previous literature.[1]

Methods

Purification

Extraction: The same extraction procedure was performed for all reactions. The crude product was dissolved in 20 ml DCM and washed three times with 25 ml deionized water. The combined organic layers were dried over anhydrous Mg_2SO_4, filtered and extracted with 10 ml DCM. Solvent was evaporated from the mixture to give a red-orange powder.

Column: Two different columns were performed to purify and separate the product mixtures. We found that by using column 2 (see below), separating **3b** from the larger macrocycles (**3e-g**) is possible, whereas column 1 favours the purification of the mixtures from side products.

Column 1: The crude product was dissolved in toluene. The column was packed with silica gel (0.063 – 0.200 mm) in 100% toluene. The product was eluted with EtOH/toluene (5:95, v:v; in total 100 mL), followed by 100% toluene. The fractions containing the products were combined, evaporated to dryness and analysed by ^{1}H NMR.

Column 2: The crude product was reconstituted in DCM. The column was packed with silica gel (0.063 – 0.200 mm) in 100% DCM. The starting eluent was DCM/diethyl ether (90:10, v:v) and the ration was changed to 80:20 and 50:50 v:v. Afterwards, 50ml ethyl acetate/DCM (50:50) was added, followed by 20 mL of pure EtOH for the final elution of products. The fractions containing the products were combined, evaporated to dryness and analysed by ^{1}H NMR.

NMR Studies

All spectra were acquired on a 500 MHz Agilent DD2 spectrometer equipped with a 5 mm inverse probe or on an 800 MHz Bruker Avance III spectrometer equipped with a He-cooled 5 mm cryoprobe. Spectra were referenced according to residual solvent signals.

2D DOSY NMR

Diffusion NMR was carried out with the Bruker standard convection compensated dstebpgp3s pulse sequence, needed for measurements in $CDCl_3$, acquiring 16 or 32 scans at 30 gradient levels. Gradient levels were incremented linearly from 5% to 95% of maximum gradient strength. Diffusion encoding gradient pulses were 0.5 ms and diffusion time was set to 300 ms. The diffusion time was optimized based on the signal to noise ratio for gradient strengths of 5% to 95% of the maximum gradient strength. Diffusion coefficients were calculated from single well resolved signals by fitting with Bruker Topspin T1/T2 data analysis module.

External Standard and calibration for DOSY NMR

Gradient strength of the probe was calibrated under typical measurement conditions against the water self-diffusion coefficient of $1.902 \cdot 10^{-9}$ m^2 s^{-1}. For quantitative estimation of analyte molecular weights, three analytes with known molecular weights and similar shape were used to establish a correlation between molecular weights and diffusion coefficients: 4,4-diaazene-1,2-diyl)dibenzoyl)chloride, cyclohexanohemicucurbit[6]uril[2] and cyclohexanohemicucurbit[8]uril[2]. The cyclohexanohemicucurbiturils (Table S1) were both provided by R. Aav et al. The experimentally determined linear regression equation y = -1.7731x - 13.418 (Figure S1) was used to establish molecular weight estimates for analytes synthesized herein.

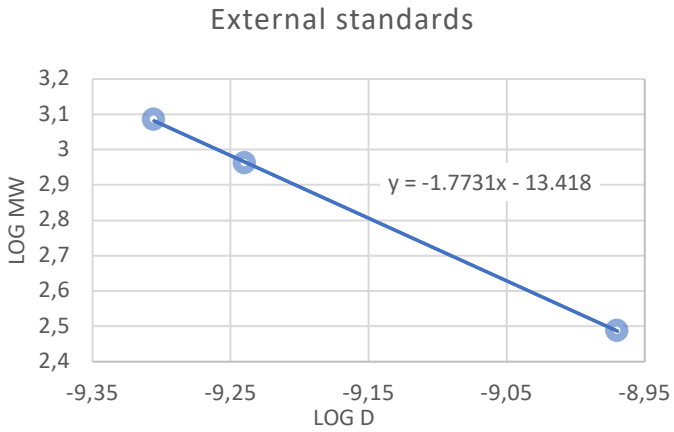

Figure S1. Graphical illustration of the external standards.

Table S1. Calibration with External Standards with Known Macrocycles

	MW (g mol^{-1})	Log MW	D (m^2 s^{-1})	Log D
4,4-diaazene-1,2-diyl)dibenzoyl)-chloride	307	2.487	$1.07 \cdot 10^{-9}$	-8.9698
cyclohexanohemicucurbit[6]uril[2]	913	2.961	$5.76 \cdot 10^{-10}$	-9.2396
cyclohexanohemicucurbit[8]uril[2]	1216	3.085	$4.95 \cdot 10^{-10}$	-9.3054

Illustrative 2D DOSY plots

Initially, attempts were made to resolve partially overlapping DOSY spectra with MNova 2D DOSY transform, but the results were inconclusive or even unreliable as peak overlap cannot often be resolved by 2D DOSY. Consequently, quantitative diffusion analysis of host-guest mixtures could not be done by a 2D DOSY transform and 2D DOSY plots are used herein solely for qualitative analysis and illustrative purposes. Diffusion coefficients for quantitative analysis were obtained by analyzing single baseline resolved peaks of mixture components by Bruker Topspin T1/T2 module diffusion functionality.

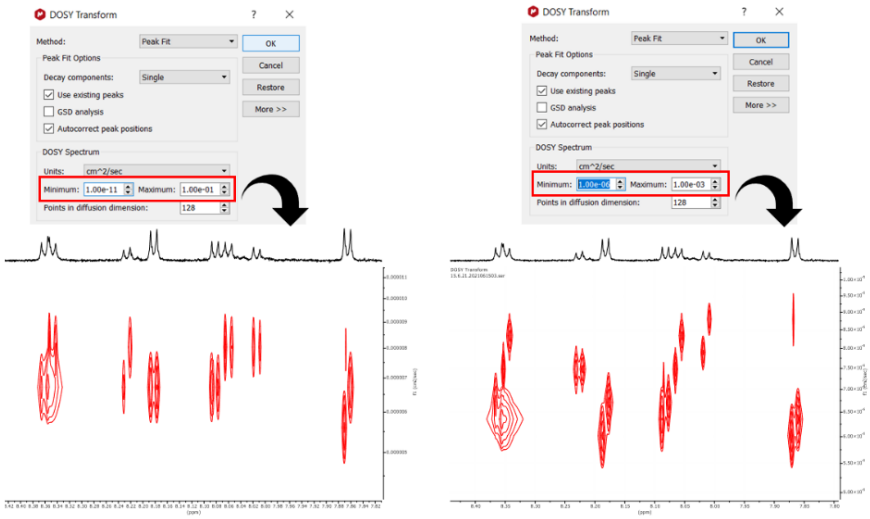

Figure S2. Illustration problem with MNova transformation.

DOSY characterization

When comparing all signals (Table S2) from all reactions and their related diffusion coefficients, obtained from both analysis methods by MNova and TopSpin, we found that the chemical shifts cannot be assigned to a single macrocycle since often differently sized macrocycles overlap in the direct proton dimension. This, together with other factors discussed in the main text and illustrated in more detail in the SI, prevented the determination of diffusion coefficients for the mixtures of the macrocycles. One possible reason for that is the ability of the macrocycles to form different isomers and therefore multiple azobenzene peaks appear overlapping in the same region. Another reason is the different results we received from different software. The processing tool with MNova allows to adjust the transformation method for the raw data to illustrate the peaks in the second dimension and already suggests the related diffusion coefficient for every peak. When applying the "Peak Fit" method, the transformation window can be chosen individually (Figure S2). We found when using small transformation windows, *e.g.*, 10^{-6} to 10^{-3}, the peaks were split over the whole 2D dimension and could not be assigned to peaks in the direct dimension anymore, whereas large transformation windows, *e.g.*, 10^{-12} to 10^{-1}, resulted in average peaks with average values, which deviated strongly from the smaller window values. Hence, TopSpin was additionally used to integrate the peak areas and to fit the obtained diffusion coefficients in the relaxation module and afterwards insert the obtained data in our regression equation obtained from external calibration (Figure S1). This explains the strongly deviating results we received from the analysis by Topspin and MNova, which made it difficult to identify distinct 1D peaks to distinct molecular weights. For completion, we present the DOSY data of all work-up mixtures and compare the diffusion coefficient obtained from both analysis methods (Table S2). We aim to demonstrate the idea behind DOSY to virtually separate molecules with different molecular weights according to their diffusion in solution. Additional factors, such as the shape and molecular interactions, restrict the application of this method and DOSY NMR was not sufficient for the characterization of our macrocycles. Nevertheless, those insight helped to understand our systems better and contributed to the obtained ESI-IM data.

Table S2. Comparison of All Results of Each Reaction Obtained from DOSY NMR with both methods.

peak	1	2	3	4	5	6	7	8	9		Method
ppm	8.36-8.35	8.34-8.33	8.22-8.21	8.17-8.16	8.08-8.07	8.06-8.05	8.01-7.99	7.86-7.84			
A4	3c	3c	3b	3c	3c	3c	3b	3c			TopSpin
	3c,d	3c,d	3b	3d	3c,d	3c,d	3b	3d			MNova
A6	3d	3c	3c	3d	3d	3d	3c	3d			TopSpin
	3b	3b	3a	3c	3b	3b	3a	3c			MNova
B4	3c	3c	3d	3b	3b	3d	3f	3b			TopSpin
	3c,d	3c,d,f,g	3g	3b	3b,c	3d,f,g	3g	3b			MNova
peak	1	2	3	4	5	6	7	8	9		
ppm	8.35-8.34	8.34-8.33	8.22-8.21	8.21-8.20	8.18-8.16	8.08-8.07	8.05-8.04	8.01-7.99	7.98-7.97		
B6	3b	3a	3b	3d	3c	3c	3d	3d	3f		TopSpin
	3b	3c,d,e	3c,d	3c,d	3c,d	3c,d,e	3c,d	3b	3b		MNova
C4	3d	oligomer	3f	3c	3c	3d	oligomer	3f	3c		TopSpin
	3c,d	3e+oligo	3g	--	3b	3b,c,d	3e+oligo	3g	3b		MNova
ppm	8.36-8.34	8.34-8.33	8.22-8.21	8.17-8.16	8.08-8.07	8.06-8.04	8.01-7.99	7.86-7.85			
C6	3c	3c	3b	3c	3c	3c	3b	3c			TopSpin
	3b	3b	--	3b	3b	3b	--	3b			MNova
peak	1	2	3	4	5	6	7	8	9	10	
ppm	8.36-8.35	8.35-8.34	8.23-8.22	8.21-8.20	8.18-8.17	8.08-8.07	8.06-8.05	8.02-8.00	7.99-7.98	7.87-7.86	
D4	3d	3d	3b	3b	3e	3d	3d	3b	3b	3e	TopSpin
	3b	3b	--	--	3b	--	--	--	--	3b	MNova
D6	3d	3d	3c	3b	3d	3d	3d	3c	3b	3d	TopSpin
	3c,d,e	3c,d,e	3b	3b	3c	3c,d,e	3c,d,e	3b	--	3c,d,e	MNova
ppm	8.36-8.34	8.33-8.32	8.23-8.21	8.17-8.16	8.08-8.07	8.06-8.05	8.01-8.00	7.86-7.85			
E4	3d	3d	3c	3d	3d	3d	3c	3d			TopSpin
	3c,d	3c,d	3b	3d	3d	3c	3b	3d			MNova
E6				3c				3c			TopSpin
				3b,c				3b,c			MNova
	1	2	3	4	5	6	7	8	9	10	
ppm	8.36-8.35	8.348-8.347	8.23-8.22	8.21-8.20	8.18-8.17	8.08-8.07	8.06-8.05	8.02-8.00	7.99-7.98	7.87-7.86	
Comparison All	**3b,c,d,(e)**	**3b,c,d, (e,g)**	**3a,b,c,d,f,g**	**3b,c,d**	**3b,c,d,e**	**3b,c,d,(e)**	**3b,c,d, (e,f,g)**	**3a,b,c,d,f,g**	**3b,c,f**	**3b,d,e**	Both methods

Mass spectrometry (ESI-MS) and ion mobility mass spectrometry (IM-MS)

The mass spectra were measured using Agilent 6560 IM-TOF mass spectrometer connected to dual ESI ion source and an ion mobility drift-tube (DT-IM). Samples were dissolved in DCM and diluted in MeOH where NaOAc or CsOAc were added to enhance ionization of the macrocycles. Samples were introduced to dual ESI ion source using direct infusion with flow rate of 5 µl/min. Samples were measured on positive polarization and parameters were optimized for maximum intensity. Nitrogen was used as dry gas and for nebulization. Dry gas temperature of 225 °C, a flow rate of 3 l/min, a nebulizer pressure of 20 psi, sheath gas temperature of 225 °C, and a sheath gas flow of 5 l/min were used. Capillary voltage between 4000 and 4500 V and fragmentor voltage of 400 V were set as source parameters. The mass spectrometer was calibrated with an ES tuning mix (from Agilent Technologies). Data were acquired using MassHunter Acquisition B.09.00 and analyzed using MassHunter Qualitative Analysis B.08.00 as software packages from Agilent Technologies, USA. In the single-field DT-IM experiments with N_2 as drift gas, the high-pressure funnel was set to 3.80 Torr. The drift tube entrance and exit voltages were set as 1700 V and 224 V, respectively. A trap filling time of 10 000 µs and a trap release time of 350 µs were used. Collision cross-section ($^{DT}CCS_{N2}$) values were determined by using multi-field measurements and the drift tube entrance voltage was varied from 1074 V to 1674 V with 100 V increments. Before sample introduction, ES tuning mix (Agilent Technologies) was measured as a quality control sample for the CCS values. IM-data was analyzed using MassHunter IM-MS Browser B.08.00. In addition to Mass Hunter, a self-developed software from Sebastian Krämer was used to fast and easy scanning of the matching *m/z* peaks out of the data.

Mainly singly and doubly charged complexes as Na^+ and Cs^+ adducts ions were observed. Macrocycles of different size but increasing charge state can have overlapping m/z values. However, isotopic distributions result in charge state information and macrocycles of different size can be identified. Further on, the ions with overlapping isotopic distributions can be isolated using ion mobility mass spectrometry. In addition, ion mobility mass spectrometry experiments would enable us to distinguish between different isomers. Here mainly overlapping *m/z* values from the macrocycles **3b** and **3d**, **3d** and **3g**, **3c** and **3f** (Table S3) were observed and were assigned due to their different charge states. In our analysis mainly **3b** and **3d** showed intense peaks, whereas the larger macrocycles **3e-g** were only found in trances in a few reactions. This could be due to the decreased ionization efficiency of the larger macrocycles or smaller quantities of **3e-g** produced in synthesis.

For every reaction the profile ESI-MS spectrum, IM arrival time distributions for individual m/z values and extracted mass spectra from IM drift peaks are shown. CCS values were measured in the gas phase and therefore conformational change in the gas phase can be different in comparison to NMR.

Table S3. Main complex ions observed in (+)ESI-MS measurements, their experimental and theoretical *m/z* values, mass accuracies and IM-MS drift times and $^{DT}CCS_{N2}$ values.

Ion		Formula	z	m/zexp	m/ztheor	MW (Da)	mass accuracy (mDa)	drift time (ms)	$^{DT}CCS_{N2}$ (Å2)
[**3b**+Na]$^{+}$	2+2	$C_{64}H_{40}N_4O_{12}Na$	1	1079.2526	1079.2535	1079.2535	-0.86	48.3	355.9
[**3b**+Cs]$^{+}$	2+2	$C_{64}H_{40}N_4O_{12}Cs$	1	1189.1687	1189.1692	1189.16918	-0.44	49.1	362.1
[**3b**+2Na]$^{2+}$	2+2	$C_{64}H_{40}N_4O_{12}Na_2$	2	551.1216	551.1214	1102.24272	0.22	25.7	377.8
[**3c**+2Na]$^{2+}$	3+3	$C_{96}H_{60}N_6O_{18}Na_2$	2	815.1864	815.1874	1630.3748	-1.0	29.8	434.1
[**3d**+2Na]$^{2+}$	4+4	$C_{128}H_{80}N_8O_{24}Na_2$	2	1079.2523	1079.2535	2158.507	-1.19	34.8	510
[**3d**+2Cs]$^{2+}$	4+4	$C_{128}H_{80}N_8O_{24}Cs_2$	2	1189.1687	1189.1692	2378.3384	-0.5	34.9	555.1
[**3e**+2Na]$^{+}$	5+5	$C_{160}H_{100}N_{10}O_{30}Na_2$	2	1343.3168	1343.31956	2686.63912	-2.76	41.26	na
[**3f**+2Cs]$^{2+}$	6+6	$C_{192}H_{120}N_{12}O_{36}Cs_2$	2	1717.3012	1717.3013	3434.6026	-0.1	42.89	757.9
[**3f**+2Na]$^{2+}$	6+6	$C_{192}H_{120}N_{12}O_{36}Na_2$	2	1607.3830	1607.3856	3214.7712	-2.6	42.79	767.3
[**3g**+2Na]$^{2+}$	8+8	$C_{256}H_{160}N_{16}O_{48}Na_2$	2	2135.5055	2135.5178	4271.0356	-12.3	49.31	na

Synthetic procedures A-E and characterization of the obtained macrocycles

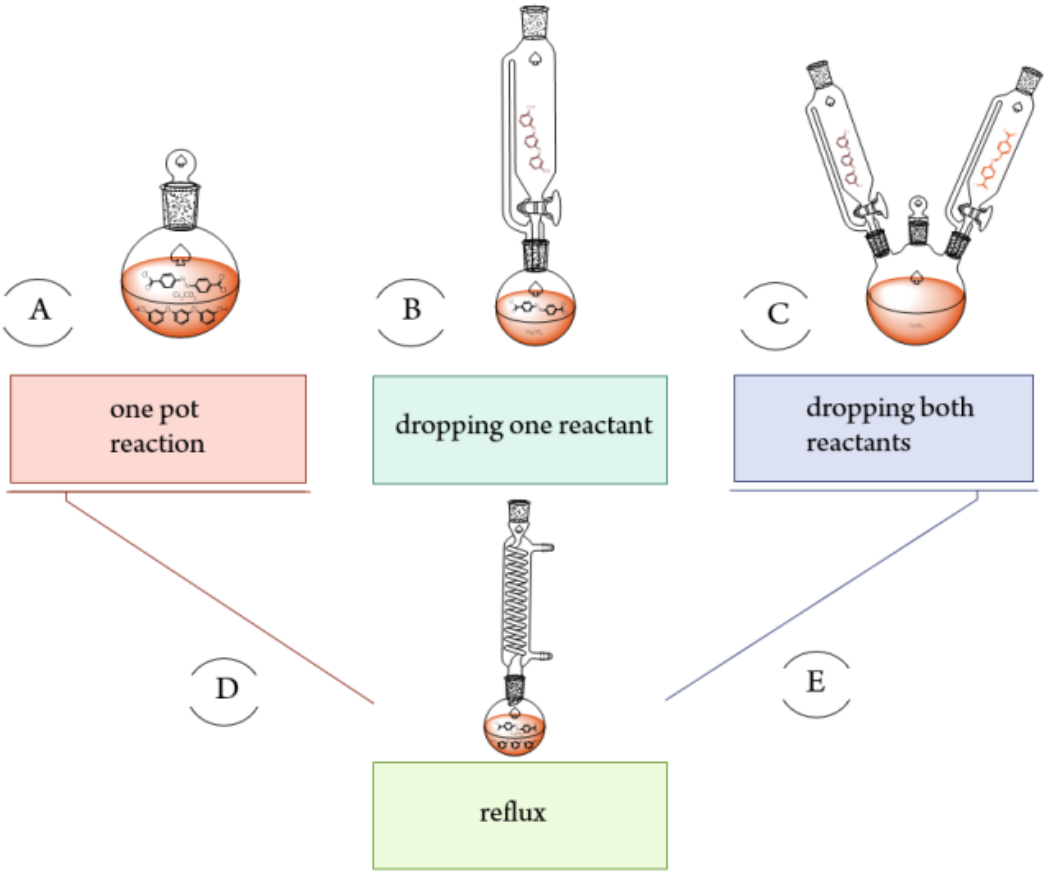

Figure S3. Reaction methods **A-E** investigated in this study.

Scheme S1. Synthetical Route to the Macrocycles **3a-g**

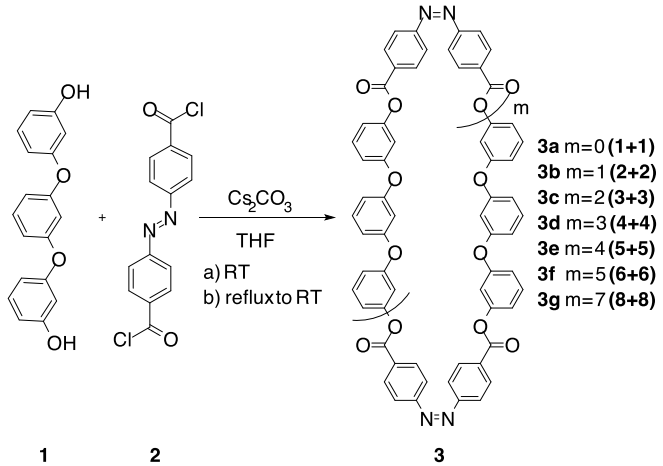

Most of the following presented proton NMR data are from the work-up mixtures of the reactions after extraction, before further purification, which is why some exhibit additional signals in the ESI-MS and NMR spectra. Our characterization is focused on the azobenzene region (7.5 to 8.5 ppm) in the ^{1}H and DOSY NMR spectra. High resolution mass spectrometry (HRMS) coupled

with ion mobility (IM) was measured for all work-up fractions after extraction and is brought below for individual reactions.

Reaction Method A

Synthetic procedure for A: One pot reaction

To a round bottom flask equipped with 3 Å molecular sieves, n equiv. of Cs_2CO_3 (n = 4, 6), 1 equiv. of 4,4-diaazene-1,2-diyl)dibenzoyl)chloride and 1 equiv. of 3,3'-(1,3-phenylenebis(oxy))diphenol were added and stirred in 24 mL THF at RT under argon atmosphere. Reaction progress was monitored with ^{1}H NMR after 3 h, 5 h, 7 h, 24 h until the reaction was complete (up to 144h). For reaction monitoring 300 µL of the mixture were taken with a syringe and the solvent was evaporated for 5 minutes. For NMR analysis, the crude product was dissolved in $CDCl_3$. After the reaction was complete, the mixture was filtered and washed with 5 mL THF and the solvent was evaporated. The extraction procedure can be found in the methods part. The conversion of 43% was reached after 118h in the presence of 4 equiv. of Cs_2CO_3 base and conversion of 35% was reached after 144h in the presence of 6 equiv. of Cs_2CO_3 base.

Reaction monitoring of the reaction A with different base equivalents

The reaction monitoring for both reactions (Figure S4) showed that at first the formation of oligomers, based on broad signals, and later the occurrence of macrocyclisation. This was observable for both reactions, albeit more strongly pronounced for the reaction with higher base equivalents.

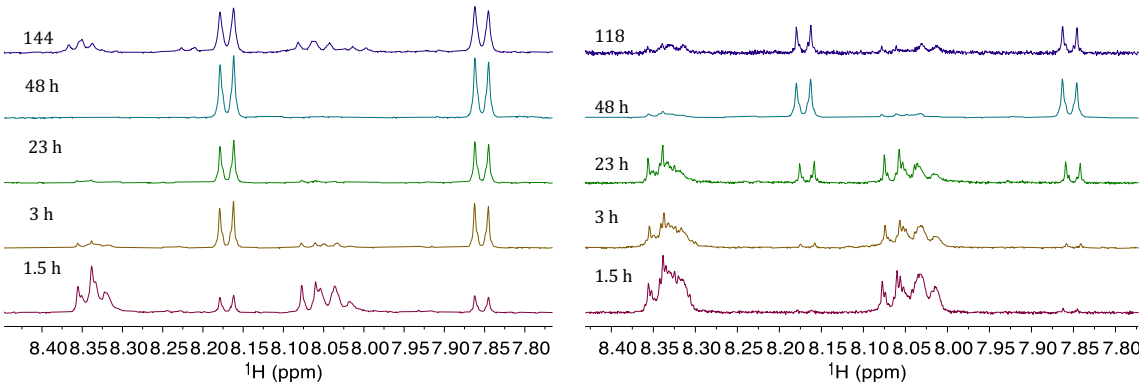

Figure S4. Reaction monitoring of the two one pot reactions **A** after different times 4 equiv. (left) and 6 equiv. (right) of Cs_2CO_3 base.

Characterization of the work-up mixtures obtained from A

The work-up mixtures were characterized with ^{1}H and DOSY NMR in the azobenzene region and ESI-MS coupled with IM and the results are presented below.

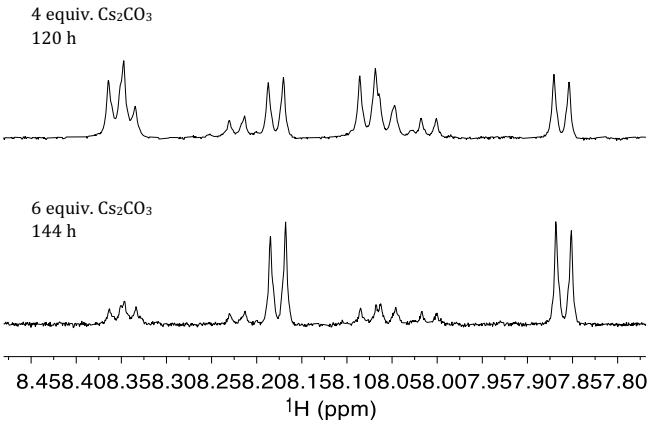

Figure S5. ^{1}H NMR azobenzene region of the 4 (above) and 6 (beneath) equivalents of Cs_2CO_3 base in the one-pot reaction **A** of the work-up phase.

NMR spectra and ESI-MS analysis from reaction A

^{1}H NMR spectrum of the 4 equivalent reaction A

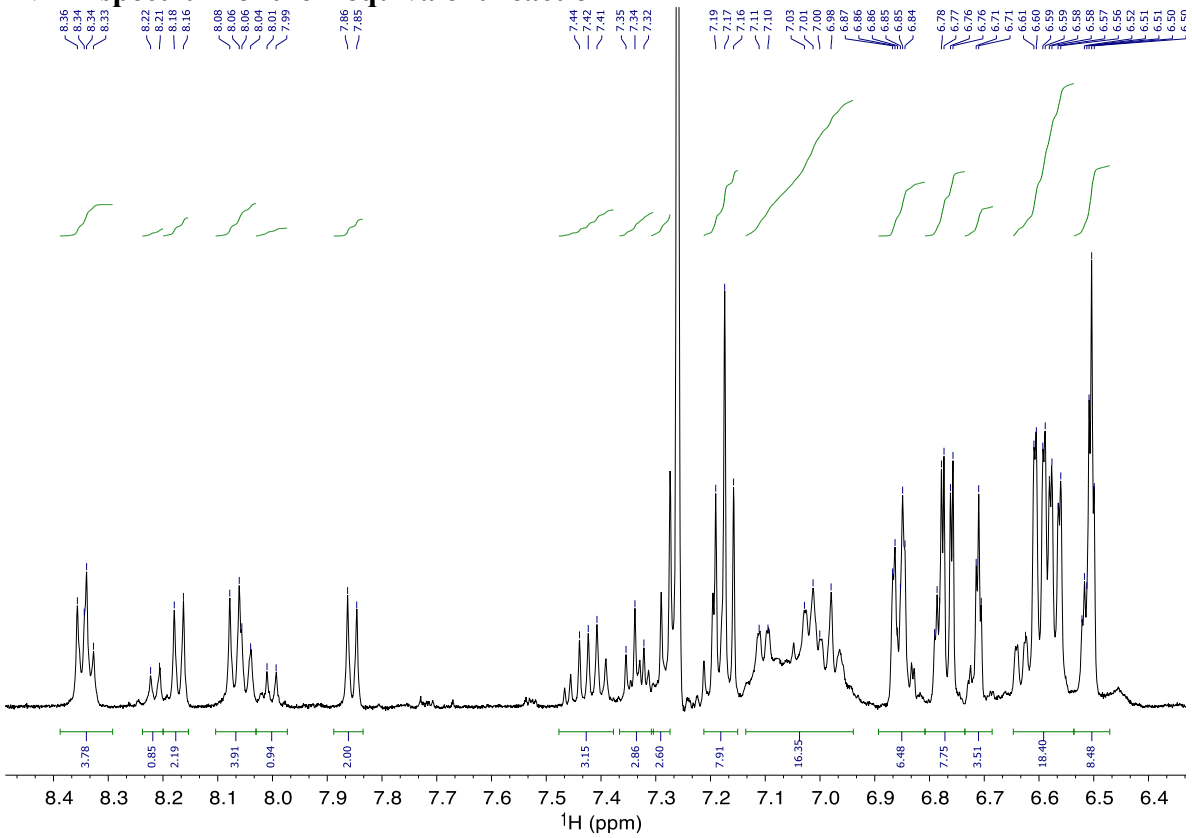

Figure S6: ^{1}H NMR from the work-up of the reaction method **A** with 4 equiv. of Cs_2CO_3 base.

^{1}H NMR (500 MHz, $CDCl_3$) δ 8.34 (dd, *J* = 6.2, 6.0 Hz, 4H), 8.21 (d, *J* = 8.3 Hz, 1H), 8.17 (d, *J* = 8.5 Hz, 2H), 8.06 (dd, *J* = 6.2, 6.0 Hz, 4H), 8.00 (d, *J* = 8.3Hz, 1H), 7.85 (d, *J* = 8.5 Hz, 2H), 7.48 – 7.38 (m, *J* = 3.5Hz 3H), 7.34 (t, *J* = 8.5Hz, 3H), 7.17 (t, *J* = 9.0 Hz, 8H), 7.14 – 6.94 (m, *J* = 8.1 Hz, 16H), 6.86 (m, *J* = 7.0, 6H), 6.81 – 6.74 (m, *J* = 2.0, 8H), 6.71 (t, *J* = 2.0 Hz, 4H), 6.58 (dddd, *J* = 2.0, 2.5, 2.0, 2.5 Hz, 18H), 6.51 (m, *J* = 2.5 Hz, 8H).

Characterization: 4 equiv. (Table 1, entry 1): HRMS, ESI$^+$: **3b (2+2)** m/z calc. for $C_{64}H_{40}N_4O_{12}$ $[M+2Na]^{2+}$ 551.1214 found 551.1214; m/z calc. for. $[M+Na]^+$ 1079.2535 found 1079.2518; m/z calc. for. $[M+Cs]^+$ 1189.1692 fond 1189.1671; **3d** (4+4) m/z calc. for $C_{128}H_{80}N_8O_{24}$ $[M+2Na]^{2+}$ 1079.2535 found 1079.2518 m/z calc. for $[M+2Cs]^{2+}$ 1189.1692 fond 1189.1671; **3e** (5+5) m/z calc. for. $C_{160}H_{100}N_{10}O_{30}$ $[M+2Na]^{2+}$ 1343.3196 found 1343.3129
DOSY NMR: D= 6.87 10^{-10} m^2 s^{-1}, MW= 902 g mol^{-1} (MNova) and D= 5.46 10^{-10} m^2 s^{-1}, MW= 1015 g mol^{-1} (TopSpin) for **3b,** D= 5.88*10^{-10} m^2 s^{-1} MW =1171 $gmol^{-1}$ and (Mnova) D= 4.55 10^{-10} m^2 s^{-1}, MW=1402.7 (TopSpin) for **3c** and D= 5.08 10^{-10} m^2 s^{-1}; MW= 1774 g mol^{-1} (MNova) for **3d.**

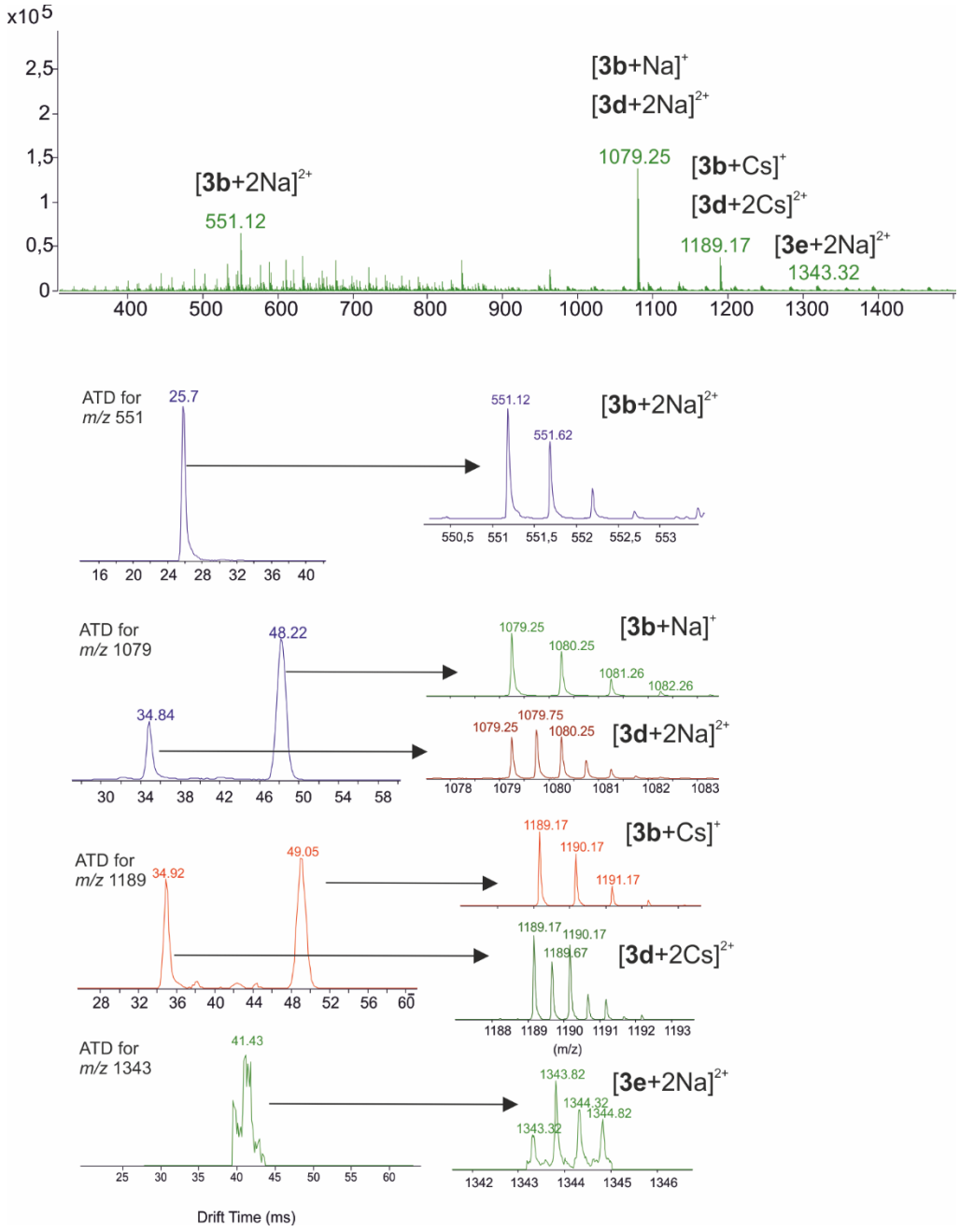

Figure S7. ESI-MS mass spectrum for **A4** and IM-MS arrival time distributions (ATDs) for different ions. Multiple peaks in ATDs correspond to different, overlapping ions. Zoomed views for MS spectra are extracted from each of the peaks to verify their identity and to compare the abundance.

DOSY Analysis of 4 equivalent reaction A

The DOSY analysis of the azobenzene region of the rection method **A** with 4 equiv. of Cs_2CO_3 base is brought below. The spectrum was illustrated and analyzed with MNova and is depicted in Figure S17. The results for the molecular weights of the macrocycles found with the external standards extracted from TopSpin are listed in Table S4.

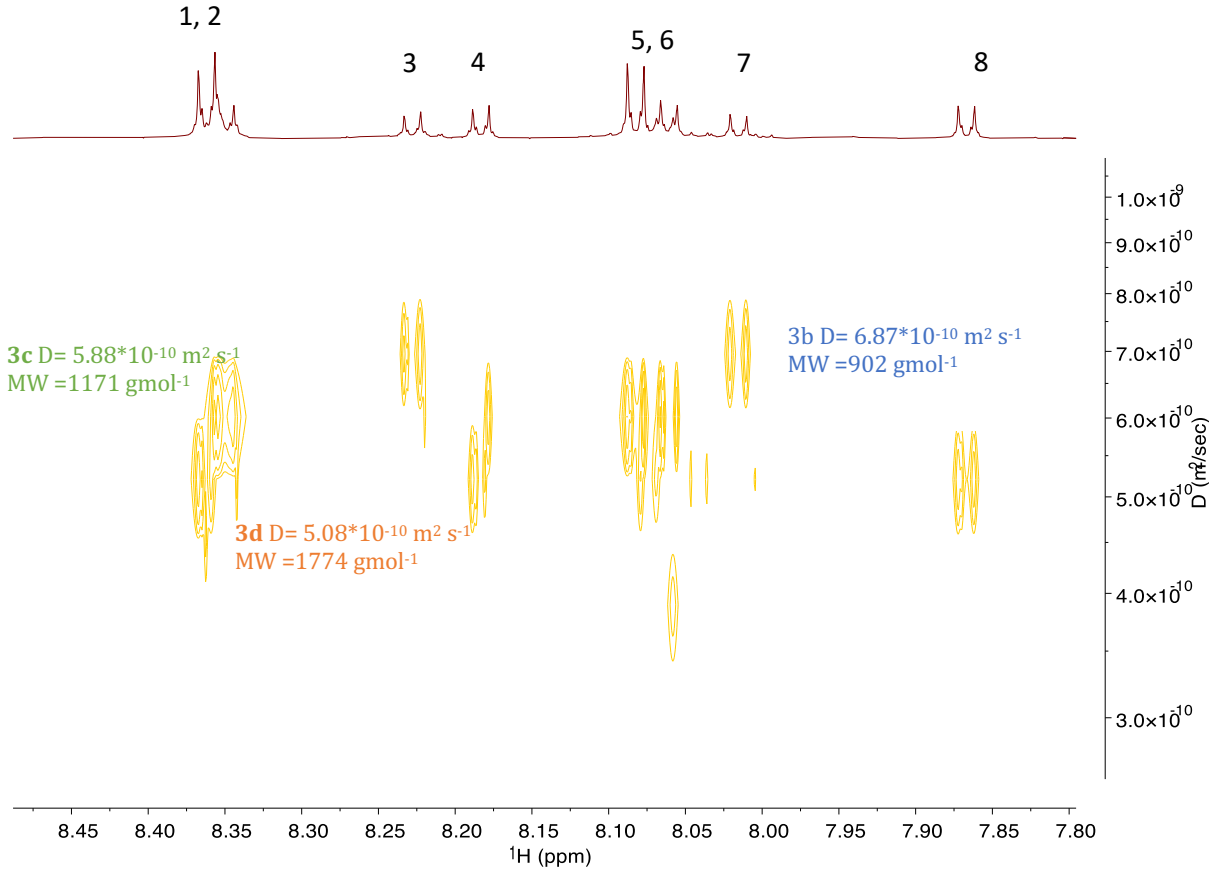

Figure S8. DOSY NMR of the reaction method **A** with 4 equiv. of Cs_2CO_3 base from MNova.

Table S4. Analysis of the Reaction Method **A** with 4 Equiv. of Cs_2CO_3 Base with TopSpin.

	1	2	3	4	5	6	7	8
ppm	8.36-8.345	8.34-8.33	8.22-8.21	8.17-8.16	8.08-8.07	8.06-8.05	8.01-7.99	7.86-7.84
D	4.55E-10	4.55E-10	5.56E-10	4.60E-10	4.85E-10	4.41E-10	5.46E-10	4.60E-10
log D	-9.34	-9.34	-9.26	-9.34	-9.31	-9.36	-9.26	-9.34
Y	3.15	3.15	2.99	3.14	3.10	3.17	3.01	3.14
calc MW	1402.7	1402.7	983.1	1371.5	1250.1	1481.5	1015.0	1375.2
Macrocycle	3+3	3+3	2+2	3+3	3+3	3+3	2+2	3+3

NMR spectrum of the reaction method A with 6 equiv. of Cs_2CO_3 base

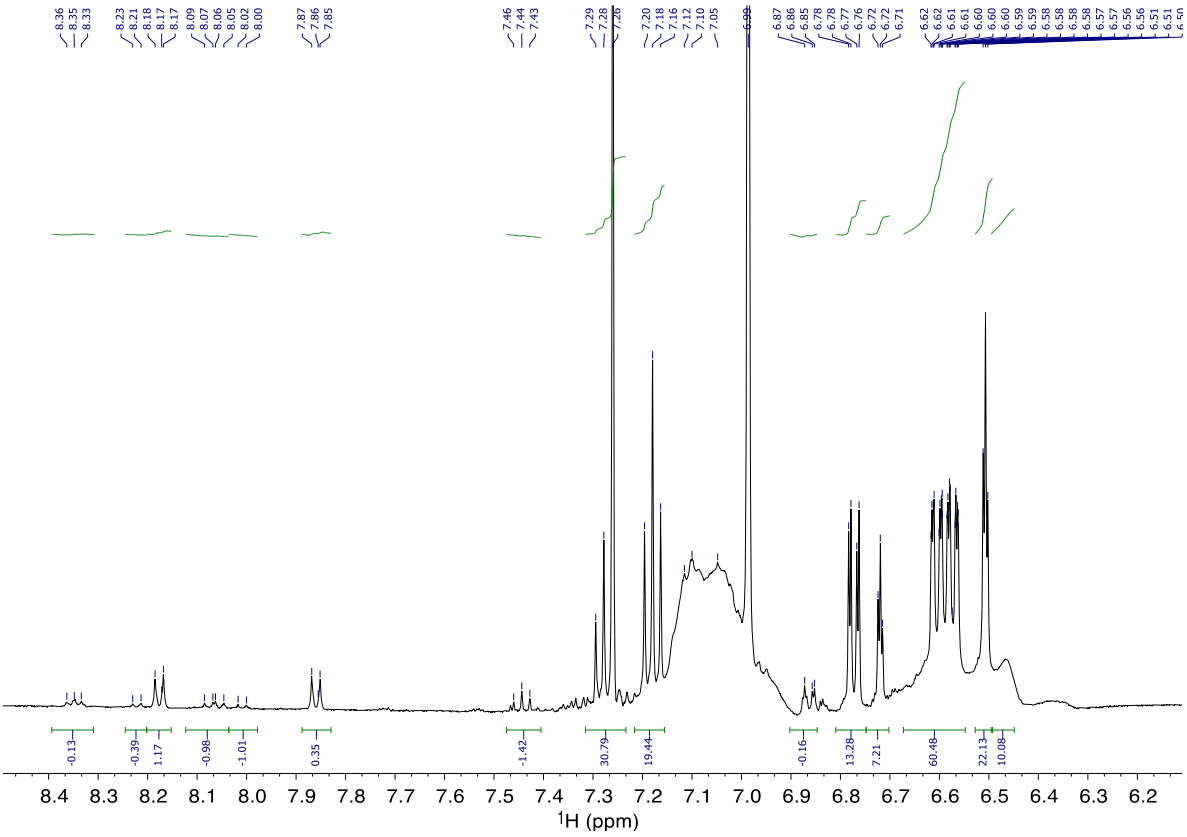

Figure S9. ^{1}H NMR of the work-up of the reaction method **A** with 6 equiv. of Cs_2CO_3 base. The work-up shows large broad additional signals in the ether precursor (aromatic) region, which indicate the formation of oligomers.

^{1}H NMR (500 MHz, $CDCl_3$) δ 8.36– 8.33 (m, dd, *J* = 8.5, 8.5 Hz ,1H), 8.18 (d, *J* = 8.5 Hz, 2H), 8.07 (dd, *J* = 8.5, 8.5 Hz, 1H), 7.86 (d, *J* = 8.5 Hz, 2H), 7.44 (t, *J* = 8.0 Hz, 1H), 7.26 (t, *J* = 8.5 Hz 34H), 7.18 (t, *J* = 8.0 Hz, 22H), 6.90 – 6.85 (m, *J* = 7.5 Hz, 2H), 6.77 (dd, *J* = 7.5, 2.0 Hz, 16H), 6.72 (t, *J* = 2.5 Hz, 9H), 6.59 (dddd, *J* = 2.5, 2.5 Hz, 64H), 6.51 (t, *J* = 2.5 Hz, 23H), 6.47 (s, 11H).

6 equiv. (Table 1, entry 2):HRMS, ESI$^+$: **3b (2+2)** m/z calc. for $C_{64}H_{40}N_4O_{12}$ $[M+2Na]^{2+}$ 551.1214 found 551.1218; m/z calc. for $[M+Na]^+$ 1079.2535 found 1079.2527; m/z calc. for $[M+Cs]^+$ 1189.1692 fond 1189,16789; **3d (4+4)** m/z calc. for $C_{128}H_{80}N_8O_{24}$ $[M+2Na]^{2+}$ 1079.2535 found 1079.2527; m/z calc. for $[M+2Cs]^{2+}$ 1189.1692 fond 1189.16789 m/z calc. for $[M+Na]^+$ 2135.5178 found 2135.5149; **3e (5+5**) m/z calc. for $C_{160}H_{100}N_{10}O_{30}$ $[M+2Na]^{2+}$ 1343.3196 found 1343.3168; **3f (6+6)** m/z calc. for. $C_{192}H_{120}N_{12}O_{36}$ $[M+2Na]^{2+}$ 1607.3856 found 1607.3830. **DOSY NMR:** D= $9.38*10^{-10}$ m^2 s^{-1} MW =468 $gmol^{-1}$ (Mnova) for **3a**, D= 7.25 10^{-10} m^2 s^{-1}, MW= 802 g mol^{-1} (MNova) for **3b**, D= $5.68*10^{-10}$ m^2 s^{-1} MW =1374 $gmol^{-1}$ (Mnova) for **3c**, D= 4.18 10^{-10} m^2 s^{-1}, MW= 1625 g mol^{-1} (TopSpin) for **3d**.The DOSY analysis of the reaction method **A** with 6

equiv. of Cs_2CO_3 base gave inadequate results when analyzed with MNova and TopSpin and only the values found for compound **3b** and **3d** match the found ESI-MS data.

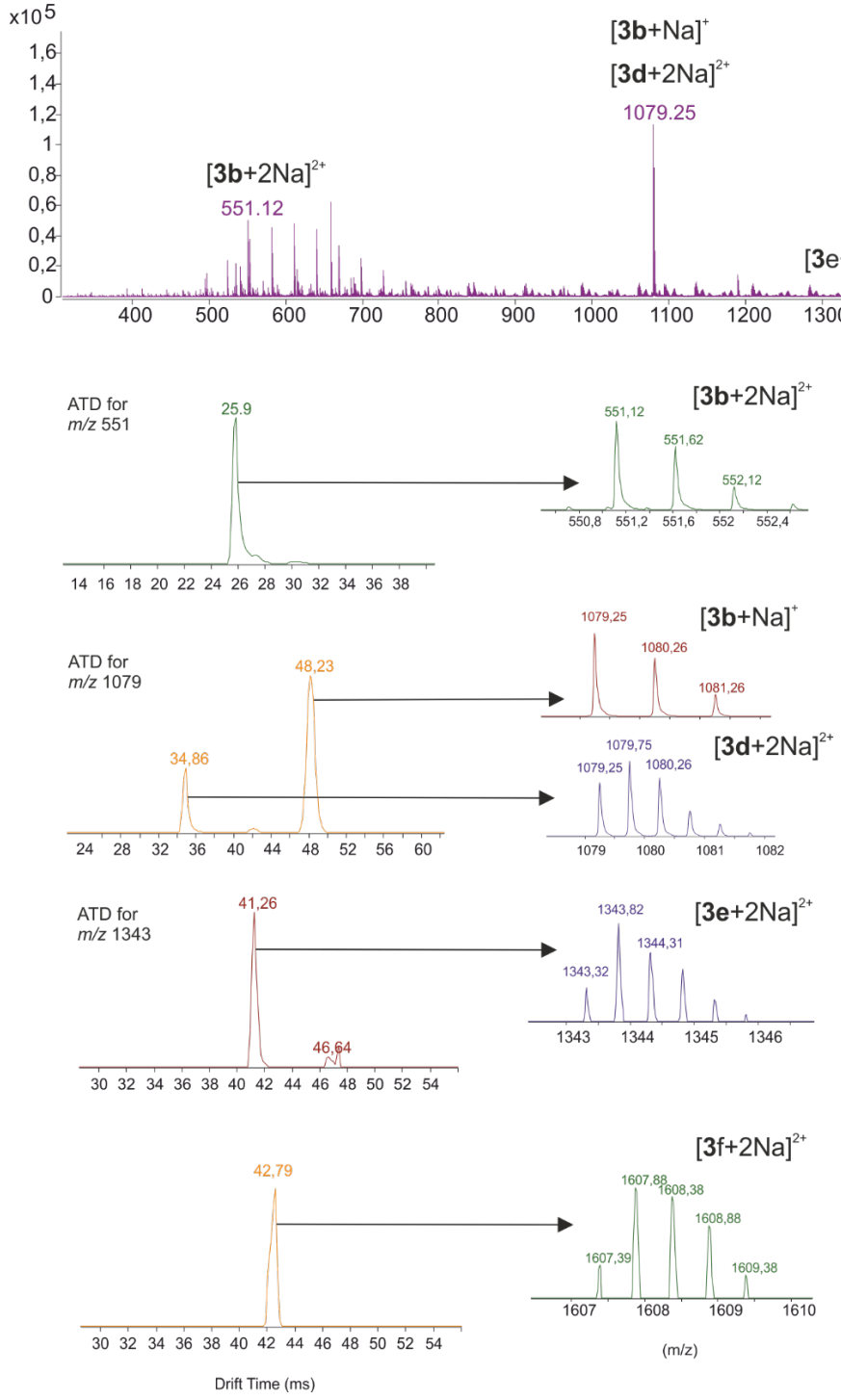

Figure S10. ESI-MS mass spectrum for **A6** and IM-MS arrival time distributions (ATDs) for different ions. Multiple peaks in ATDs correspond to different, overlapping ions. Zoomed views for MS spectra are extracted from each of the peaks to verify their identity and to compare the abundance.

DOSY analysis of the reaction method A with 6 equiv. of Cs_2CO_3 base

The DOSY analysis of the azobenzene region of the reaction method **A** with 6 equiv. of Cs_2CO_3 base is brought below. The spectrum was illustrated and analyzed with MNova and is depicted in Figure S11. The results of the found macrocycles with the external standards extracted from TopSpin are listed in Table S5.

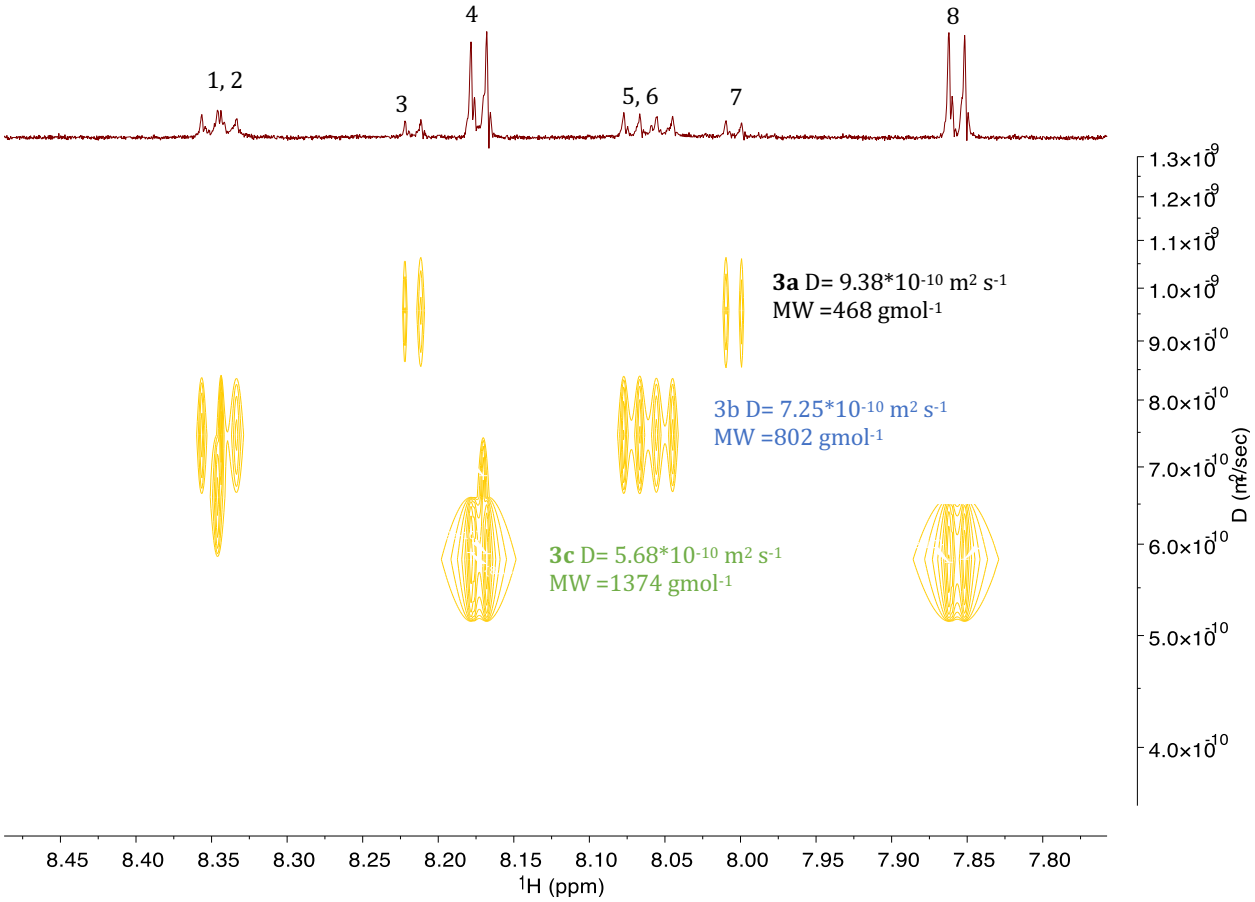

Figure S11. DOSY spectrum of work-up of the reaction method **A** with 6 equiv. of Cs_2CO_3 base illustrated with MNova.

Table S5. DOSY Analysis with TopSpin of the Work-up the Reaction Method **A** with 6 Equiv. of Cs_2CO_3 Base

	1	2	3	4	5	6	7	8
ppm	8.35-8.34	8.34-8.33	8.22-8.21	8.18-8.17	8.08-8.05	8.05-8.05	8.01-8.00	7.86-7.85
D	4.184E-10	4.716E-10	4.447E-10	4.186E-10	4.263E-10	4.263E-10	4.945E-10	4.496E-10
log D	-9.38	-9.33	-9.35	-9.38	-9.37	-9.37	-9.31	-9.35
Y	3.21	3.12	3.16	3.21	3.20	3.20	3.08	3.16
calc MW	1625.0	1314.3	1458.5	1623.6	1572.0	1572.0	1208.3	1430.5
Macrocycle	4+4	3+3	3+3	4+4	4+4	4+4	3+3	4+4

Reaction Method B

Synthetic procedure of the reaction B: Dropping one reactant (1)

In a 3-neck round bottom flask equipped with 3 Å molecular sieves, n equiv. of Cs_2CO_3 (n= 2, 4, 6, 8) and 1 equiv. of 4,4-diaazene-1,2-diyl)dibenzoyl)chloride were stirred in 12 mL THF for 5 minutes. Afterwards, 1 equiv. of 3,3'-(1,3-phenylenebis(oxy))diphenol was dissolved in 6 mL THF and added dropwise over 1 h to the solution. The solution was stirred at RT under argon atmosphere and reaction progress was monitored with ^{1}H NMR, similarly to as described in reaction method **A**, after 3, 5, 7, 24 h until the reaction was complete (up to 7 days). After the reaction was complete, the mixture was filtered and washed with 5 mL THF and the solvent was evaporated. The mixture was extracted (see methods) and evaporated to give 27% (4 equiv.) and 92% (6 equiv.) conversion to the macrocycles.

Reaction monitoring of the reaction B with different base equivalents

Smaller base equivalents and short reaction times (2 equiv. in red) led to the formation of oligomers.

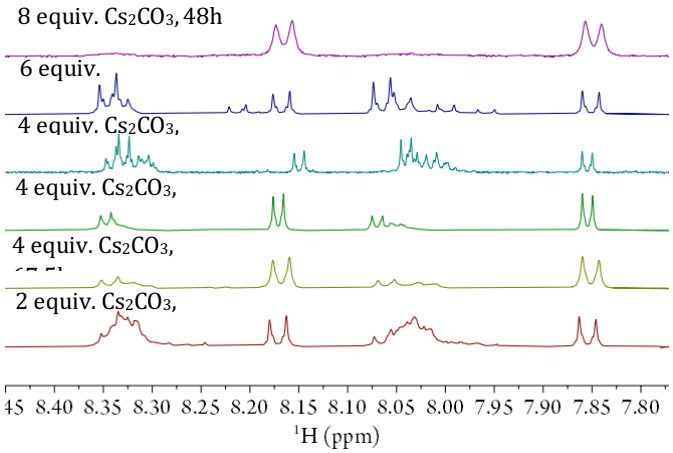

Figure S12. Monitoring of all different equiv. of base used in reaction method **B**.

Characterization of the work-up mixtures obtained from B

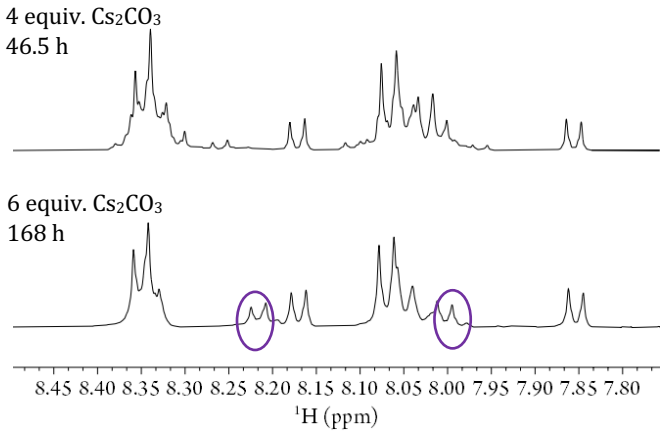

Figure S13. ^{1}H NMR azobenzene region of the reaction method **B** with 4 (above) and 6 (below) equiv. of Cs_2CO_3 base for the work-up phases.

NMR spectra and analysis from reaction B

NMR spectrum of the 4 equivalent reaction **B**

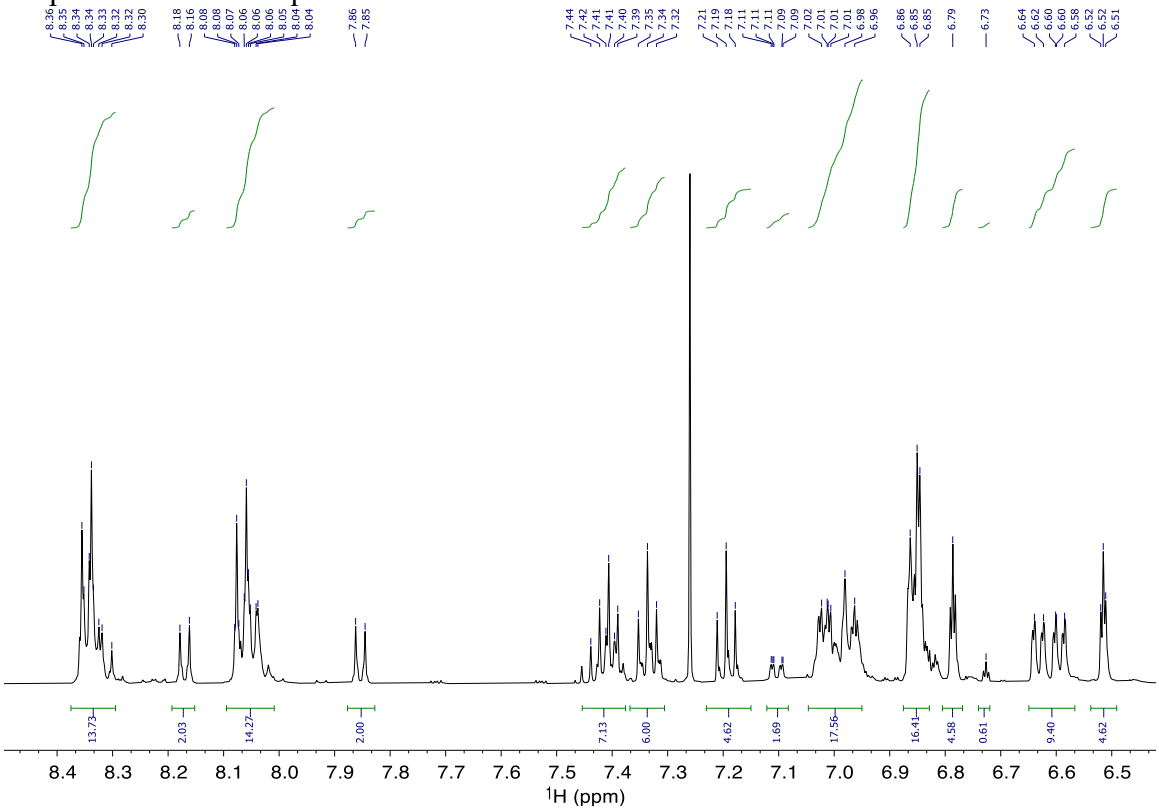

Figure S14. ^{1}H NMR of the work-up of the reaction method **B** with 4 equiv. of Cs_2CO_3 base.

^{1}H NMR (500 MHz, $CDCl_3$) δ 8.34 (m, *J* = 1.5, 2.0, 3.0 Hz, 14H), 8.17 (d, *J* = 8.5 Hz, 2H), 8.09 – 8.01 (m, *J* = 1.5, 2.0, 3.0 Hz, 14H), 7.85 (d, *J* = 8.5 Hz, 2H), 7.45 – 7.38 (m, *J* = 8.0, Hz 7H), 7.34 (t, *J* = 8.5 Hz, 6H), 7.19 (t, *J* = 8.0 Hz, 5H), 7.12 – 7.08 (m, *J* = 1.5, 2H), 7.05 – 6.95 (m, *J* =5.0, 9.0, 18H), 6.88 – 6.83 (m, *J* = 6.0, 16H), 6.79 (s, 5H), 6.73 (s, 1H), 6.65 – 6.57 (dddd, *J* = 8.0, 9H), 6.52 (t, *J* = 2.5 Hz, 5H).

4 equiv. (Table 1, entry 3): HRMS, ESI: **3b (2+2)** m/z calc. for. $C_{64}H_{40}N_4O_{12}$ $[M+2Na]^{2+}$ = 551.1214 found 551.1216; m/z calc. for $[M+Na]^+$ 1079.2535 found 1079.2535; m/z calc. for $[M+Cs]^+$ 1189.1692 fond 1189,1690; **3c (3+3)** m/z calc. for $C_{96}H_{60}N_6O_{18}$ $[M+3Na]^{3+}$ 1079.2535 found 1079.2535 and $[M+3Cs]^{3+}$ 1189.1692 fond 1189.1690; **3d** (4+4) m/z calc. for $C_{128}H_{80}N_8O_{24}$ $[M+2Na]^{2+}$ 1079.2535 found 1079.2535; m/z calc. for $[M+2Cs]^{2+}$ 1189.1692 fond 1189.1690; **3f** (6+6) m/z calc. for $C_{192}H_{120}N_{12}O_{36}$ $[M+2Na]^{2+}$ 1607.3856 found 1607.3813; m/z calc. for $[M+2Cs]^{2+}$ 1717.3013 fond 1717.3004.

DOSY NMR: D= 6.77 10^{-10} m^2 s^{-1}, MW= 932 g mol^{-1} (MNova) and D= 5.17 10^{-10} m^2 s^{-1}, MW= 1116 g mol^{-1} (TopSpin) for **3b**, D= 5.50*10^{-10} m^2 s^{-1} MW =1477 $gmol^{-1}$(Mnova) for **3c,** D= 4.39 10^{-10} m^2 s^{-1}, MW= 2494 g mol^{-1} (MNova) and D= 3.78 10^{-10} m^2 s^{-1}, MW= 1945 g mol^{-1} (TopSpin)

for **3d**, D= 3.95*10^{-10} m^2 s^{-1} MW =3204 gmol^{-1} (Mnova) for **3f** and D= 3.54*10^{-10} m^2 s^{-1} MW =4180gmol^{-1} (Mnova) for **3g.**

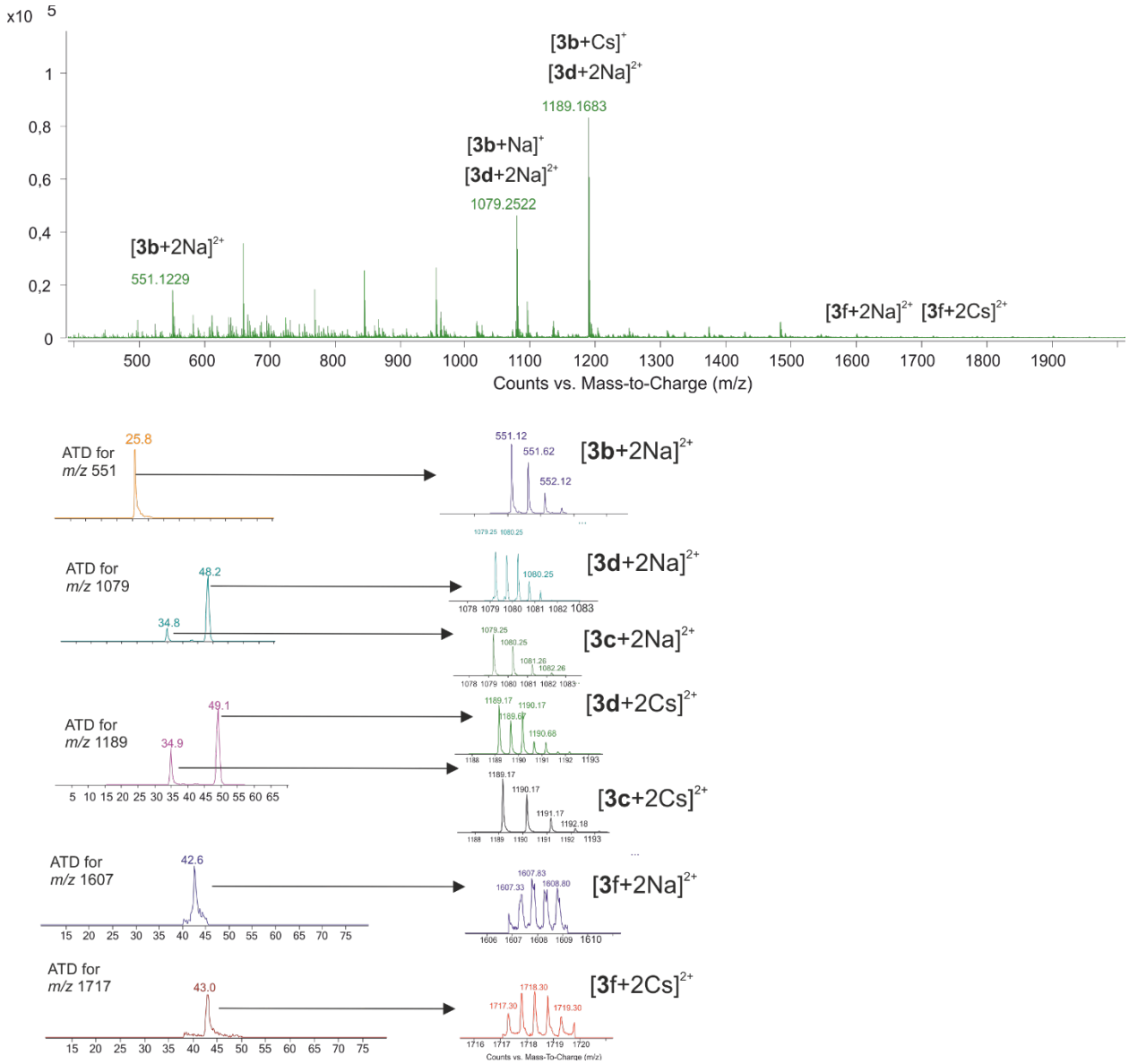

Figure S15. ESI-MS mass spectrum for **B4** (entry 3) and IM-MS arrival time distributions (ATDs) for different ions. Multiple peaks in ATDs correspond to different, overlapping ions. Zoomed views for MS spectra are extracted from each of the peaks to verify their identity and to compare the abundance.

DOSY Analysis of 4 equivalent reaction B

The DOSY analysis of the azobenzene region of the reaction method **B** with 4 equiv. of Cs_2CO_3 base is brought below. The spectrum was illustrated and analyzed with MNova and is depicted in Figure S16. The results of the found macrocycles with the external standards extracted from TopSpin are listed in Table S6.

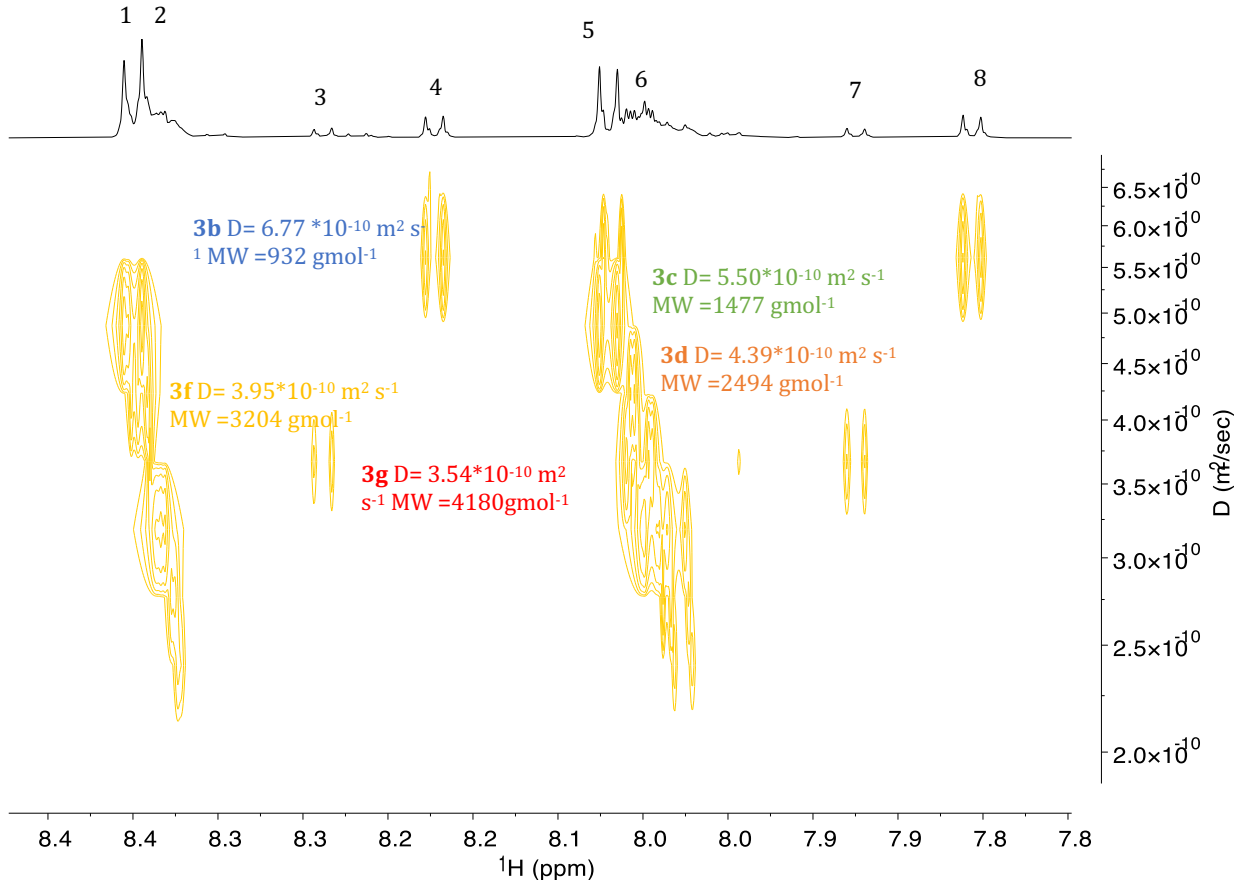

Figure S16. DOSY spectrum of the work-up of the reaction method **B** with 4 equiv. of Cs_2CO_3 base illustrated with MNova.

Table S6. TopSpin Analysis of the Work-up of the Reaction Method **B** with 4 equiv. of Cs_2CO_3 Base

	1	2	3	4	5	6	7	8
ppm	8.35-8.34	8.34-8.33	8.22-8.21	8.18-8.17	8.08-8.05	8.05-8.05	8.01-8.00	7.86-7.85
D	4.519E-10	4.519E-10	3.781E-10	4.835E-10	5.172E-10	3.856E-10	3.052E-10	4.799E-10
log D	-9.34	-9.34	-9.42	-9.32	-9.29	-9.41	-9.52	-9.32
Y	3.15	3.15	3.29	3.10	3.05	3.27	3.45	3.11
calc MW	1417.6	1417.6	1944.7	1257.5	1115.9	1878.1	2843.0	1274.2
Macrocycle	3+3	3-3	4+4	2+2	2+2	4+4	6+6	2+2

NMR data of the reaction method **B** with 6 equiv. of Cs_2CO_3 base

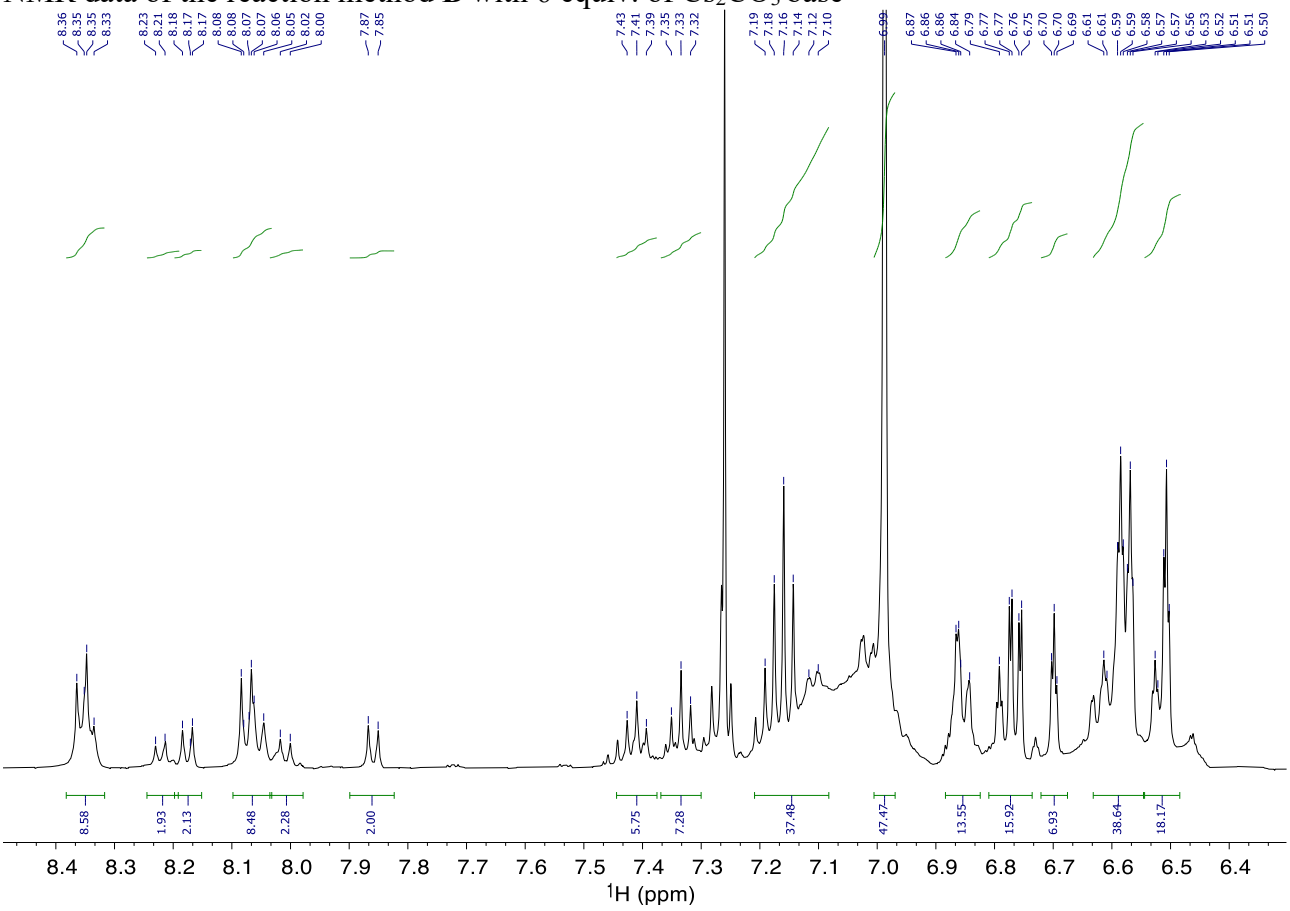

Figure S17. ^{1}H NMR of the reaction method **B** with 6 equiv. of Cs_2CO_3 base acquired in toluene-d_8.

^{1}H NMR (500 MHz, $CDCl_3$) δ 8.35 (dd, *J* = 8.5, 8.0, 9H), 8.22 (d, *J* = 8.0 Hz, 2H), 8.18 (d, *J* = 8.5 Hz, 2H), 8.06 (dd, *J* = 8.5, 8.0 Hz, 9H), 8.01 (d, *J* = 8.0 Hz, 2H), 7.86 (d, *J* = 8.5 Hz, 2H), 7.41 (t, *J* = 8.0 Hz, 6H), 7.33 (t, *J* = 8.5 Hz, 8H), 7.21 – 7.08 (m, *J* = 8.5 Hz, 38H), 6.99 (s, 48H), 6.88 – 6.82 (m, *J* = 2.5, 1.5 Hz, 14H), 6.81 – 6.74 (m, *J* = 2.5 Hz, 16H), 6.70 (t, *J* = 2.5 Hz, 7H), 6.63 – 6.55 (m, *J* = 8.0Hz, 39H), 6.54 – 6.48 (m, *J* = 2.5 Hz, 19H).

Characterization: 6 equiv. (Table 1, entry 4): HRMS, ESI$^+$: **3b** (2+2) m/z calc. for $C_{64}H_{40}N_4O_{12}$ $[M+2Na]^{2+}$ 551.1214 found 551.1214; m/z calc. for $[M+Na]^+$ 1079.2535 found 1079.2530; m/z calc. for $[M+Cs]^+$ 1189.1692 fond 1189,1696; **3d** (4+4) m/z calc. for $C_{128}H_{80}N_8O_{24}$ $[M+2Na]^{2+}$ 1079.2535 found 1079.2530; m/z calc. for $[M+2Cs]^{2+}$ 1189.1692 fond 1189.1696.

DOSY NMR: D= 817 10^{-10} m^2 s^{-1}, MW= 496.1 g mol^{-1} (MNova) for **3a**, D= 6.15 10^{-10} m^2 s^{-1}, MW= 1152 g mol^{-1} (MNova) and D= 5.80 10^{-10} m^2 s^{-1}, MW= 911 g mol^{-1} (TopSpin) for **3b**, D= 5.48*10^{-10} m^2 s^{-1} MW =1492 gmol^{-1} (Mnova) for **3c**, D= 4.85 10^{-10} m^2 s^{-1}, MW= 1969 g mol^{-1} (MNova) and D= 3.69 10^{-10} m^2 s^{-1}, MW= 2035 g mol^{-1} (TopSpin) for **3d,** D= 4.31 10^{-10} m^2 s^{-1}, MW= 2604 g mol^{-1} (MNova) and D= 3.07 10^{-10} m^2 s^{-1}, MW= 2861 g mol^{-1} (TopSpin) for **3f**.

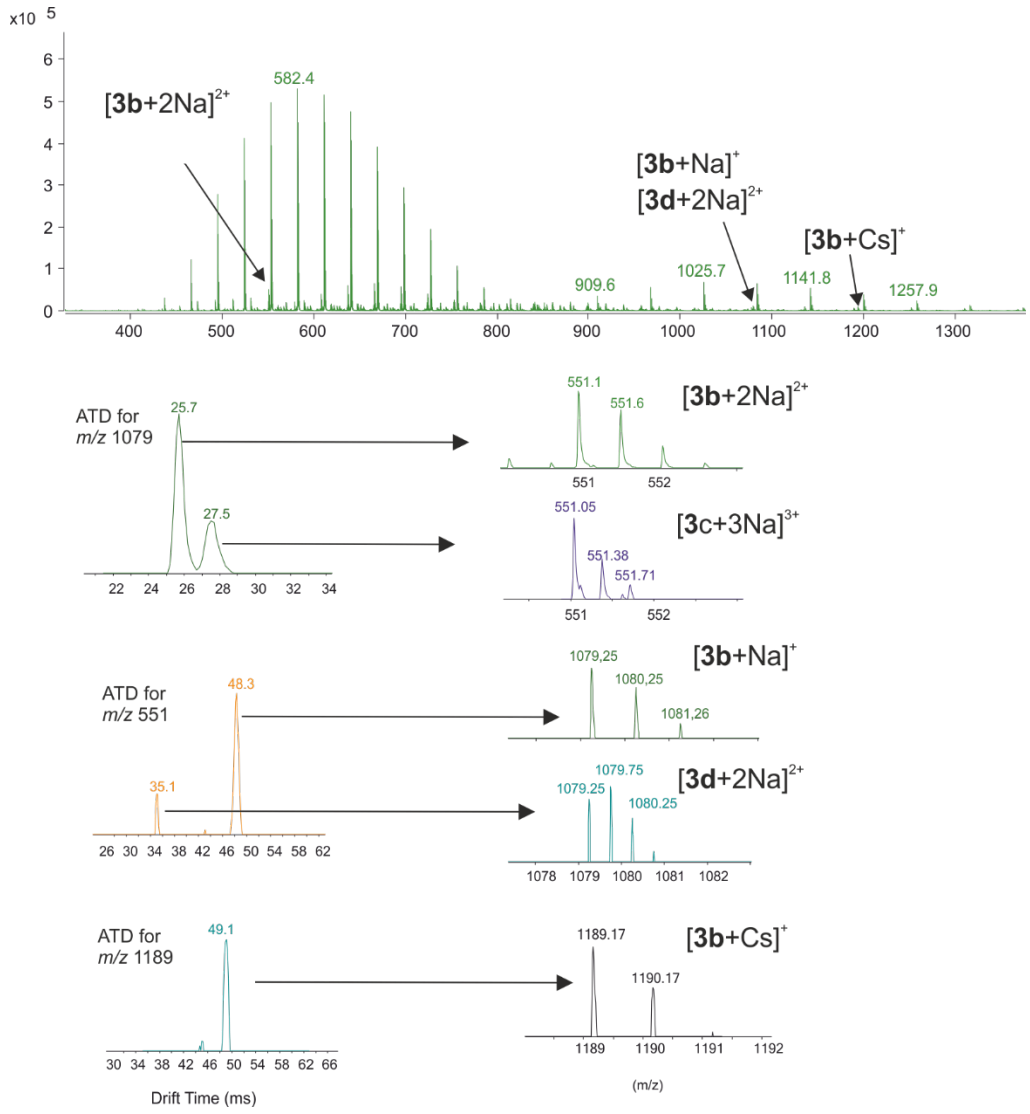

Figure S18. ESI-MS mass spectrum for **B6** (entry 4) and IM-MS arrival time distributions (ATDs) for different ions. Multiple peaks in ATDs correspond to different, overlapping ions. Zoomed views for MS spectra are extracted from each of the peaks to verify their identity and to compare the abundance.

DOSY Analysis of 6 equivalent reaction B

The DOSY analysis of the azobenzene region of the reaction method **B** with 6 equiv. of Cs_2CO_3 base is brought below. The spectrum was illustrated and analyzed with MNova and is depicted in Figure S19. The results of the found macrocycles with the external standards extracted from TopSpin are listed in Table S7.

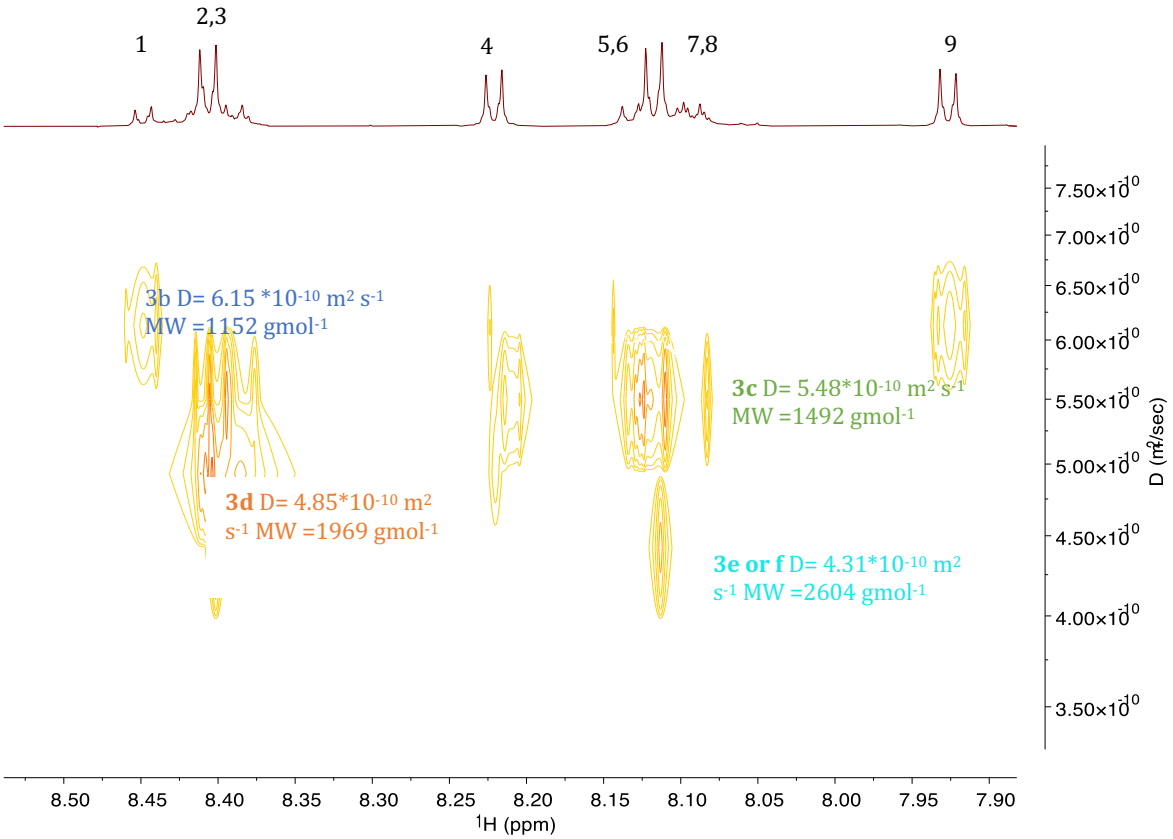

Figure S19. DOSY spectrum of the work-up for the reaction method **B** with 6 equiv. of Cs_2CO_3 base illustrated with MNova. Since the solvent in this spectraum ($CDCl_3$) differs from the one in the ^1H spectra in toluene-d_8 above, somewhat different isomer peaks and ppm shifts were observed in the direct dimension in comparison to Table 7.

Table S7. TopSpin Analysis of the Work-Up of the Reaction Method **B** with 6 Equiv. of Cs_2CO_3 Base

	1	2	3	4	5	6	7	8	9
ppm	8.35-8.34	8.34-8.33	8.22-8.21	8.21-8.20	8.18-8.16	8.08-8.07	8.05-8.04	8.01-7.99	7.98-7.97
D	5.8E-10	8.17E-10	5.969E-10	3.685E-10	4.677E-10	4.843E-10	3.685E-10	3.559E-10	3.068E-10
log D	-9.24	-9.09	-9.22	-9.43	-9.33	-9.31	-9.43	-9.45	-9.51
Y	2.96	2.70	2.94	3.31	3.13	3.10	3.31	3.34	3.45
calc MW	910.7	496.1	865.5	2035.4	1333.8	1253.8	2035.4	2164.9	2816.8
Macrocycle	2+2	1+1	2+2	4+4	3+3	3+3	4+4	4+4	6+6

Reaction Method C

Synthetic procedure for C: Dropping both reactants (1 and 2)
In a 3-neck round bottom flask equipped with 3 Å molecular sieves, n equiv. of Cs_2CO_3 (n= 4, 6) were dissolved in 10 mL THF and stirred at RT under argon atmosphere for 5 minutes. Two dropping funnels, one with 1 equiv. of 3,3'-(1,3-phenylenebis(oxy))diphenol (35.00 mg, 118.9 μmol) dissolved in 6 mL THF and one with 1 equiv. of 4,4-diaazene-1,2-diyl)dibenzoyl)-chloride (36.53 mg, 118.9 μmol) in 6 mL THF were connected and the reactants were added dropwise over 15-20 min. to the reaction mixture. The mixture was stirred at RT under argon atmosphere and reaction progress was monitored with ^{1}H NMR, similarly to as described above, after 1, 3, 5, 7, 24 h until the reaction was complete (up to 4 days). After the reaction was complete, the mixture was filtered and washed with 5 mL THF and the solvent was evaporated and extracted. The mixture was dried under vacuum to give 37.7 mg (60%; 4 equiv.) and 26.9 mg (43%; 6 equiv.), respectively, as a red-orange powder.

Reaction monitoring of the reaction C with different base equivalents
The broad main peaks for 4 equiv. of base can be assigned to oligomeric species, whereas in the 6 equiv. reaction sharp signals appear. Reaction monitoring of both of the reactions **C** after the same reaction time (24h), showed that the higher amount of base accelerated the ring closing reaction, contrary to the reaction method **A**, where the 4 equiv. reaction showed faster macrocyclisation.

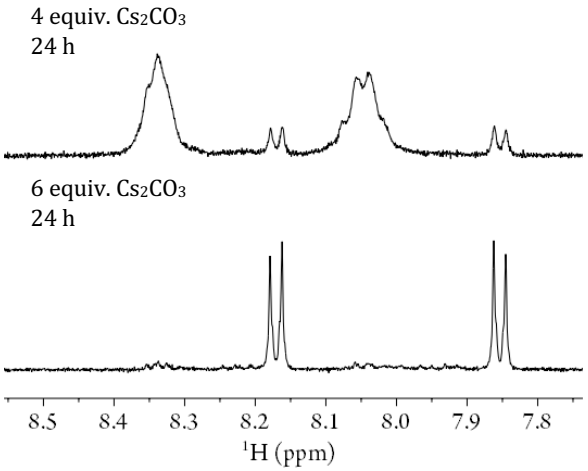

Figure S20. Reaction monitoring of the reaction **C** after 24 h of the 4 equiv. (above) and 6 equiv. (below) of Cs_2CO_3 base.

Characterization of the work-up mixtures obtained from C
As a result, it could be observed that longer reaction times and slow reactant addition result in higher overall conversion (98 h vs. 49 h).

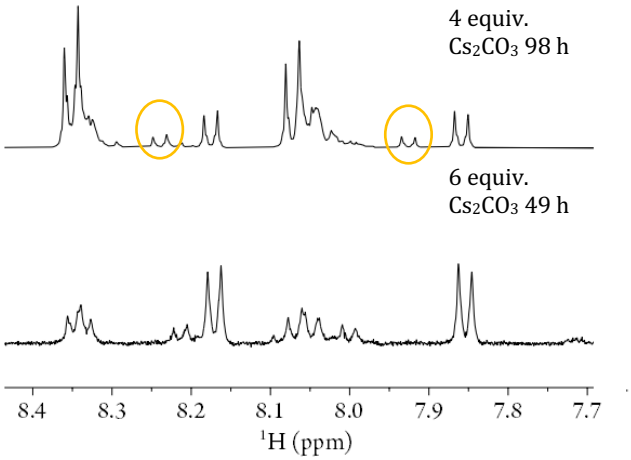

Figure S21. ^{1}H NMR azobenzene region of the reaction method **C** with 4 (above) and 6 (below) equiv. of Cs_2CO_3 base .

NMR spectra and analysis from reaction C

NMR data of the reaction method **C** with 4 equiv. of Cs_2CO_3 base

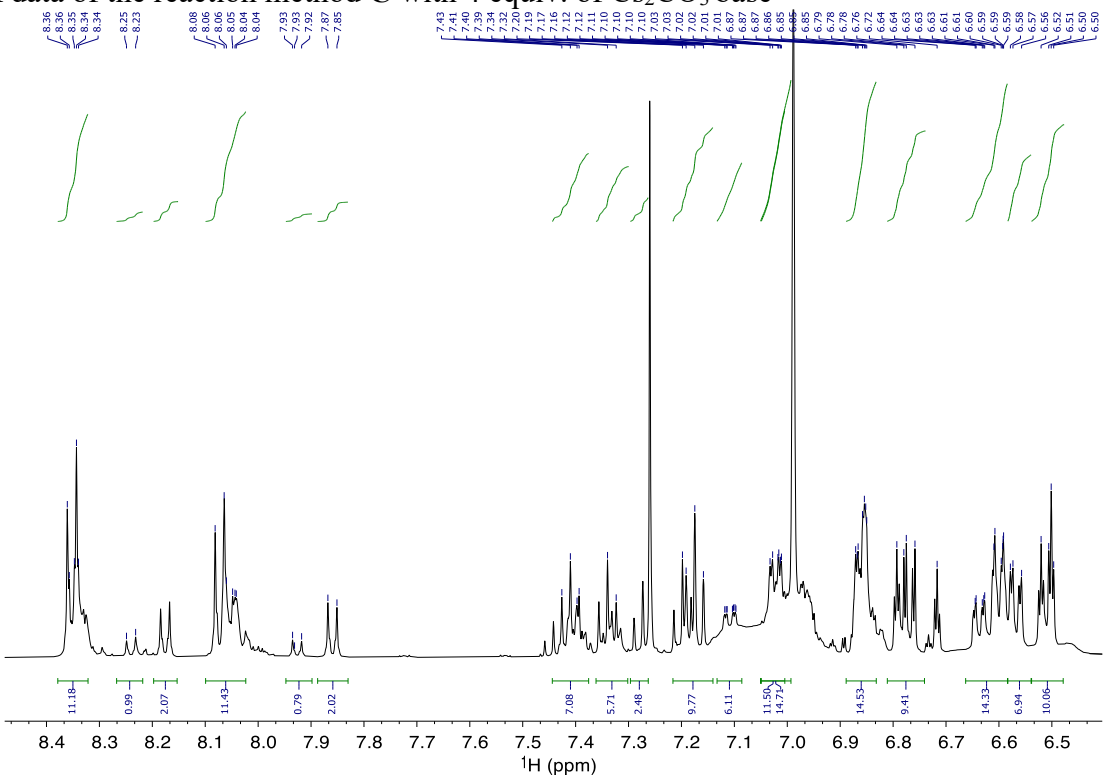

Figure S22. ^{1}H NMR of the work-up of the reaction method **C** with 4 equiv. of Cs_2CO_3 base.

^{1}H NMR (500 MHz, $CDCl_3$) δ 8.36 – 8.32 (m, *J* = 10.5, 6.0, 11H), 8.24 (d, *J* = 8.5 Hz, 1H), 8.20 – 8.16 (d, , *J* = 8.5, 2H), 8.08 – 8.03 (m, *J* = 10.5, 6.0, 11H), 7.93 (d, *J* = 8.5 Hz, 1H), 7.86 (d, *J* =

8.5 Hz, 2H), 7.44 – 7.36 (m, *J* = 8.0, 7H), 7.33 (d, *J* = 8.5 Hz, 6H), 7.23 – 7.13 (m, *J* = 3.5, 10H), 7.12– 7.08 (dddd, *J* = 2.0, 2.5, 6H), 7.07 – 7.01 (m, *J* = 2.0, 1.5, 12H), 6.90 – 6.83 (m, *J* = 2.5, 2.0, 15H), 6.78 (dd, *J* = 2.5, 2.0 Hz, 1H), 6.72 (t, *J* = 1.5, 3H), 6.65 – 6.55 (m, *J* = 8.0, 20H), 6.53 – 6.49 (m, *J* = 7.5, 10H)

Characterization: 4 equiv. (Table 1, entry 5): HRMS, ESI^+: **3b** (2+2) m/z calc. for $C_{64}H_{40}N_4O_{12}$ $[M+2Na]^{2+}$ 551.1214 found 551.1222; m/z calc. for $[M+Na]^+$ 1079.2535 found 1079.2534*;* m/z calc. for $[M+Cs]^+$ 1189.1692 fond 1189.1689*;* **3d** (4+4) $C_{128}H_{80}N_8O_{24}$ $[M+2Na]^{2+}$ 1079.2535 found 1079.2534*;* m/z calc. for $[M+2Cs]^{2+}$ 1189.1692 fond 1189.1689; **DOSY NMR:** D= 6.53 10^{-10} m^2 s^{-1}, MW= 1009 g mol^{-1} (MNova) for **3b,** D= 5.57 10^{-10} m^2 s^{-1}, MW= 1437 g mol^{-1} (MNova) and D= 4.17 10^{-10} m^2 s^{-1}, MW= 1633 g mol^{-1} (TopSpin) for **3c**, D= 4.75 10^{-10} m^2 s^{-1}, MW= 2067 g mol^{-1} (MNova) and D= 3.62 10^{-10} m^2 s^{-1}, MW= 2099 g mol^{-1} (TopSpin) for **3d**, D= 4.29*10^{-10} m^2 s^{-1} MW =2627 $gmol^{-1}$ (Mnova) for **3e** or **3f** and D= 3.61*10^{-10} m^2 s^{-1} MW =3977 $gmol^{-1}$(Mnova) for **3g.**

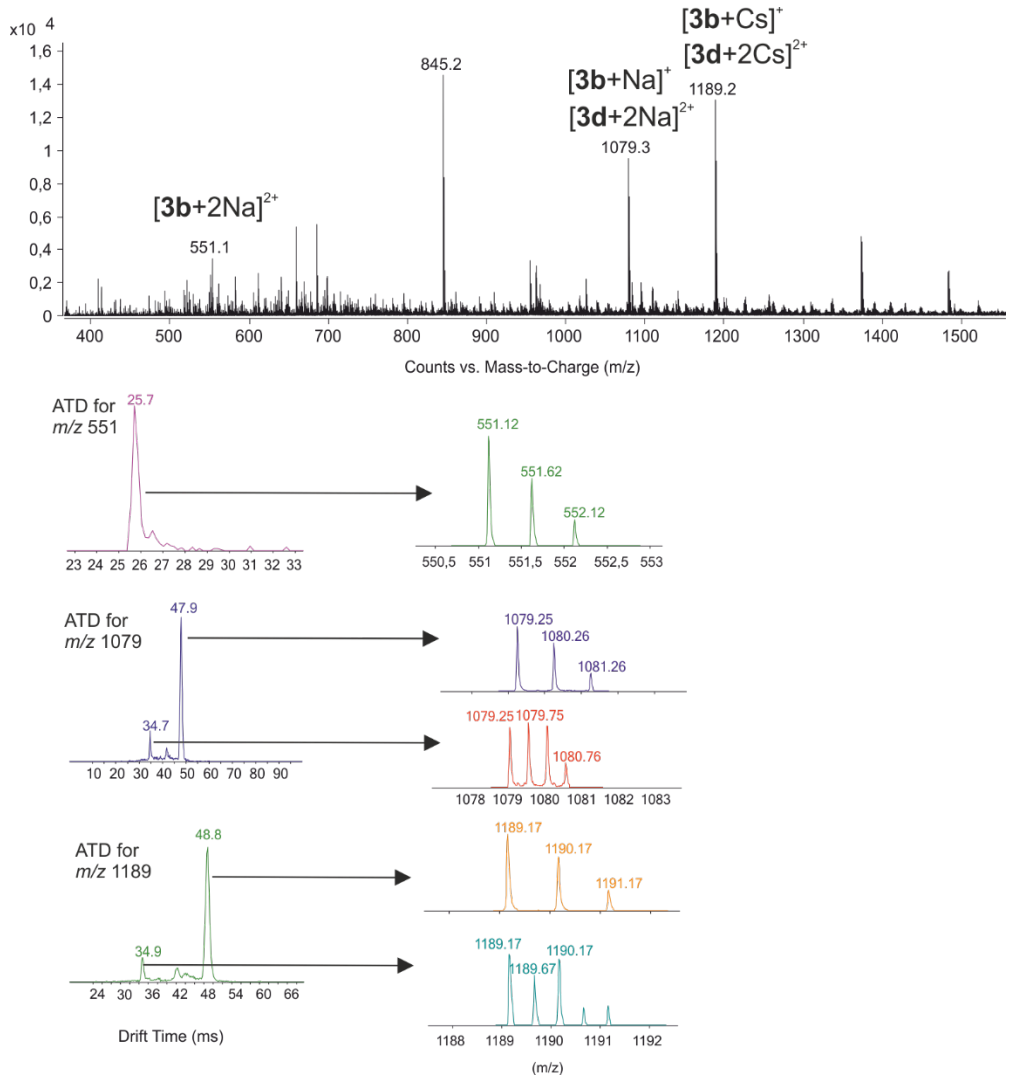

Figure S23. ESI-MS mass spectrum for **C4** (entry 5) and IM-MS arrival time distributions (ATDs) for different ions. Multiple peaks in ATDs correspond to different, overlapping ions. Zoomed views for MS spectra are extracted from each of the peaks to verify their identity and to compare the abundance.

DOSY Analysis of 4 equivalent reaction C

The DOSY analysis of the azobenzene region of the reaction method **C** with 4 equiv. of Cs_2CO_3 base is brought below. The spectrum was illustrated and analyzed with MNova and is depicted in Figure S24. The results of the found macrocycles with the external standards extracted from TopSpin are listed in Table S8.

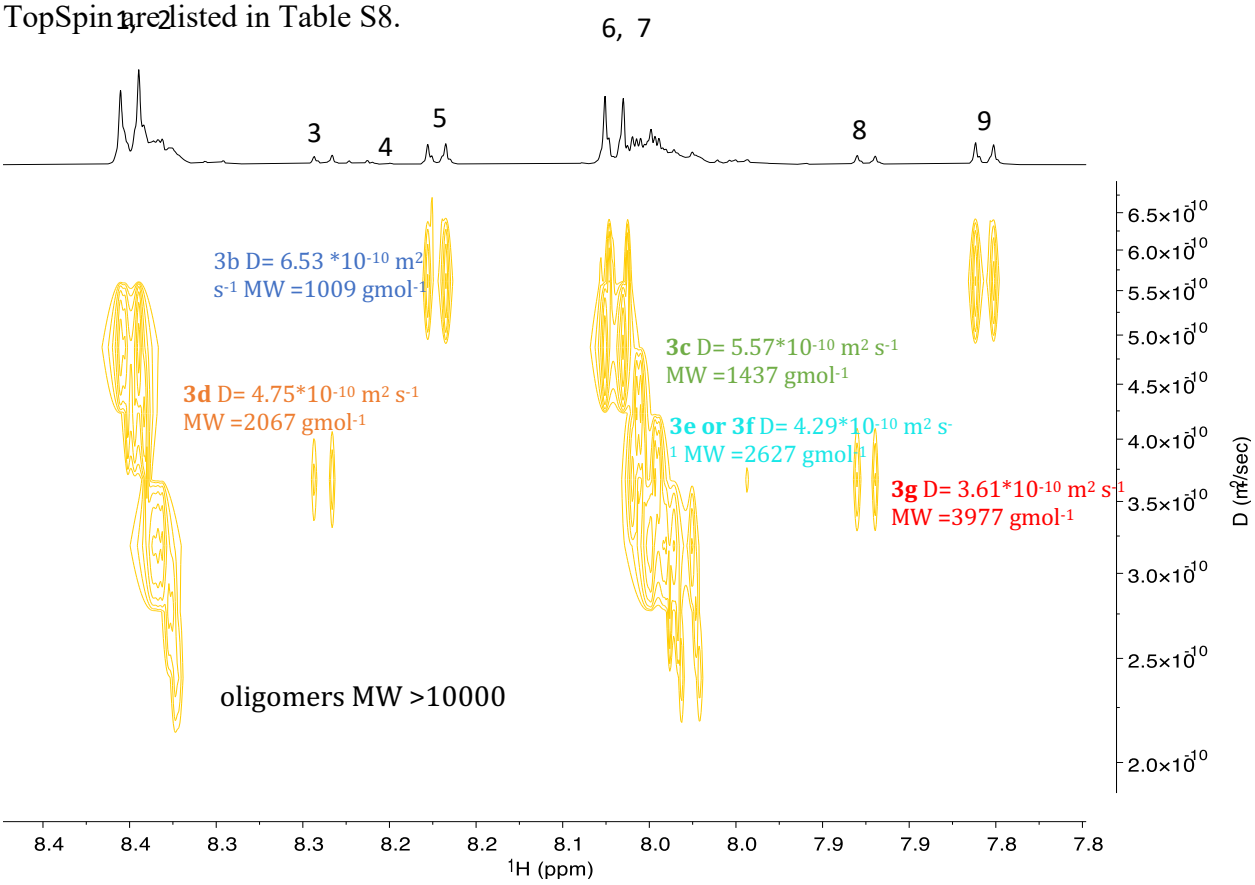

Figure S24. DOSY spectrum of work-up of the reaction method **C** with 4 equiv. of Cs_2CO_3 base illustrated with MNova. In this sample, small amounts oligomers with large molecular weights were formed.

Table S8. TopSpin Analysis of the Work-up of the Reaction Method **C** with 4 Equiv. of Cs_2CO_3 Base

	1	2	3	4	5	6	7	8	9
ppm	8.35-8.34	8.33-8.32	8.24-8.23	8.22-8.20	8.17-8.16	8.07-8.06	8.06-8.04	7.93-7.92	7.86-7.85
D	3.62E-10	2.39E-10	2.80E-10	4.16E-10	4.17E-10	4.08E-10	2.66E-10	2.82E-10	4.18E-10
log D	-9,44	-9,62	-9,55	-9,38	-9,38	-9,39	-9,58	-9,55	-9,38
Y	3,32	3,64	3,52	3,21	3,21	3,23	3,56	3,52	3,21
calc MW	2098.6	4376.2	3314.5	1639.6	1633.3	1702.1	3632.6	3279.1	1625.7
Macrocycle	4+4	oligomer	6+6	3+3	3+3	4+4	oligomer	6+6	3+3

NMR data of the reaction method **C** with 6 equiv. of Cs_2CO_3 base

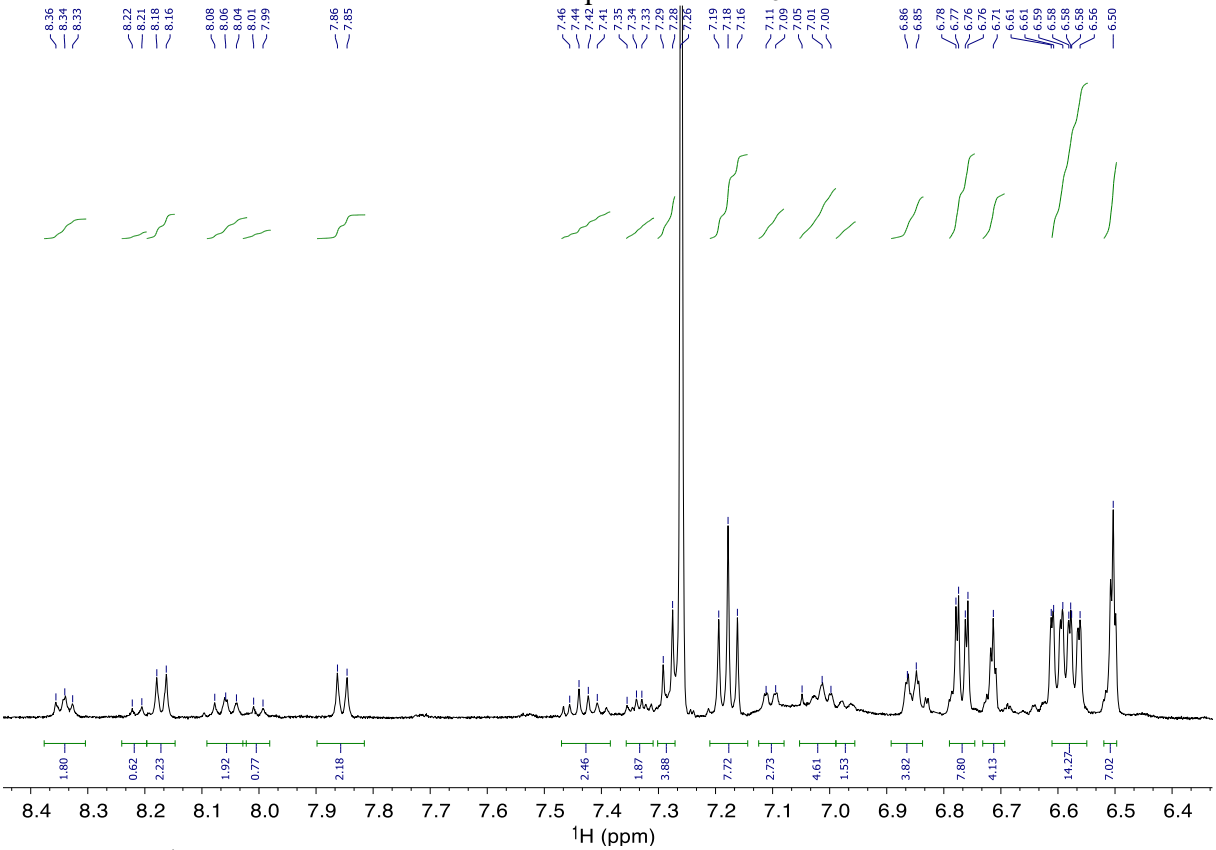

Figure S25. ^{1}H NMR of the reaction method **C** with 6 equiv. of Cs_2CO_3 base.

^{1}H NMR (500 MHz, $CDCl_3$) δ 8.34 (dd, *J* = 8.0, 6.5, Hz, 2H), 8.21 (d, *J* = 8.5 Hz, 1H), 8.17 (d, *J* = 8.5 Hz, 2H), 8.09 – 8.02 (dd, *J* = 8.0, 6.5 2H), 8.00 (d, *J* = 8.5 Hz, 1H), 7.85 (d, *J* = 8.5 Hz, 2H), 7.43 (m, *J* = 8.5 Hz, 2H), 7.36 – 7.31 (m, *J* = 8.0 Hz, 2H), 7.28 (d, *J* = 8.5 Hz, 4H), 7.18 (t, *J* = 8.0 Hz, 8H), 7.10 (d, *J* = 8.0 Hz, 3H), 7.05 – 6.99 (m, *J* = 7.5 Hz 5H), 6.97 (d, *J* = 8.5 Hz, 2H), 6.86 (d, *J* = 8.0 Hz, 4H), 6.77 (dd, *J* = 2.5, 2.0 Hz, 8H), 6.71 (s, 4H), 6.61 – 6.55 (dd, *J* = 2.5, 2.0 Hz, 14H), 6.50 (s, 7H).

Characterization: 6 equiv. (Table 1, entry 6): HRMS, ESI$^+$: **3b** (2+2) m/z calc. for $C_{64}H_{40}N_4O_{12}$ $[M+2Na]^{2+}$ 551.1214 found 551.1213; m/z calc. for $[M+Na]^+$ 1079.2535 found 1079.2518; m/z calc. for $[M+Cs]^+$ 1189.1692 fond 1189.1686 **3d** (4+4) m/z calc. for $C_{128}H_{80}N_8O_{24}$ $[M+2Na]^{2+}$ 1079.2535 found 1079.2518; m/z calc. for. $[M+2Cs]^{2+}$ 1189.1692 fond 1189.1686. **DOSY NMR:** D= 6.44 10^{-6} m^2 s^{-1}, MW= 1038 $gmol^{-1}$ (MNova) and D= 4.58 10^{-10} m^2 s^{-1}, MW= 1384 $gmol^{-1}$ (TopSpin) for **3b** , D= 4.58 10^{-6} m^2 s^{-1}, MW= 1384.3 (TopSpin) for **3c**. The found macrocycles deviate from the analysis with ESI-MS.

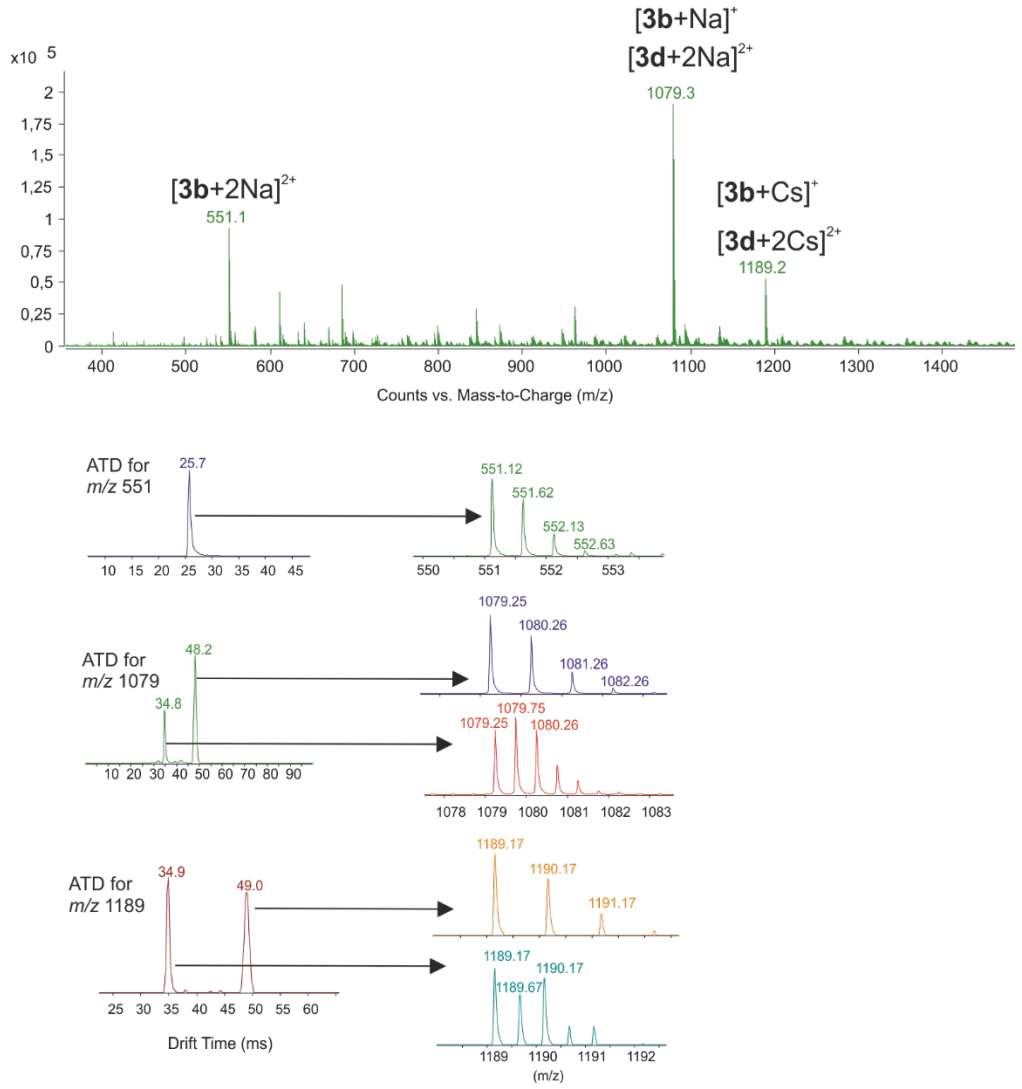

Figure S26. ESI-MS mass spectrum for **C6** (entry 6) and IM-MS arrival time distributions (ATDs) for different ions. Multiple peaks in ATDs correspond to different, overlapping ions. Zoomed views for MS spectra are extracted from each of the peaks to verify their identity and to compare the abundance.

DOSY analysis of reaction method C with 6 equiv. of Cs_2CO_3 base

The DOSY analysis of the azobenzene region of the reaction method **C** with 6 equiv. of Cs_2CO_3 base is brought below. The spectrum was illustrated and analyzed with MNova and is depicted in Figure S27. The results of the found macrocycles with the external standards extracted from TopSpin are listed in Table S9.

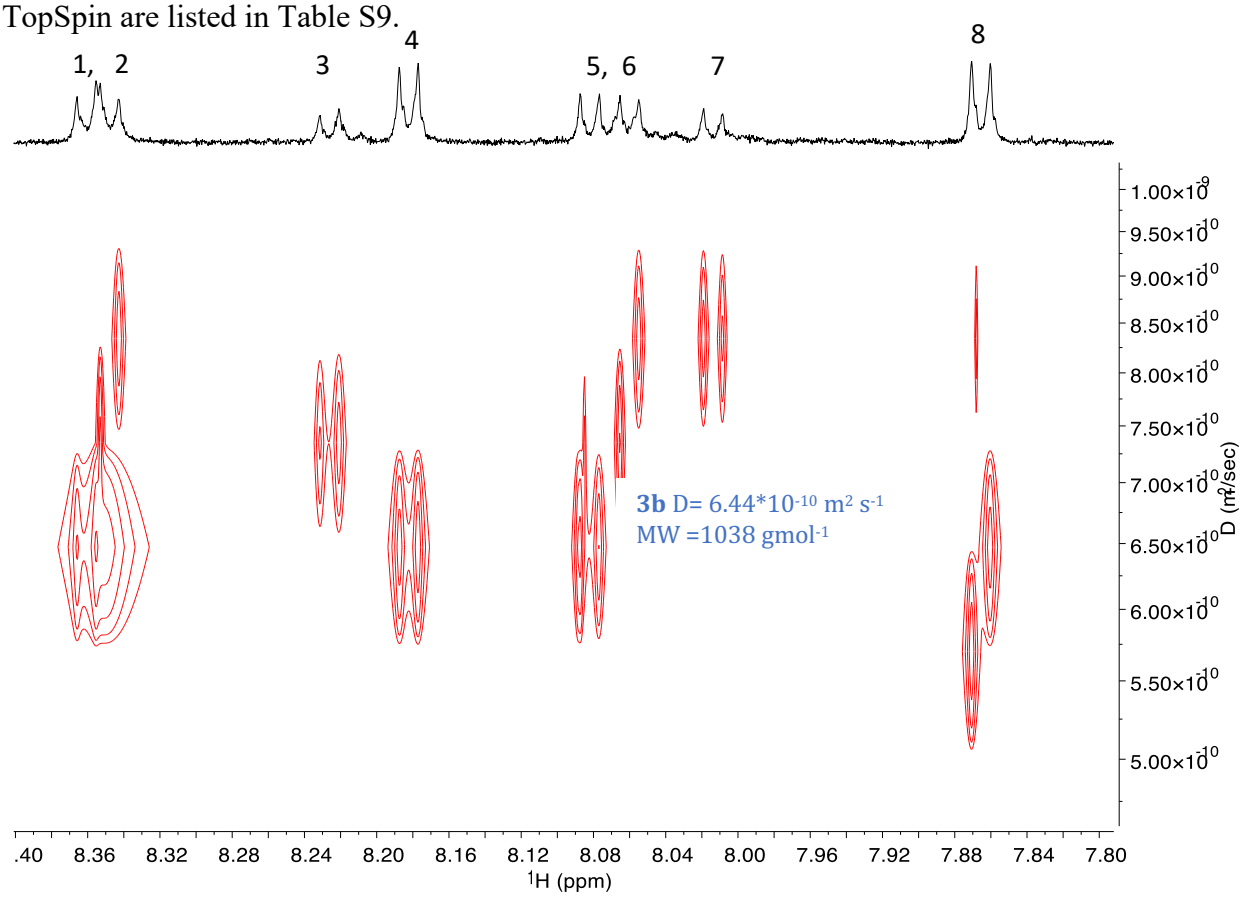

Figure S27. DOSY spectrum of work-up of the reaction method **C** with 6 equiv. of Cs_2CO_3 base illustrated with MNova.

Table S9. TopSpin Analysis of the Reaction Method **C** with 6 Equiv. of Cs_2CO_3 Base

	1	2	3	4	5	6	7	8
ppm	8.36-8.34	8.34-8.33	8.22-8.21	8.17-8.16	8.08-8.07	8.055-8.04	8.01-7.99	7.86-7.85
D	4.58E-10	4.58E-10	5.91E-10	4.63E-10	4.73E-10	4.619E-10	5.75E-10	4.59E-10
log D	-9.34	-9.34	-9.23	-9.33	-9.33	-9.34	-9.24	-9.34
Y	3.14	3.14	2.94	3.13	3.12	3.13	2.97	3.14
calc MW	1384.3	1384.3	880.6	1357.9	1307.9	1363.6	925.3	1381.1
Macrocycle	3+3	3+3	2+2	3+3	3+3	3+3	2+2	3+3

Reaction Method D

Synthetic procedure for D: One pot reaction and reflux

To a round bottom flask equipped with 3 Å molecular sieves n equiv. of Cs_2CO_3 (n= 4, 6), 1 equiv. of 4,4-diaazene-1,2-diyl)dibenzoyl)chloride and 1 equiv. of 3,3'-(1,3-phenylenebis(oxy))diphenol was added and stirred at RT under argon atmosphere. The reaction was refluxed at 80˚C for 7 h and then cooled to RT and stirred overnight under argon atmosphere. Reaction progress was monitored after 5, 7, 24 h with ^{1}H NMR, similarly to the previous reaction methods, until the reaction was complete (up to 29 h). After the reaction was complete, the mixture was filtered and washed with 5 mL THF and the solvent was evaporated. The conversion of 67% was reached after 26h in the presence of 4 equiv. of base and conversion of 75% was reached after 29h in the presence of 6 equiv. of base.

Reaction monitoring of the reaction D with different base equivalents

Reaction monitoring indicated that the reaction was complete after 5h of refluxing since the peaks did not change after that anymore. However, longer stirring at RT after refulxing led to higher conversions.

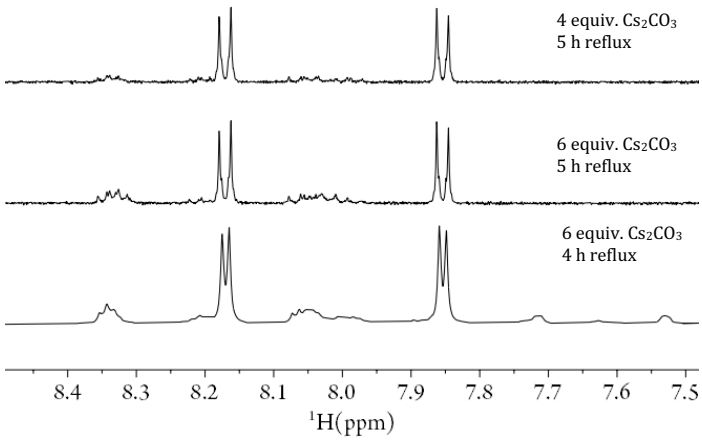

Figure S28. Reaction monitoring of the reaction **D** after 4 h and 5 h of refluxing, 4 equiv. (above spectrum) and 6 equiv. (middle and beneath) of Cs_2CO_3 base.

Characterization of the work-up mixtures obtained from D

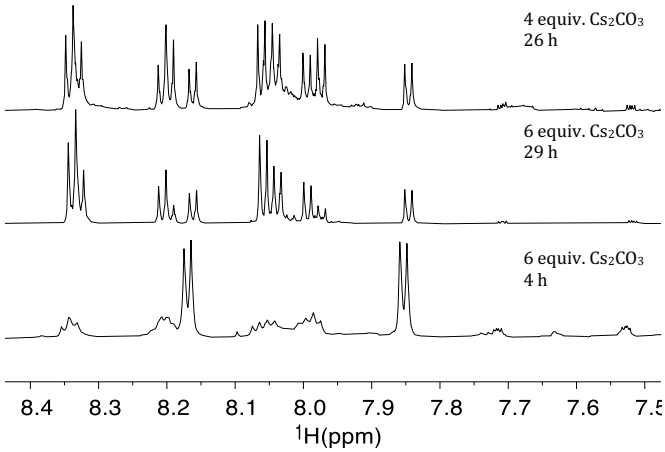

Figure S29. ^{1}H NMR azobenzene region of the reaction method **D** with 4 (above) and 6 (below) equiv. of Cs_2CO_3 base for the work-up phases.

NMR spectra and analysis from reaction D

NMR spectra of the reaction method **D** with 4 equiv. of Cs_2CO_3 base

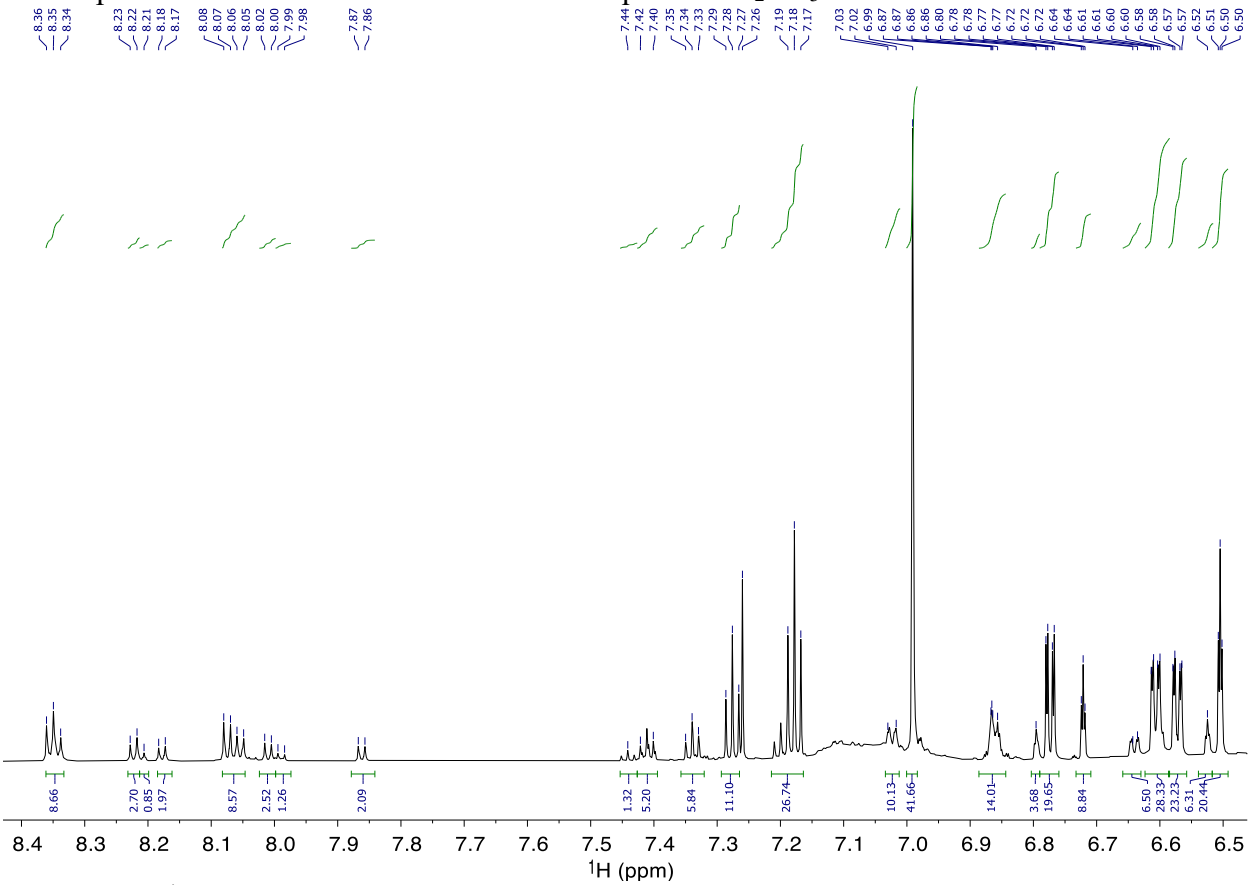

Figure S30. ^{1}H NMR of the work-up of the reaction method **D** with 4 equiv. of Cs_2CO_3 base.

^{1}H NMR (800 MHz, $CDCl_3$) δ 8.35 (dd, *J* = 8.8, 8.4 Hz, 9H), 8.22 (m, *J* = 8.0 Hz, 3H), 8.18 (d, *J* = 8.0 Hz, 2H), 8.08 – 8.05 (dd, *J* = 8.8, 8.4, Hz 9H), 8.01 (d, *J* = 8.0 Hz, 3H), 7.99 (d, *J* = 8.0 Hz, 1H), 7.86 (d, *J* = 8.0 Hz, 2H), 7.41 (t, *J* = 8.0 Hz, 5H), 7.36 – 7.32 (m, dd, *J* = 8.5 Hz, 6H), 7.18 (t, *J* = 8.0 Hz, 27H), 7.02 (m, *J* = 8.8 Hz, 10H), 6.99 (s, 42H), 6.89 – 6.84 (m, *J* = 8.8 Hz, 14H), 6.79 (m, *J* = 2.4, 4H), 6.77 (dd, *J* = 2.4, 2.4 Hz, 20H), 6.72 (t, *J* = 2.4 Hz, 9H), 6.64 (dd, *J* = 8.0, 8.0 Hz, 7H), 6.62 – 6.58 (dd, *J* = 2.4, 2.4 Hz, 28H), 6.57 (dd, *J* = 8.1, 2.3, 0.8 Hz, 23H), 6.52 (s, 6H), 6.50 (t, *J* = 2.4 Hz, 20H).

Characterization: 4 equiv. (Table 1, entry 7): HRMS, ESI$^-$ **3a** (1+1) m/z calc. for $C_{64}H_{40}N_4O_{12}$ $[M+Na]^+$ 551.1212 found 551.1224; **3b** (2+2) m/z calc. for $C_{64}H_{40}N_4O_{12}$ $[M+2Na]^{2+}$ 551.1214 found 551.1213; m/z calc. for $[M+Na]^+$ 1079.2535 found 1079.2520*;* m/z calc. for $[M+Cs]^+$ 1189.1692 fond 1189.1704; **3d** (4+4**)** m/z calc. for $C_{128}H_{80}N_8O_{24}$ $[M+2Na]^{2+}$ 1079.2535 found 1079.2520; **3e** (5+5) m/z calc. for $C_{160}H_{100}N_{10}O_{30}$ $[M+2Na]^{2+}$ 1343.3196 found 1343.3196; **DOSY NMR:** D= 6.47 10^{-10} m^2 s^{-1}, MW= 1034 g mol^{-1} (MNova) and D= 4.66 10^{-10} m^2 s^{-1}, MW= 1342 g mol^{-1} (TopSpin) for **3b** and D= 5.01 10^{-10} m^2 s^{-1}, MW= 1832 g mol^{-1} (MNova) and D= 3.79 10^{-10} m^2 s^{-1}, MW= 1940 g mol^{-1} (TopSpin) for **3d** and D= 3.34 10^{-10} m^2 s^{-1}, MW= 2420 g mol^{-1} (TopSpin) for **3e**.

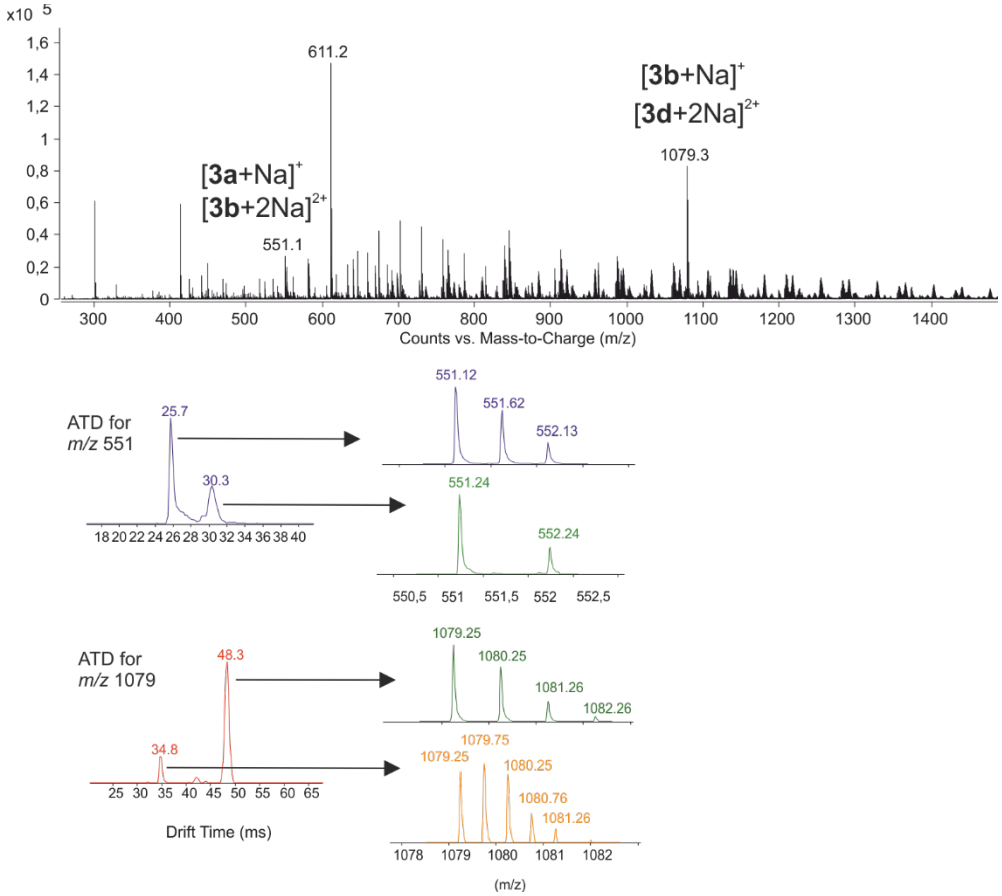

Figure S31. ESI-MS mass spectrum for **D4** (entry 7) and IM-MS arrival time distributions (ATDs) for different ions. Multiple peaks in ATDs correspond to different, overlapping ions. Zoomed views for MS spectra are extracted from each of the peaks to verify their identity and to compare the abundance.

DOSY analysis of the reaction method D with 4 equiv. of Cs_2CO_3 base

The DOSY analysis of the azobenzene region of the reaction method **D** with 4 equiv. of Cs_2CO_3 base is brought below. The spectrum was illustrated and analyzed with MNova and is depicted in Figure S32. The results of the found macrocycles with the external standards extracted from TopSpin are listed in Table S10.

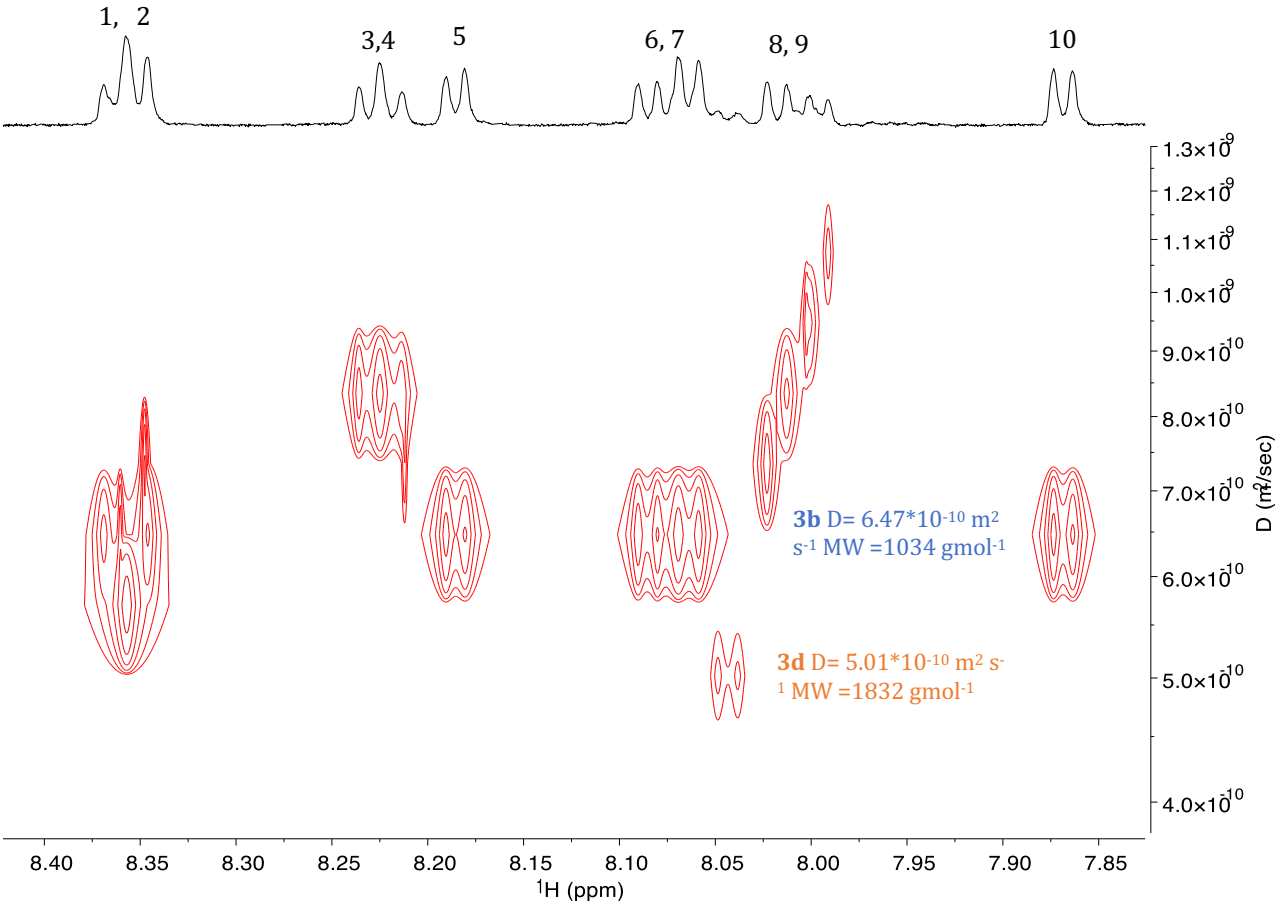

Figure S32. DOSY spectrum of work-up of the reaction method **D** with 4 equiv. of Cs_2CO_3 base illustrated with MNova.

Table S10. TopSpin Analysis of the Work-up of the Reaction Method **D** with 4 Equiv. of Cs_2CO_3 Base

	1	2	3	4	5	6	7	8	9	10
ppm	8.36-8.35	8.35-8.34	8.23-8.22	8.22-8.21	8.18-8.17	8.08-8.07	8.06-8.05	8.02-8.00	7.99-7.98	7.87-7.86
D	3.622E-10	3.861E-10	4.44E-10	4.166E-10	3.342E-10	3.807E-10	3.786E-10	4.347E-10	4.66E-10	3.579E-10
log D	-9.44	-9.41	-9.35	-9.38	-9.48	-9.42	-9.42	-9.36	-9.33	-9.45
Y	3.32	3.27	3.17	3.21	3.38	3.28	3.29	3.18	3.13	3.33
calc MW	2098.6	1873.8	1462.6	1637.5	2420.4	1921.2	1940.1	1518.5	1342.4	2143.5
Macrocycle	4+4	4+4	2+2	2+2	5+5	4+4	4+4	2+2	2+2	5+5

NMR spectra of the the reaction method D with 6 equiv. of Cs_2CO_3 base

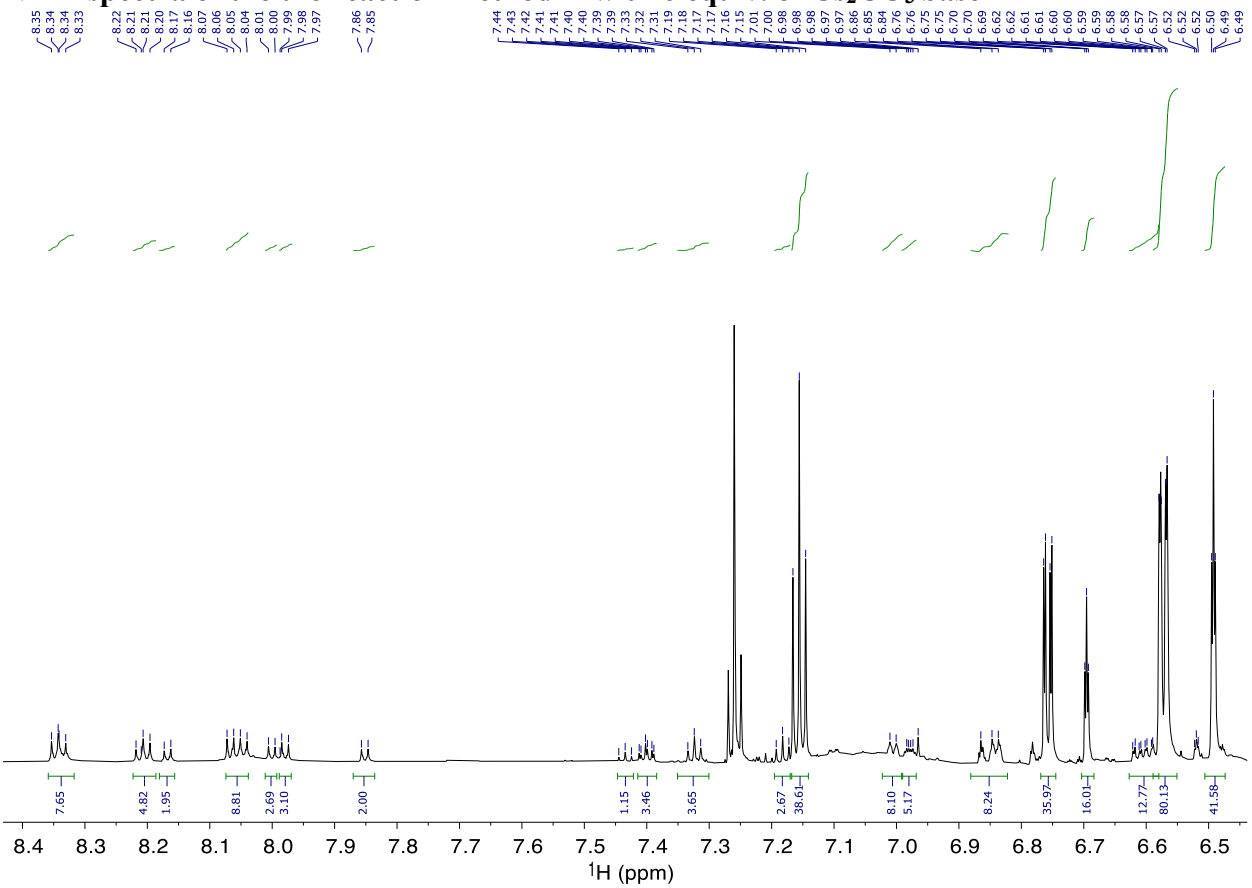

Figure S33. ^{1}H NMR of the work-up of the reaction method **D** with 6 equiv. of Cs_2CO_3 base.

^{1}H NMR (800 MHz, $CDCl_3$) δ 8.34 (dd, *J* = 8.8, 8.0 Hz, 8H), 8.21 (m, *J* = 6.4, 2.4 Hz, 5H), 8.17 (d, *J* = 8.8 Hz, 2H), 8.06 (dd, *J* = 8.0, 8.8 Hz, 9H), 8.00 (d, *J* = 8.8 Hz, 3H), 7.99 – 7.97 (d, *J* = 8.8 Hz, 3H), 7.86 (d, *J* = 8.8 Hz, 2H), 7.43 (t, *J* = 2.4 Hz, 1H), 7.40 (m, *J* = 2.4, 2.4 Hz, 3H), 7.32 (t, *J* = 2.4 Hz, 4H), 7.18 (t, *J* = 8.8 Hz, 3H), 7.16 (t, *J* = 8.0 Hz, 39H), 7.01 (d, *J* = 7.2 Hz, 8H), 6.98 (dd, *J* = 2.4, 2.4 Hz, 5H), 6.88 – 6.82 (m, *J* = 8.0 Hz, 8H), 6.79 – 6.75 (m, , *J* = 2.4, 2.4, 36H), 6.70 (t, *J* = 2.4 Hz, 16H), 6.61 (dddd, *J* = 2.4, 2.4 Hz, 13H), 6.57 (dd, *J* = 7.4, 2.4 Hz, 80H), 6.49 (t, *J* = 2.4 Hz, 42H).

Characterization 6 equiv. (Table 1, entry 8): HRMS, ESI^+: **3b** (2+2) m/z calc. for $C_{64}H_{40}N_4O_{12}$ $[M+2Na]^{2+}$ 551.1214 found 551.1220; m/z calc. for. $[M+Na]^+$ 1079.2535 found 1079.2532*;* m/z calc. for $[M+Cs]^+$ 1189.1692 fond 1189.1694; **3d** (4+4) m/z calc. for $[M+2Cs]^{2+}$ 1189.1692 fond 1189.1694. **DOSY NMR:** D= 6.37 10^{-10} m^2 s^{-1}, MW= 1065 g mol^{-1} (MNova) and D= 5.72 10^{-10} m^2 s^{-1}, MW= 936 g mol^{-1} (TopSpin) for **3b**, D= 5.00 10^{-10} m^2 s^{-1}, MW= 1476 g mol^{-1} (MNova) and D= 4.52 10^{-10} m^2 s^{-1}, MW= 1420 g mol^{-1} (TopSpin) for **3c**, D= 4.79 10^{-10} m^2 s^{-1}, MW= 2002 g mol^{-1} (MNova) and D= 3.70 10^{-10} m^2 s^{-1}, MW= 2021 g mol^{-1} (TopSpin) for **3d,** D= 4.25*10^{-10} m^2 s^{-1} MW =2680 $gmol^{-1}$ (Mnova) for **3e**.

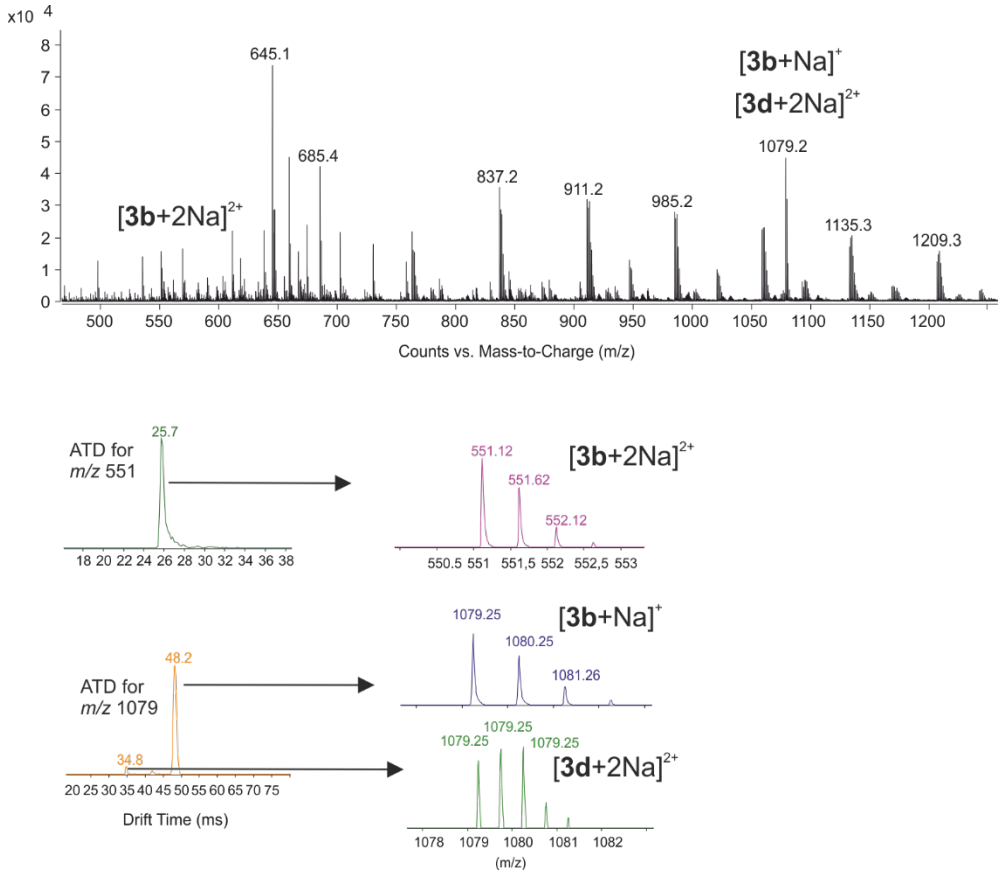

Figure S34. ESI-MS mass spectrum for **D6** (entry 8) and IM-MS arrival time distributions (ATDs) for different ions. Multiple peaks in ATDs correspond to different, overlapping ions. Zoomed views for MS spectra are extracted from each of the peaks to verify their identity and to compare the abundance.

DOSY analysis of the reaction method D with 6 equiv. of Cs_2CO_3 base

The DOSY analysis of the azobenzene region of the reaction method **D** with 6 equiv. of Cs_2CO_3 base is brought below. The spectrum was illustrated and analyzed with MNova and is depicted in Figure S35. The results of the found macrocycles with the external standards extracted from TopSpin are listed in Table S11.

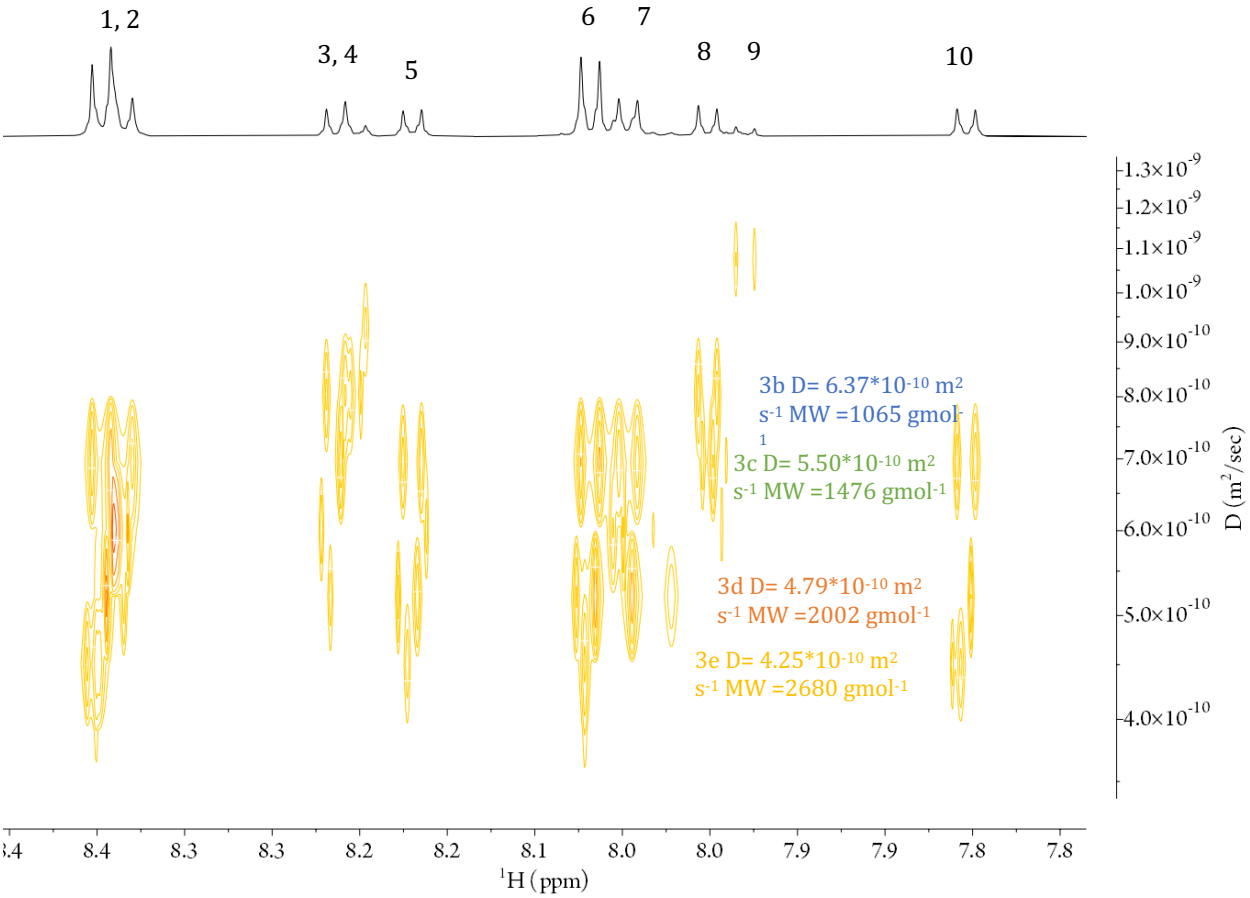

Figure S35. DOSY analysis of the work-up of the reaction method **D** with 6 equiv. of Cs_2CO_3 base

Table S11. TopSpin Analysis of the Reaction Method **D** with 6 Equiv. of Cs_2CO_3 Base

	1	2	3	4	5	6	7	8	9	10
ppm	8.36-8.35	8.348-8.347	8.23-8.22	8.21-8.20	8.18-8.17	8.08-8.07	8.06-8.05	8.02-8.00	7.99-7.98	7.87-7.86
D	3.7E-10	4.012E-10	4.941E-10	5.785E-10	3.915E-10	4.171E-10	4.236E-10	4.515E-10	5.712E-10	3.934E-10
log D	-9.43	-9.40	-9.31	-9.24	-9.41	-9.38	-9.37	-9.35	-9.24	-9.41
Y	3.31	3.24	3.08	2.96	3.26	3.21	3.20	3.15	2.97	3.26
calc MW	2020.8	1750.6	1210.0	914.9	1828.2	1634.0	1589.8	1419.8	935.7	1812.6
Macrocycle	4+4	4+4	3+3	2+2	4+4	4+4	4+4	3+3	2+2	4+4

Reaction Method E

Synthetic procedure for E: Dropping both reactants (1 and 2) and refluxing
In a 3-neck round bottom flask equipped with 3 Å molecular sieves n equiv. of Cs_2CO_3 (n= 4, 6) were dissolved in 12 mL THF and stirred at RT under argon atmosphere for 5 minutes. Two dropping funnels, one with 1 equiv. of 3,3'-(1,3-phenylenebis(oxy))diphenol (42.8 mg, 145.4 µmol) dissolved in 6 mL THF extra dry and one with 1 equiv. of 4,4-diaazene-1,2-diyl)dibenzoyl)chloride (44.66 mg, 145.4 µmol) in 6 mL THF were connected and both reactants were added dropwise over 15-20 min to the reaction mixture. Immediately afterwards the reaction was heated to 80˚C and refluxed for 6h and afterwards cooled to RT. The mixture was stirred under argon atmosphere and reaction progress was monitored with ^{1}H NMR, similarly to as described above, after 4, 6, 23, 49, 53h until the reaction was completed (up to 7 days). After the reaction was complete, the mixture was filtered and washed with 5 mL THF and the solvent was evaporated. The mixture was extracted and evaporated to give 98% after 168h in the presence of 4 equiv. of base and 56% conversion after 120h in the presence of 6 equiv. of base.

Reaction monitoring of the reaction E with different base equivalents
After a long stirring time at RT for 168h for the 4 equiv. base reaction (left), all peaks are overlapping for this reaction, however after the purification they appear separated again in the spectrum (work-up).

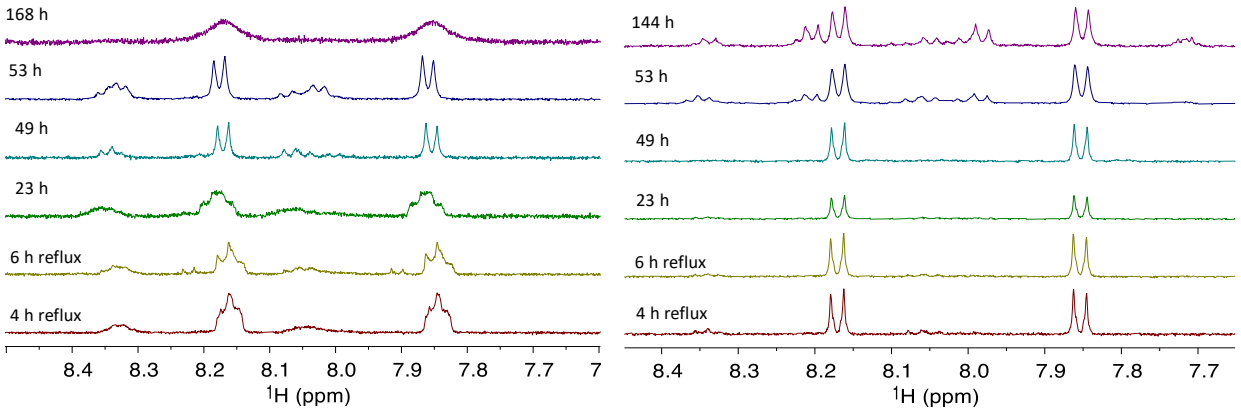

Figure S36. Reaction monitoring of the reaction the reaction method **E** with 4 (above) and 6 (below) equiv. of Cs_2CO_3 base

Characterization of the work-up mixtures obtained from E

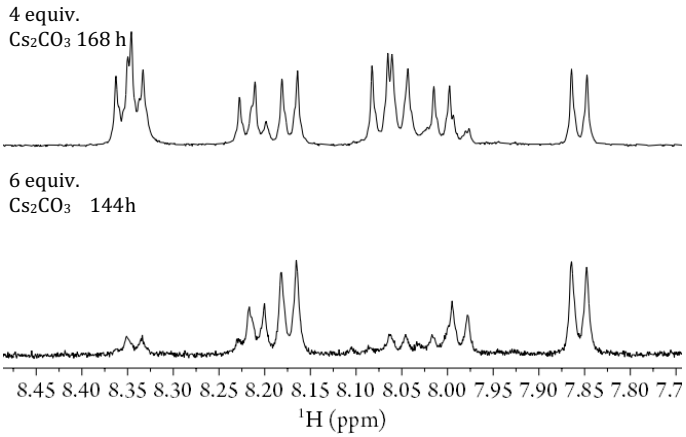

Figure S37. ^{1}H NMR azobenzene region of the reaction method **E** with 4 (above) and 6 (below) equiv. of Cs_2CO_3 base of the work-up phase.

NMR spectra and analysis from reaction E

NMR spectra of the reaction method **E** with 4 equiv. of Cs_2CO_3 base

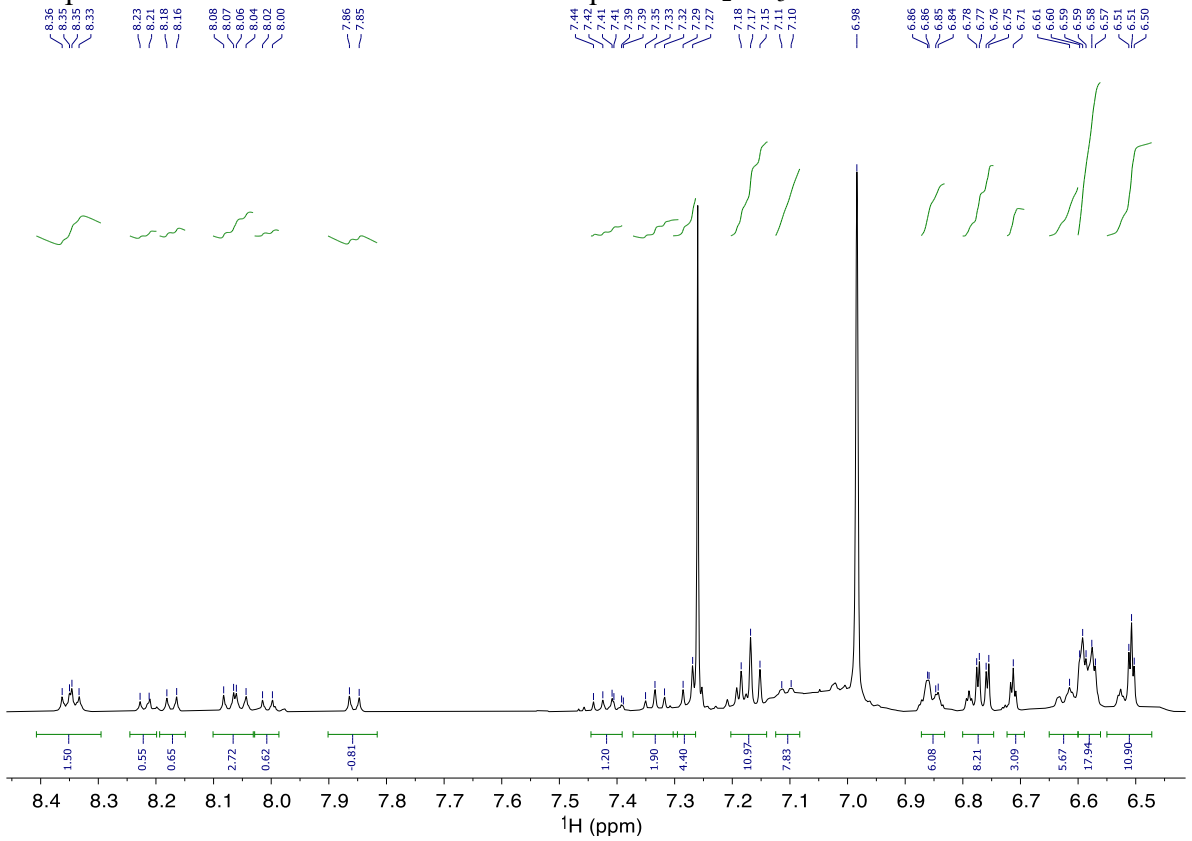

Figure S38. ^{1}H NMR for the reaction method **E** with 4 equiv. of Cs_2CO_3 base.

^{1}H NMR (500 MHz, $CDCl_3$) δ 8.35 (dd, *J* = 8.5, 8.0 Hz, 5H), 8.22 (d, *J* = 8.0 Hz, 2H), 8.17 (d, *J* = 8.5 Hz, 2H), 8.06 (dd, *J* = 8.5, 8.0 Hz, 5H), 8.01 (d, *J* = 8.0 Hz, 2H), 7.86 (d, *J* = 8.5 Hz, 2H), 7.45 – 7.39 (m, *J* = 8.0, 3H), 7.33 (t, *J* = 8.0 Hz, 5H), 7.28 (d, *J* = 8.5 Hz, 6H), 7.17 (t, *J* = 8.5 Hz, 13H), 7.11 (d, *J* = 8.0 Hz, 9H), 6.87 – 6.83 (m, *J* = 8.0, 7H), 6.77 (dd, *J* = 2.5, 2.5 Hz, 10H), 6.71 (t, *J* = 2.4 4H), 6.61 (s, 7H), 6.60 – 6.56 (m, *J* = 5.5, 3.0 19H), 6.51 (t, *J* = 2.5 Hz, 14H).

Characterization: 4 equiv. (Table 1, entry 9): HRMS, ESI$^+$: **3b (2+2)** m/z calc. for $C_{64}H_{40}N_4O_{12}$ $[M+2Na]^{2+}$ 551.1214 found 551.1218; m/z calc. for $[M+Na]^+$ 1079.2535 found 1079.2524; **3d** (4+4) $C_{128}H_{80}N_8O_{24}$ $[M+2Na]^{2+}$ 1079.2535 found 1079.2524. **DOSY NMR:** D= 6.27 10^{-10} m^2 s^{-1}, MW= 1089 g mol^{-1} (MNova) for **3b**, D= 5.34*10^{-10} m^2 s^{-1} MW =1579 $gmol^{-1}$ (Mnova) **for 3c,** D= 4.70 10^{-10} m^2 s^{-1}, MW= 2118 g mol^{-1} (MNova) and D= 3.61 10^{-10} m^2 s^{-1}, MW= 2112 g mol^{-1} (TopSpin) for **3d;** D= 4.04 10^{-10} m^2 s^{-1}, MW= 3018 g mol^{-1} (MNova) for **3f.**

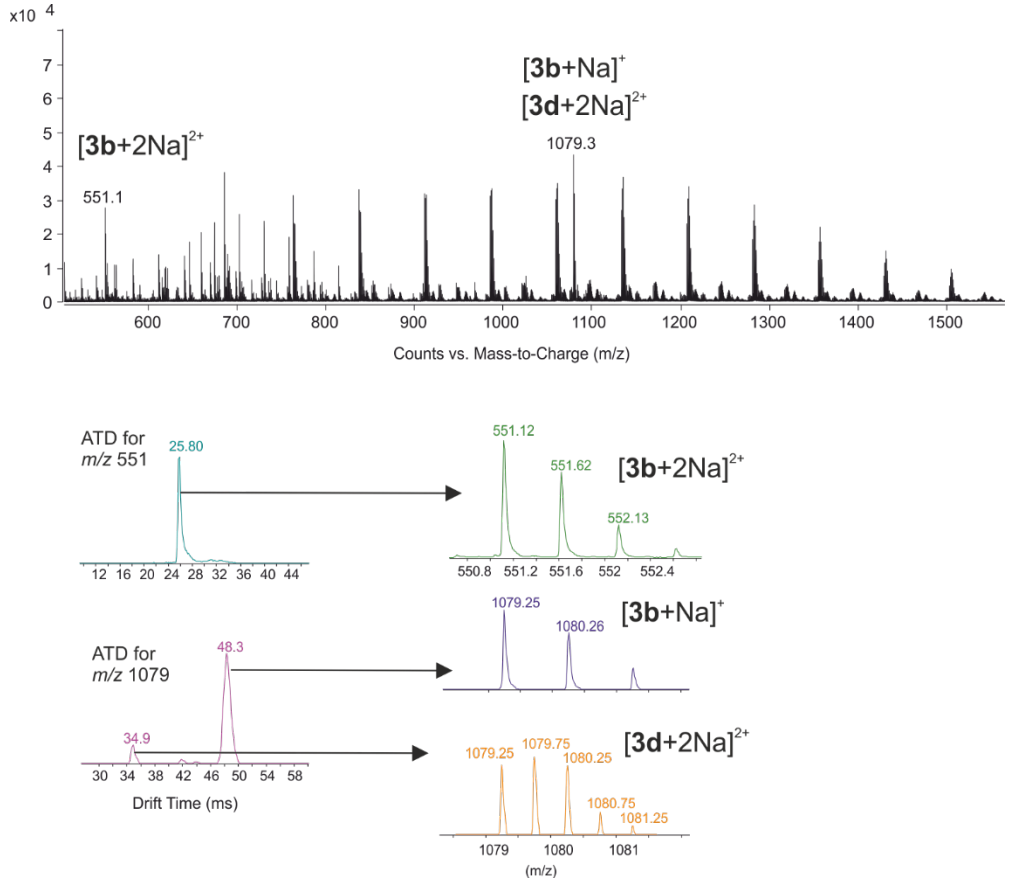

Figure S39. ESI-MS mass spectrum for **E4** (entry 9) and IM-MS arrival time distributions (ATDs) for different ions. Multiple peaks in ATDs correspond to different, overlapping ions. Zoomed views for MS spectra are extracted from each of the peaks to verify their identity and to compare the abundance.

DOSY Analysis of the reaction method E with 4 equiv. of Cs_2CO_3 base

The DOSY analysis of the azobenzene region of the reaction method **E** with 4 equiv. of Cs_2CO_3 base is brought below. The spectrum was illustrated and analyzed with MNova and is depicted in Figure S40. The results of the found macrocycles with the external standards extracted from TopSpin are listed in Table S12.

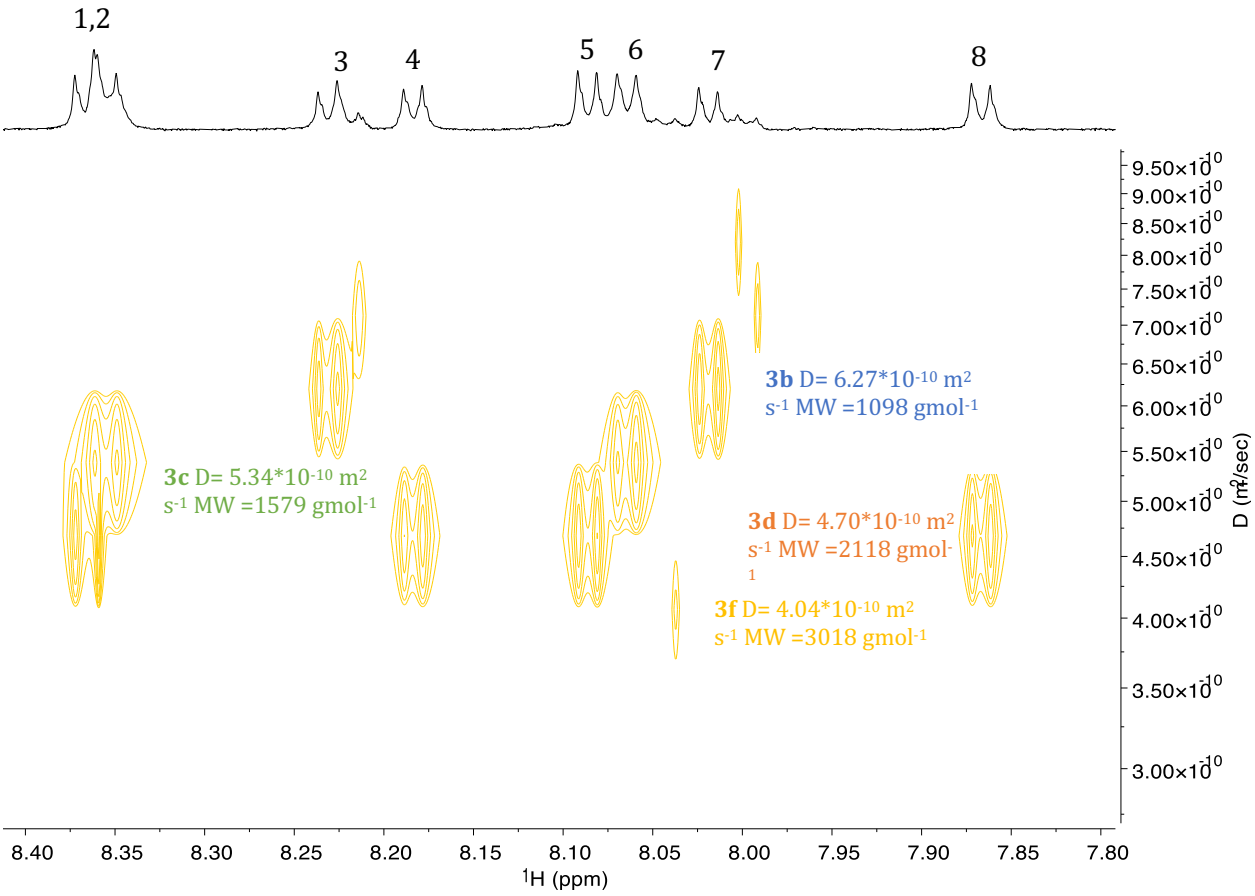

Figure S40. DOSY analysis of the work-up of the reaction method **E** with 4 equiv. of Cs_2CO_3 base.

Table S12. TopSpin Analysis of the Reaction Method **E** with 4 Equiv. of Cs_2CO_3 Base

	1	2	3	4	5	6	7	8
ppm	8.36-8.34	8.33-8.32	8.23-8.21	8.17-8.16	8.08-8.07	8.06-8.05	8.01-8.00	7.86-7.85
D	3.72E-10	3.629E-10	4.555E-10	3.516E-10	3.655E-10	3.609E-10	4.553E-10	3.556E-10
log D	-9.43	-9.44	-9.34	-9.45	-9.44	-9.44	-9.34	-9.45
Y	3.30	3.32	3.15	3.34	3.31	3.32	3.15	3.34
calc MW	2001.6	2091.4	1397.8	2212.1	2065.1	2112.0	1398.9	2168.2
Macrocycle	4+4	4+4	3+3	4+4	4+4	4+4	3+3	4+4

NMR spectra of the reaction method **E** with 6 equiv. of Cs_2CO_3 base

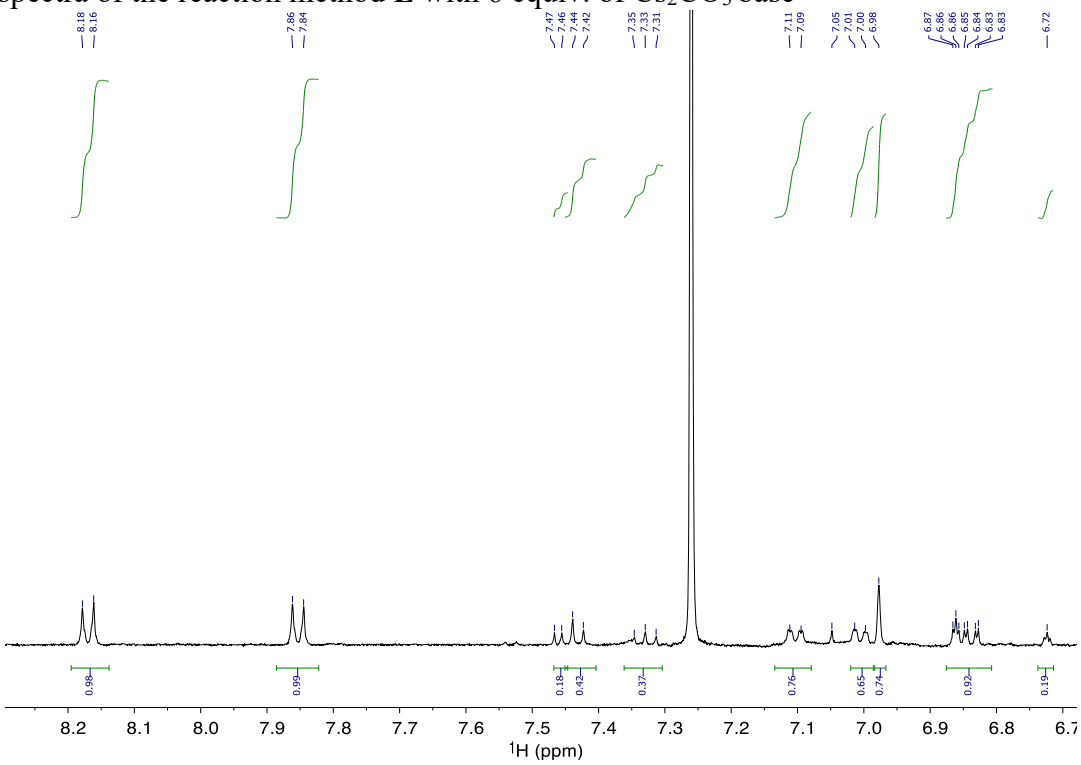

Figure S41. ^{1}H NMR for the reaction method **E** with 6 equiv. of Cs_2CO_3 base.

^{1}H NMR (500 MHz, $CDCl_3$) δ 8.17 (d, *J* = 8.5 Hz, 1H), 7.85 (d, *J* = 8.4 Hz, 1H), 7.10 (d, *J* = 8.5 Hz, 1H), 7.01 (d, *J* = 8.2 Hz, 1H), 6.98 (s, 1H), 6.88 – 6.81 (m, 1H).

Characterization 6 equiv. (Table 1, entry 10): HRMS, ESI$^+$: **3b (2+2)** m/z calc. for $C_{64}H_{40}N_4O_{12}$ $[M+2Na]^{2+}$ 551.1214 found 551.1212; m/z calc. for $[M+Na]^+$ 1079.2535 found 1079.2538; m/z calc. for $[M+Cs]^+$ 1189.1692 fond 1189.1704; **3d** (4+4) $C_{128}H_{80}N_8O_{24}$ $[M+2Na]^{2+}$ 1079.2535 found 1079.2538; m/z calc. for $[M+Na]^+$ 2135.5178 found 2135.5162; **3e (5+5)** m/z calc. for $C_{160}H_{100}N_{10}O_{30}$ $[M+2Na]^{2+}$ 1343.3196 found 1343.1386; **3f (6+6)** m/z calc. for $C_{192}H_{120}N_{12}O_{36}$ $[M+2Na]^{2+}$ 1607.3856 found 1607.3869; **3g** (8+8) m/z calc. for $C_{256}H_{160}N_{16}O_{48}$ $[M+2Na]^{2+}$ 2135.5177 found 2135.5162. **DOSY NMR*:*** D= 6.16 10^{-10} m^2 s^{-1}, MW= 1149 g mol^{-1} (MNova) for **3b**; D= 5.39 10^{-10} m^2 s^{-1}, MW= 1548 g mol^{-1} (MNova) and D= 4.43 10^{-10} m^2 s^{-1}, MW= 1470 g mol^{-1} (TopSpin) for **3c**.

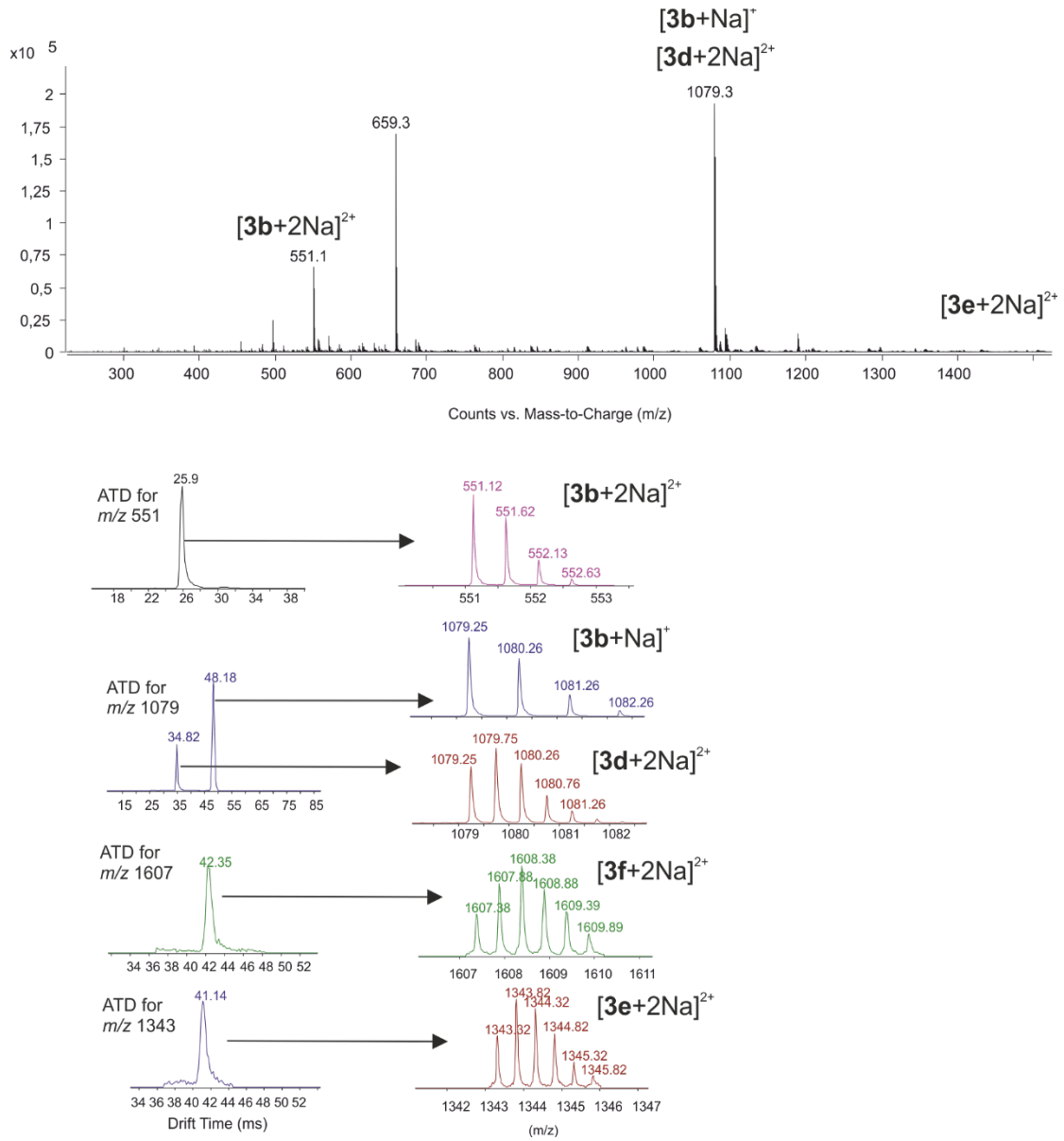

Figure S42. ESI-MS mass spectrum for **E6** (entry 10) and IM-MS arrival time distributions (ATDs) for different ions. Multiple peaks in ATDs correspond to different, overlapping ions. Zoomed views for MS spectra are extracted from each of the peaks to verify their identity and to compare the abundance.

DOSY Analysis of the reaction method E with 6 equiv. of Cs_2CO_3 base

The DOSY analysis of the azobenzene region of the reaction method **E** with 6 equiv. of Cs_2CO_3 base is brought below. The spectrum was illustrated and analyzed with MNova and is depicted in Figure S43. The results of the found macrocycles with the external standards extracted from TopSpin are listed in Table S13.

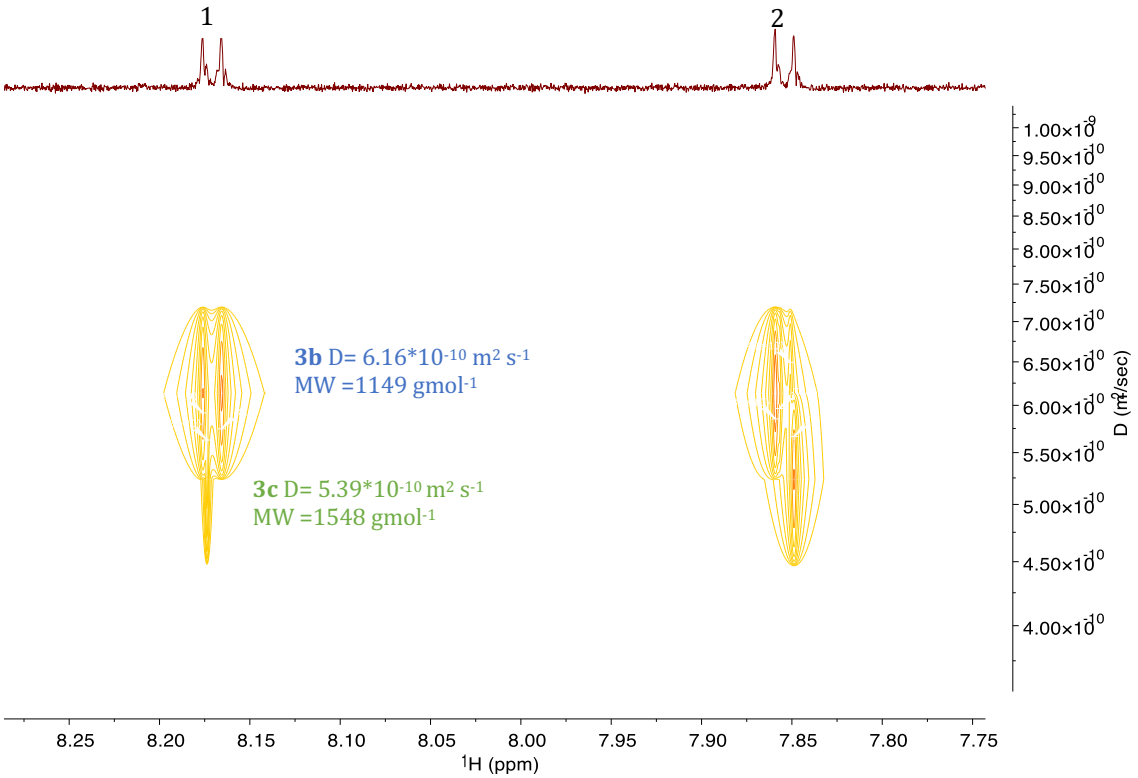

Figure S43. DOSY analysis of the reaction method **E** with 4 equiv. of Cs_2CO_3 base.

Table S13. TopSpin Analysis of the Reaction Method **E** with 4 Equiv. of Cs_2CO_3 Base

	1	2
ppm	8.18-8.17	7.86-7.85
D	4.192E-10	4.428E-10
log D	-9.38	-9.35
Y	3.21	3.17
calc MW	1619.5	1469.6
Macrocycle	3+3	3+3

Characterization of the separated compound obtained from method B

Characterization and NMR data of *E,Z*-3b

The compound with suggested conformation ***E,Z*-3b** was isolated applying column 2 the reaction method **B** with 4 equiv. of Cs_2CO_3 base. The characterization of the isolated compound with ^1H, ^{13}C, COSY, HSQC and DOSY NMR is brought below. With ESI-MS we could see traces of the compound **3d** and a small amount of impurity, which eluted together with the macrocycle in the column and we were not able to separate it from **3b**. This could be because of intermolecular interactions with **3b**.

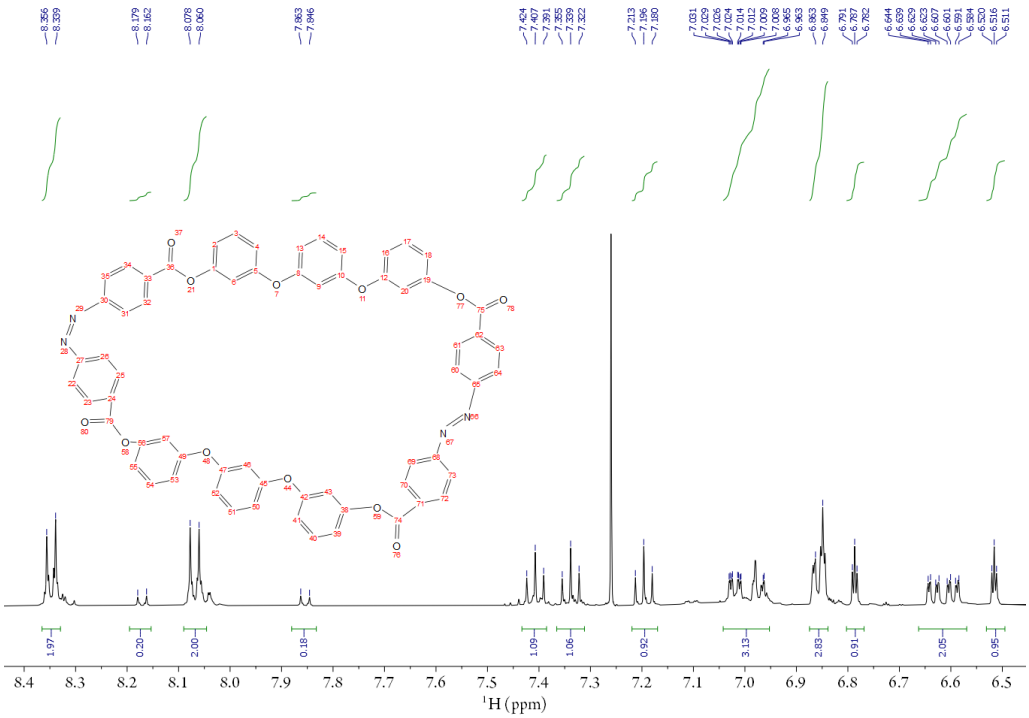

Figure S44. ^1H NMR of the compound ***E,Z*-3b** in $CDCl_3$.

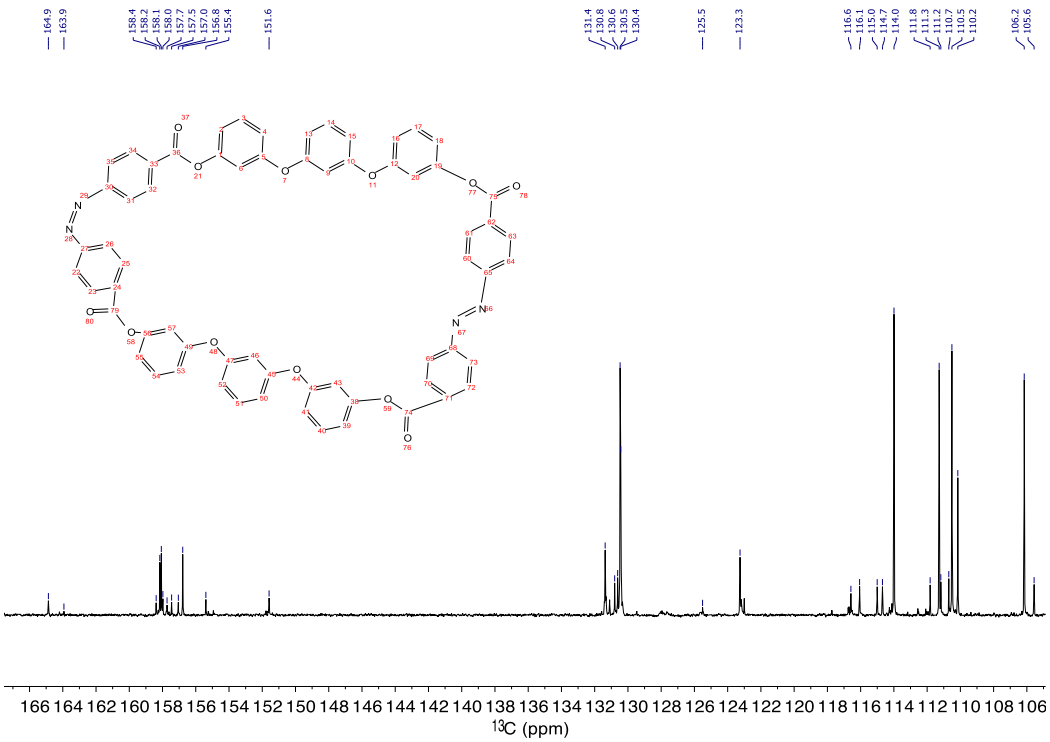

Figure S45. ^{13}C NMR of ***E,Z*-3b** in $CDCl_3$.

^{1}H NMR (500 MHz, $CDCl_3$) δ 8.35 – 8.34 (d, *J* = 8.5 Hz, 12H); 8.18– 8.16 (d, *J* = 8.5 Hz, 0.2H); 8.08–8.06 (d, *J* = 8.5 Hz, 2H); 7.86 – 7.85 (d, *J* = 8.5 Hz, 0.2H) (22,23,25,26,31,32,34,35,60,61,63,64,69,70,72,73, azobenzene-H), 7.42 – 7.40 (t, *J* = 8.5 Hz, 1H); 7.35 – 7.33 (t, *J* = 8.0 Hz, 1H) 3;17;40;54), 7.19 – 7.17 (t, *J* = 8.5 Hz, 1H) (14;51), 7.03 – 6.96 (dddd, *J* = 2.5, 2.0 Hz, 3H); 6.86 – 6.84 (d, *J* = 7.0 Hz, 3H) (2,4,16,18,39,41,53,55), 6.79 (t, *J* = 2.0 Hz, 1H), 6.64 – 6.58 (dddd, *J* = 2.5, 2.0 Hz, 2H) (13,15,50,52), 6.52 (t, *J* = 2.0 Hz, 1H) (9,46). **^{13}C NMR** (201 MHz, $CDCl_3$) δ 164.9; 163.9, (O**C**=O; 36,75,74,79), 158.4; 158.2; 158.1(N-**C**Ar; 27,30,65,68), 158.0; 157.7, 157.5, 157.1 (Ar**C**-O-**C**Ar-Ar**C**-O-**C**Ar-; 5,12,42,49), 156.78; 155.39; 151.59, (8,10,45,47), 131.4 (23,25,32,34,61,63,70,72), 130.6; 130.5; 130.4 (3,17,4054), 125.51; 123.26 (22,25,31,35,60,64,69,73), 130.8; 116.6; 116.1; 115.0; 114.7;114.0; 111.8 (2,4,16,18,39,41,53,55), 111.3; 111.2; 110.70; 110.5(13,15,50,52), 106.2 (6,20,43,57), 105.7(9,46). **HRMS**, ESI$^+$: m/z calc. for $C_{64}H_{40}N_4O_{12}$ $[M+2Na]^{2+}$ 551.1214 found 551.1228; $[M+Na]^+$ 1079.2535 found 1079.2535, $[M+Cs]^+$ 1189.1692 found 1189.1700.

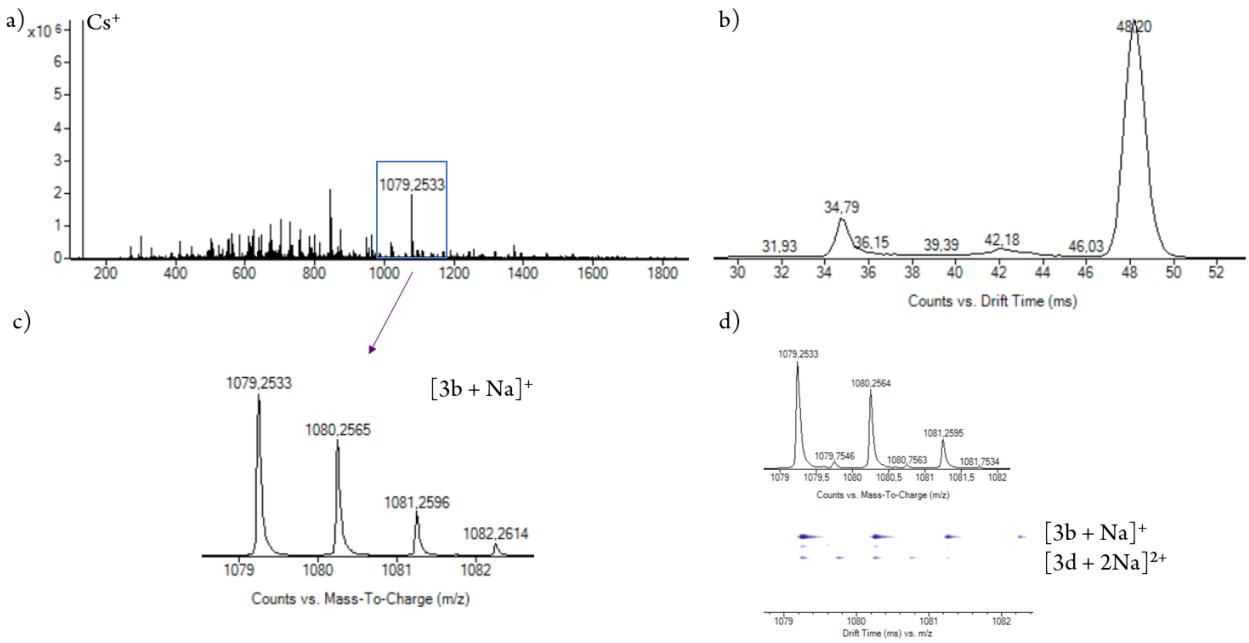

Figure S46. a) Full ESI-MS spectra of **E,Z-3b** b) drift time of the whole spectrum c) extracted IM of the main compound **3b** and d) small amount of overlapping **3d**.

DOSY Spectrum:

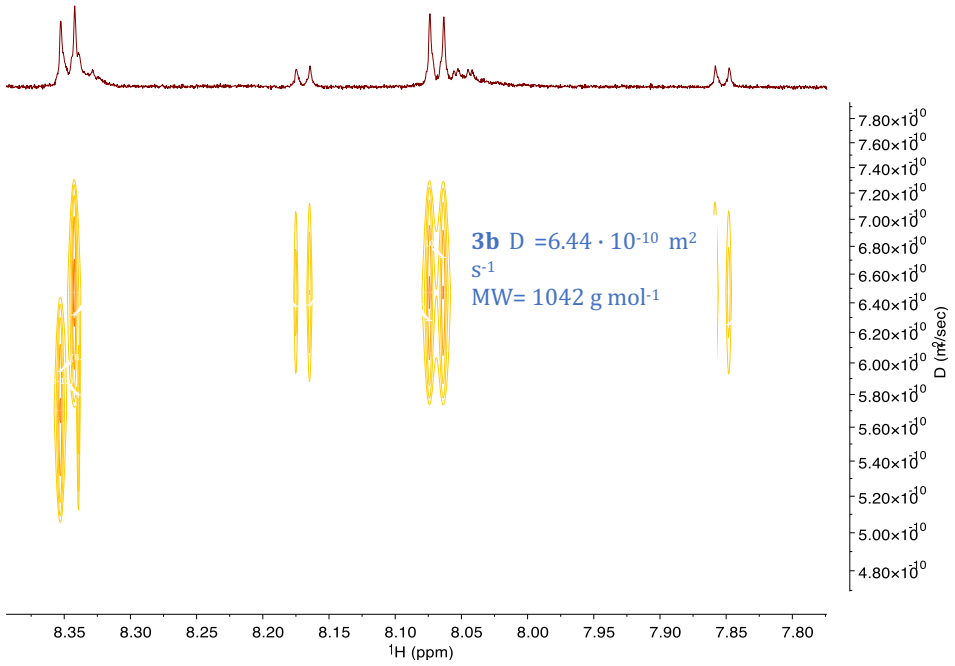

Figure S47. DOSY NMR of the isolated ***E,Z*-3b** in toluene-d_8.

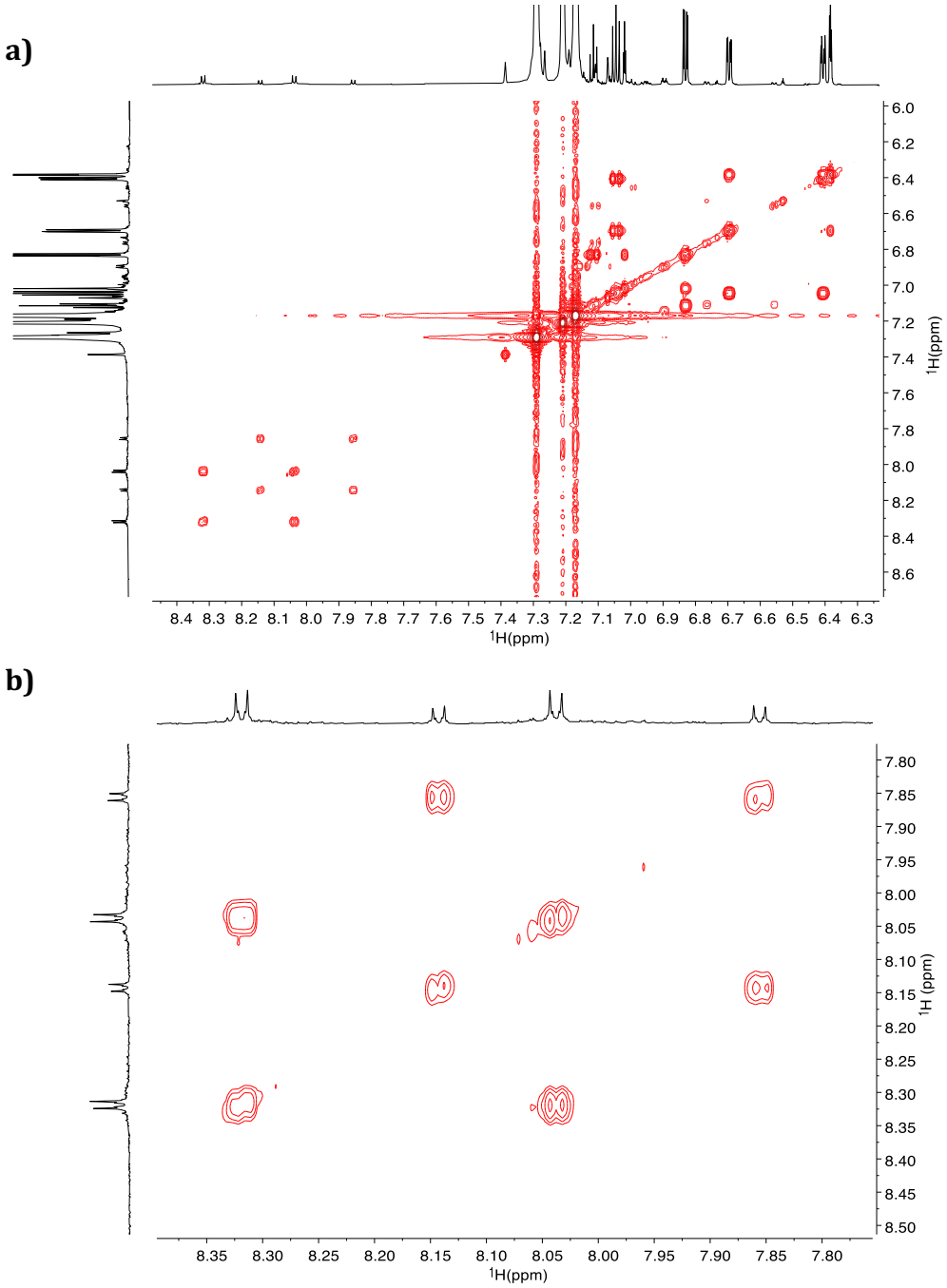

Figure S48. COSY (H-H) NMR of the separated ***E,Z*-3b** a) full spectrum b) zoomed in azobenzene region in toluene-d_8.

a)

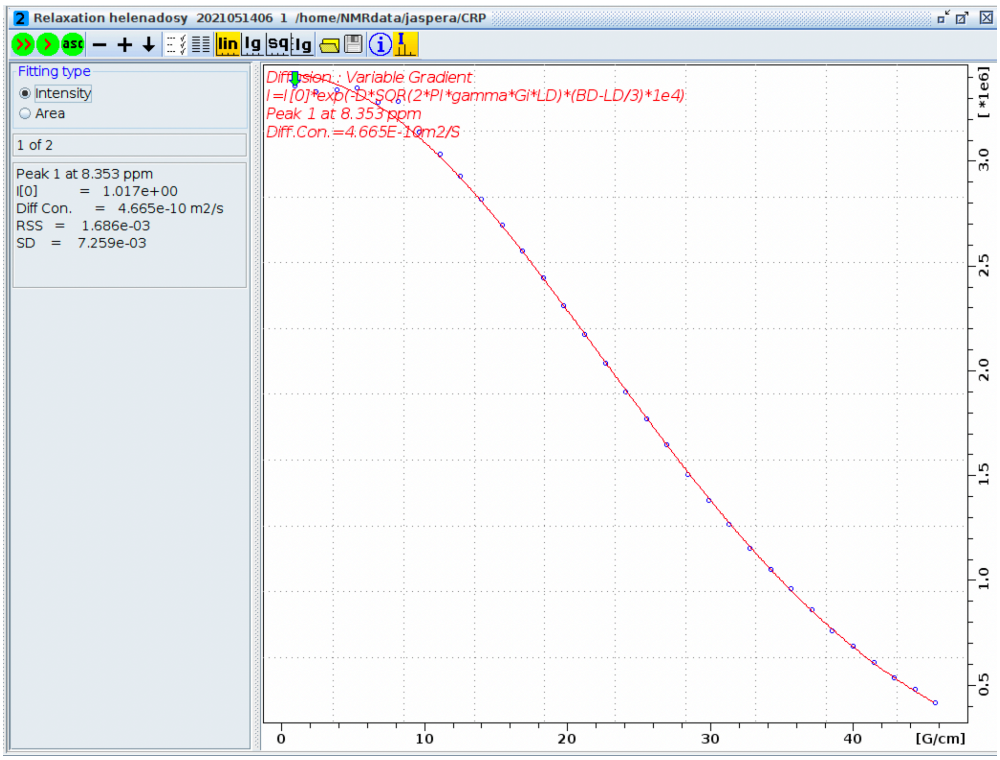

b)

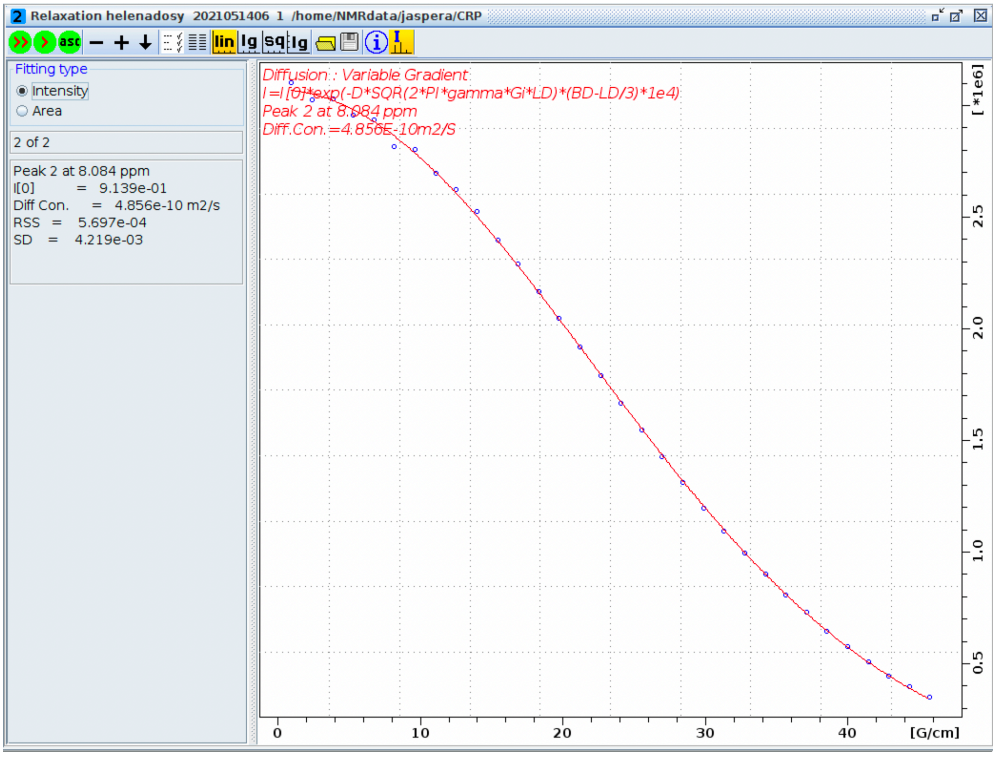

Figure 49. a) and b) DOSY exponential fit of the decay of some signals attributed to a single to a mono-exponential function. The sample **3b** was analyzed with Topspin in the T1/T2 relaxation module, the integration is obtained for the 4 azobenzene proton peaks between 7.5 and 8.5 ppm.

Theoretical calculations

Ground state conformational search for the ***E,E*-3b** and ***Z,Z*-3b** compounds representing 2+2 macrocycle framework was carried out in chloroform at PCM[3,4]/B3LYP[5,6]/6-311G(d.p)[7] level using the Gaussian16[8] software package and the lack of imaginary frequencies in harmonic vibrational analysis was observed for each optimized structure. The geometries of the lowest energy ***Z,Z*-3b** and ***E,E*-3b** conformers were subsequently used in TD-DFT[9] calculations of respective UV/Vis spectra. For calculations of spectral properties, the CAM-B3LYP[10] range-separated hybrid functional with mild Coulombic attenuation was tuned to achieve better description of the measured counterparts. For both studied structures the best match with experimental spectrum was observed at PCM/*m*CAM-B3LYP (α = 0.03. β = 0.97. μ = 0.24) /6-311G(d.p) level of theory. The simulated spectrum was convoluted with the Gaussian broadening function of 0.2 eV HWHH. D3 version of empirical dispersion correction with Becke-Johnson damping[11] was applied for all DFT and TD-DFT calculations.

Table S14. Calculated Spectral Properties for Studied Compounds at PCM/*m*CAM-B3LYP +GD3BJ/6-311G(d.p) Level

***E,E*-3b**			***Z,Z*-3b**		
Excited state	Excitation energy, nm	Oscillator strength	Excited state	Excitation energy, nm	Oscillator strength
1.	508.85	0.0173	1.	514.39	0.0002
2.	501.43	0.0021	2.	514.03	0.0852
3.	348.3	0.1196	3.	305.32	0
4.	340.47	2.1945	4.	304.54	0.0429
5.	323.6	0.0029	5.	296.44	0.0083
6.	322.15	0.1171	6.	295.91	0.4234
7.	300.48	0.001	7.	281.17	0.0089
8.	294.13	0.2775	8.	280.17	0.3776
9.	289.76	0.0146	9.	277.78	0.347
10.	289.09	0.056	10.	276.54	0.0857
11.	284.19	0.2399	11.	266.9	0.1677
12.	282.63	0.0476	12.	266.83	0.0505
13.	260.73	0.0117	13.	260.69	0.0021
14.	260.63	0.0031	14.	260.47	0.0067
15.	259.09	0.0023	15.	259.74	0.0119
16.	258.93	0	16.	257.72	0.4012
17.	256.29	0.0021	17.	251.55	0.0202
18.	253.26	0.0008	18.	251.53	0.0287
19.	251.61	0.0446	19.	249.8	0.0082
20.	251.52	0.0078	20.	249.75	0.0059
21.	248.34	0	21.	246.29	0.3824
22.	248.33	0.0261	22.	246.24	0.0219
23.	246.25	0.003	23.	245.66	0.0138
24.	246.14	0.0493	24.	245.57	0.0379
25.	241.34	0.0279	25.	240.17	0.0137
26.	241.21	0.0799	26.	240.15	0.0033
27.	240.66	0.0182	27.	236	0.0023
28.	240.63	0.0051	28.	235.94	0.0146
29.	239.18	0	29.	235.8	0.0124
30.	238.15	0.0499	30.	235.75	0.036

It is worth noting that the sum of oscillator strength values for the 30 lowest electronic transitions is higher than 2.6 for both ***E,E*-3b** and ***Z,Z*-3b** species, thus pointing to an elevated number of oscillating electrons in accordance with Thomas-Reiche-Kuhn rule, which is consistent with the polymer-like extended macrocycle origin. However, for ***E,E*-3b** case the high oscillator strength value is associated with the single $S_0 \rightarrow S_4$ transition while for ***Z,Z*-3b** structure the total oscillator strength is distributed between multiple transitions with varied oscillator strengths of lower magnitude which are forming the main high-energy absorption band between 220 and 320 nm.

Table S15-17 show the main contributions to the target electronic excitation natural transition orbitals (NTO-s) for the low-energy states of selected ***E,E*-3b** and ***Z,Z*-3b** structures. The NTO-s for $S_0 \rightarrow S_4$ transition of ***E,E*-3b** structure in low-energy symmetric C_2 representation reveal the patterns of intra ligand charge transfer (ILCT) character. For ***Z,Z*-3b** structure. the absorption bands both in the low-energy region ($S_0 \rightarrow S_2$) and in the high-energy region represented by $S_0 \rightarrow S_6$ excitation associated with the highest oscillator strength were likewise due to ILCT-type transitions. It is also evident that NTO-s of symmetric 2+2 macrocycle appear in pairs due to inversion of the phase of orbitals in one of the side chains.

Table S15. Dominant Hole and Particle NTO-s for $S_0 \rightarrow S_4$ Transitions (340 nm, Oscillator Strength 2.19) from PCM/*m*CAM-B3LYP+GD3BJ/6-311G(d.p) Level Calculations for ***E,E*-3b** Structure, λ is the Contribution of Respective NTO-s

	Dominant hole	Particle
$\lambda = 0.83$	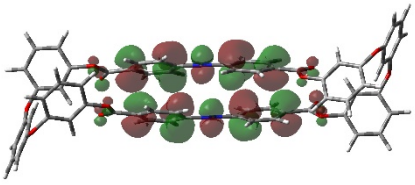	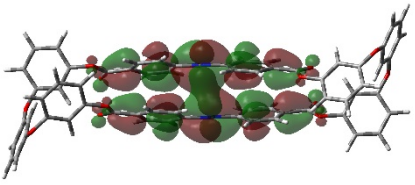

Table S16. Dominant Hole and Particle NTO-s for $S_0 \rightarrow S_2$ Transitions (514 nm, Oscillator Strength 0.09) from PCM/*m*CAM-B3LYP+GD3BJ/6-311G(d.p) Level Calculations for ***Z,Z*-3b** Structure, λ is the Contribution of Respective NTO-s

	Dominant hole	Particle
$\lambda = 0.51$	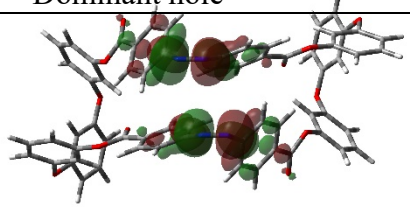	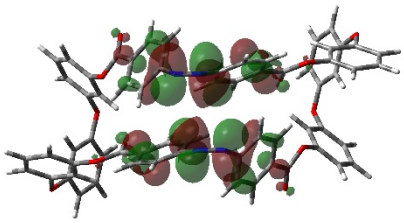
$\lambda = 0.49$	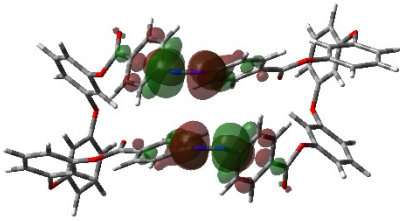	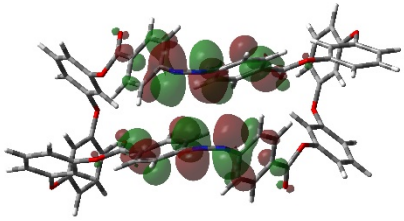

Table S17. Dominant Hole and Particle NTO-s for $S_0 \rightarrow S_6$ Transitions (296 nm, Oscillator Strength 0.42) from PCM/mCAM-B3LYP+GD3BJ/6-311G(d.p) Level Calculations for ***Z,Z*-3b** Structure, λ is the Contribution of Respective NTO-s

	Dominant hole	Particle
$\lambda = 0.49$	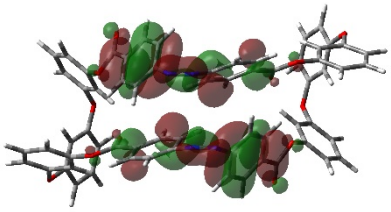	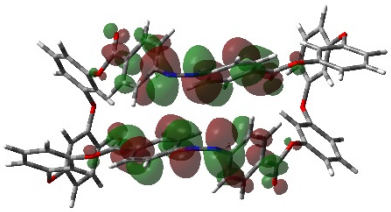
$\lambda = 0.43$	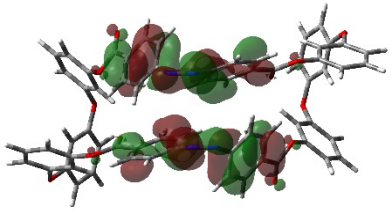	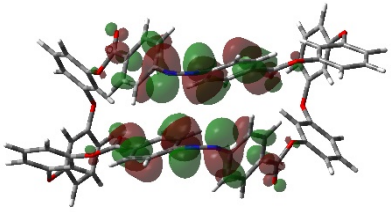

References

1. Zhou, Q., Su, L., Jiang, T., Zhang, B., Chen, R., Jiang, H., Ye, Y., Zhu, M., Han, D., Shen, J., Dai, G., & Li, Z. Copper/iron-catalyzed Ullmann coupling of diiodo- and dibromoarenes and diphenols for the synthesis of aryl ether macrocycles. **2014**, *Tetrahedron*, *70*(6). https://doi.org/10.1016/j.tet.2013.12.089

2. Prigorchenko. E.; Öeren. M.; Kaabel. S.; Fomitšenko. M.; Reile. I.; Järving. I.; Tamm. T.; Topić. F.; Rissanen. K.; Aav. R. Template-Controlled Synthesis of Chiral Cyclohexylhemicucurbit[8]Uril. *Chemical Communications* **2015**, *51* (54). https://doi.org/10.1039/C5CC04101E
3. Cancès, E.; Mennucci, B.; Tomasi, J. A New Integral Equation Formalism for the Polarizable Continuum Model: Theoretical Background and Applications to Isotropic and Anisotropic Dielectrics. *The Journal of Chemical Physics* **1997**, *107* (8), 3032–3041. https://doi.org/10.1063/1.474659
4. Mennucci, B.; Cancès, E.; Tomasi, J. Evaluation of Solvent Effects in Isotropic and Anisotropic Dielectrics and in Ionic Solutions with a Unified Integral Equation Method: Theoretical Bases, Computational Implementation, and Numerical Applications. *The Journal of Physical Chemistry B* **1997**, *101* (49), 10506–10517. https://doi.org/10.1021/jp971959k
5. Becke, A. D. Density-functional Thermochemistry. III. The Role of Exact Exchange. *The Journal of Chemical Physics* **1993**, *98* (7), 5648–5652. https://doi.org/10.1063/1.464913
6. Lee, C.; Yang, W.; Parr, R. G. Development of the Colle-Salvetti Correlation-Energy Formula into a Functional of the Electron Density. *Physical Review B* **1988**, *37* (2), 785–789. https://doi.org/10.1103/PhysRevB.37.785
7. Frisch, M. J.; Pople, J. A.; Binkley, J. S. Self-consistent Molecular Orbital Methods 25. Supplementary Functions for Gaussian Basis Sets. *The Journal of Chemical Physics* **1984**, *80* (7), 3265–3269. https://doi.org/10.1063/1.447079
8. Frisch, M.; Trucks, G.; Schlegel, H.; Scuseria, G.; Robb, M.; Cheeseman, J.; Scalmani, G.; Barone, V.; Petersson, G.; Nakatsuji, H.; Li, X.; Caricato, M.; Marenich, A.; Bloino, J.; Janesko, B.; Gomperts, R.; Mennucci, B.; Hratchian, H.; Ortiz, J.; Izmaylov, A.; Sonnenberg, J.; Williams-Young, D.; Ding, F.; Lipparini, F.; Egidi, F.; Goings, J.; Peng, B.; Petrone, A.; Henderson, T.; Ranasinghe, D.; Zakrzewski, V.; Gao, J.; Rega, N.; Zheng, G.; Liang, W.; Hada, M.; Ehara, M.; Toyota, K.; Fukuda, R.; Hasegawa, J.; Ishida, M.; Nakajima, T.; Honda, Y.; Kitao, O.; Nakai, H.; Vreven, T.; Throssell, K.; Montgomery, J.; Peralta, J.; Ogliaro, F.; Bearpark, M.; Heyd, J.; Brothers, E.; Kudin, K.; Staroverov, V.; Keith, T.; Kobayashi, R.; Normand, J.; Rachavachari, K.; Rendell, A.; Burant, J.; Iyengar, S.; Tomasi, J.; Cossi, M.; Millam, J.; Klene, M.; Adamo, C.; Cammi, R.; Ochterski, J.; Martin, R.; Morokuma, K.; Farkas, O.; Foresman, J.; Fox, D. Gaussian 16, Revision C.01. *Gaussian, Inc.: Wallingford, CT* **2016**.
9. Runge, E.; Gross, E. K. U. Density-Functional Theory for Time-Dependent Systems. *Physical Review Letters* **1984**, *52* (12), 997–1000. https://doi.org/10.1103/PhysRevLett.52.997
10. Yanai, T.; Tew, D. P.; Handy, N. C. A New Hybrid Exchange–Correlation Functional Using the Coulomb-Attenuating Method (CAM-B3LYP). *Chemical Physics Letters* **2004**, *393* (1–3), 51–57. https://doi.org/10.1016/j.cplett.2004.06.011
11. Grimme, S.; Ehrlich, S.; Goerigk, L. Effect of the damping function in dispersion corrected density functional theory. *J. Comp. Chem.* **2011,** 32, 1456-65. https://doi.org/10.1002/jcc.21759